AERO-MAP: A data compilation and modelling approach to understand spatial variability in fine and coarse mode aerosol composition

Natalie M. Mahowald[1], Longlei Li[1], Julius Vira[2], Marje Prank[2], Douglas S. Hamilton[3], Hitoshi Matsui[4], Ron L. Miller[5], P. Louis Lu[1,6], Ezgi Akyuz[7], Daphne Meidan[1], Peter Hess[8], Heikki Lihavainen[9], Christine Wiedinmyer[10], Jenny Hand[11], Maria Grazia Alaimo[12], Célia Alves[13], Andres Alastuey[14], Paulo Artaxo[15], Africa Barreto[16], Francisco Barraza[17], Silvia Becagli[18], Giulia Calzolai[18], Shankararaman Chellam[19], Ying Chen[20], Patrick Chuang[21], David D. Cohen[22], Cristina Colombi[23], Evangelia Diapouli[24], Gaetano Dongarra[12], Konstantinos Eleftheriadis[24], Johann Engelbrecht[25], Corinne Galy-Lacaux[26], Cassandra Gaston[27], Dario Gomez[28], Yenny González Ramos[29,16], Roy M. Harrison[30], Chris Heyes[31], Barak Herut[32,33], Philip Hopke[34,35], Christoph Hüglin[36], Maria Kanakidou[37,38,39], Zsofia Kertesz[40], Zbigniew Klimont[31], Katriina Kyllönen[2], Fabrice Lambert[41,42], Xiaohong Liu[43], Remi Losno[44], Franco Lucarelli[18], Willy Maenhaut[45], Beatrice Marticorena[46], Randall V. Martin[47], Nikolaos Mihalopoulos[37,48], Yasser Morera-Gómez[49], Adina Paytan[50], Joseph Prospero[26], Sergio Rodríguez[51,16], Patricia Smichowski[28], Daniela Varrica[12], Brenna Walsh[47], Crystal Weagle[48], Xi Zhao[43]

[1]Department of Earth and Atmospheric Sciences, Cornell University, Ithaca, NY, 14853, USA

[2] Finnish Meteorological Institute, Helsinki, Finland

[3] Department of Marine, Earth and Atmospheric Sciences, North Carolina State, Raleigh, NC, USA

[4] Graduate School of Environmental Studies, Nagoya University, Nagoya, Japan 464-8601

[5] National Aeronautics and Space Administration, Goddard Institute for Space Studies, Columbia University, NY, NY 10025

[6] Earth and Climate Section, Nicholas School of the Environment, Duke University, Durham, NC, 27708, USA

[7] Eurasia Institute of Earth Sciences, Istanbul Technical University, 34467 Istanbul, Turkey

[8] Department of Biological and Environmental Engineering, Cornell University, Ithaca NY, USA

[9] SIOS Knowledge Centre, Postboks 156, 9171 Longyearbyen, Norway

[10] Cooperative Institute for Research in Environmental Sciences at the University of Colorado Boulder, Boulder, CO, USA

[11] Cooperative Institute for Research in the Atmosphere, Colorado State University, Fort Collins, CO, USA,

[12] Dip. Scienze della Terra e del Mare, University of Palermo, Italy

[13] Centre for Environmental and Marine Studies (CESAM), Department of Environment, University of Aveiro, 3810-193, Aveiro, Portugal

[14] Institute of Environmental Assessment and Water Research (IDAEA-CSIC), 08034, Barcelona, Spain

[15] Instituto de Fisica,Universidade de Sao Paulo, 05508-090, Sao Paulo, SP, Brazil

[16] Izaña Atmospheric Research Center (IARC), Agencia Estatal de Meteorología (AEMET), Santa Cruz de Tenerife, Spain
[17] Saw Science, Invercargill, New Zealand
[18] Department of Physics and Astronomy, Universita di Firenze and INFN-Firenze, 50019 Sesto Fiorentino, Italy
[19] Department of Civil & Environmental Engineering, Texas A&M University, College Station, TX 77843-3136, USA
20 Dept. Environ. Sci. Engr. Fudan University Jiangwan Campus 2005 Songhu Road, Shanghai, China
[21] Earth & Planetary Sciences Department, Institute of Marine Sciences, University of California, Santa Cruz, CA, 95064 , USA.
[22] Centre for Accelerator Science, Australian Nuclear Science and Technology Organisation, New Illawarra Rd, Lucas Heights, NSW, Australia
[23] Environmental Monitoring Sector, Arpa Lombardia, Via Rosellini 17, 20124 Milan, Italy
[24] Environmental Radioactivity & Aerosol Technology for Atmospheric & Climate impact Lab, INRaSTES, N.C.S.R. Demokritos, 15341 Ag. Paraskevi, Attiki, Greece
[25] Desert Research Institute (DRI), 2215 Raggio Parkway, Reno, Nevada 89512-1095
[26] Laboratoire d Aerologie, Universite de Toulouse, CNRS, Observatoire Midi Pyrenees, Toulouse, France
[27] Rosenstiel School of Marine and Atmospheric Science, University of Miami, Miami, FL, 33149, US
[28] Comision Nacional de Energia Atomica, Gerencia Química, Av. Gral Paz 1499, B1650KNA, San Martin, Buenos Aires, Argentina
[29] Scientific Department, CIMEL, Paris, France.
[30] School of Geography, Earth and Environmental Sciences, University of Birmingham, Edgbaston, Birmingham B15 2TT, United Kingdom
[31] Energy, Climate and Environment Program, International Institute for Applied Systems Analysis, 2361 Laxenburg, Austria
[32] Israel Oceanographic & Limnological Research, Tel Shikmona, Haifa, 31080, Israel
[33] University of Haifa, Haifa, 3103301, Israel
[34] Clarkson University, Potsdam, NY, USA,
[35] Department of Public Health Sciences, University of Rochester School of Medicine and Dentistry, Rochester, NY, USA,
[36] Swiss Federal Laboratories for Materials Science and Technology(EMPA), CH-8600 Duebendorf, Switzerland
[37] Environmental Chemical Processes Laboratory (ECPL), Department of Chemistry, University of Crete, Heraklion, Greece.
[38] Center of Studies of Air quality and Climate Change, Institute for Chemical Engineering Sciences, Foundation for Research and Technology Hellas, Patras, Greece.
[39] Excellence Chair, Institute of Environmental Physics, University of Bremen, Bremen, Germany
40 HUN-REN Institute for Nuclear Research (ATOMKI), Debrecen, Hungary
[41] Geography Institute, Pontificia Universidad Catolica de Chile, Santiago, 7820436, Chile
[42] Center for Climate and Resilience Research, Santiago, Chile
[43] Department of Atmospheric Sciences, Texas A&M University, College Station, TX 77843
[44] Institut de Physique du Globe de Paris, Universite de Paris, Paris, France
[45] Department of Chemistry, Ghent University, Gent, Belgium
[46] Laboratoire Interuniversitaire des Systemes Atmospheriques (LISA), Universit«es Paris Est-Paris Diderot-Paris 7, UMR CNRS 7583, Cr«eteil, France
[47] Energy, Environmental and Chemical Engineering, Washington University, St. Louis, MO, USA.
[48] Institute for Environmental Research and Sustainable Development, National Observatory of Athens, Pendeli, Greece

[49] Universidad de Navarra, Instituto de Biodiversidad y Medioambiente BIOMA, Irunlarrea 1, 31008, Pamplona, España
[50] Earth and Planetary Science, University of California, Santa Cruz, CA, USA
[51] Consejo Superior de Investigaciones Científicas, IPNA CSIC, Tenerife, Canary Islands, Spain.

Correspondence to: Natalie M. Mahowald (mahowald@cornell.edu)

Abstract. Aerosol particles are an important part of the Earth-climate system, and their concentrations are spatially and temporally heterogeneous, as well as variable in size and composition. Particles can interact with incoming solar radiation and outgoing long wave radiation, change cloud properties, affect photochemistry, impact surface air quality, change the albedo of snow and ice, and modulate carbon dioxide uptake by the land and ocean. High particulate matter concentrations at the surface represent an important public health hazard. There are substantial datasets describing aerosol particles in the literature or in public health databases, but they have not been compiled for easy use by the climate and air quality modelling community. Here we present a new compilation of $PM_{2.5}$ and PM_{10} surface observations, including measurements of aerosol composition, focusing on the spatial variability across different observational stations. Climate modelers are constantly looking for multiple independent lines of evidence to verify their models, and in situ surface concentration measurements, taken at the level of human settlement, present a valuable source of information about aerosols and their human impacts that are complementary to the column averages or integrals often retrieved from satellites. We demonstrate a method for comparing the datasets to output from global climate models that are the basis for projections of future climate and large-scale aerosol transport patterns that influence local air quality. Annual trends and seasonal cycles are discussed briefly and included in the compilation. Overall, most of the planet or even the land fraction does not have sufficient observations of surface concentrations, and especially particle composition, to characterize and understand the current distribution of particles. Climate models without ammonium nitrate aerosols omit ~10% of the globally averaged surface concentration of aerosol particles in both $PM_{2.5}$ and PM_{10} size fractions, with up to 50% of the surface concentrations not included in some regions. In these regions, climate model aerosol forcing projections are likely to be incorrect, as they do not include important trends in short lived climate forcers.

Deleted: global average mass

Deleted: particles

1 Introduction

Intergovernmental Panel on Climate Change (IPCC) reports (IPCC, 2021; Gulev et al., 2021; Szopa et al., 2021) and other community assessments have highlighted the role of uncertainties in human-induced changes to aerosol concentration and composition in limiting our ability to project future climate. Aerosol particles are also a major contributor to air pollution, which reduces life expectancy and quality of life (Burnett et al., 2018). Aerosol particles are suspended liquids or solids in the atmosphere originating from diverse natural and anthropogenic sources and composed of a wide variety of chemicals

(e.g., sea salts, dust, sulfate, nitrate, black carbon, organic carbon). Particles interact with incoming solar radiation, outgoing long wave radiation, change cloud properties and lifetimes, and modify atmospheric photochemistry (Mahowald et al., 2011; Kanakidou et al., 2018; Bellouin et al., 2020). Once deposited on the surface, they can modify land and ocean biogeochemistry, as well as the albedo of snow and ice surfaces (Mahowald et al., 2017; Hansen and Nazarenko, 2004; Skiles et al., 2018). Satellite remote sensing retrievals provide important information about the temporal and spatial distribution of aerosol particles, but challenges remain in quantifying the aerosol size and chemical composition (Kahn et al., 2005; Tanré et al., 1997; Remer et al., 2005, Castellanos et al., 2024). In addition, the AERONET surface remote sensing network provides some information about loading, size and absorbing aerosol properties related to composition (Holben et al., 2001; Dubovik et al., 2002; Schuster et al., 2016; Gonçalves Ageitos et al., 2023; Obiso et al., 2023). Both the magnitude of the aerosol effects on climate, and sometimes their sign, are dependent on the composition and size of particles (Mahowald et al., 2011, 2014a; Bond et al., 2013; IPCC, 2021). In addition, one cannot understand the impact of humans on aerosol particles without identifying the sources of particles, which determine their chemical composition. Obtaining information about the composition and size of particles in many cases requires in situ observations, which are often limited in space and time (Hand et al., 2017; Philip et al., 2017; Yang et al., 2018; Collaud Coen et al., 2020).

The climate and aerosol modelling community, especially under the auspices of AEROCOM, has compiled datasets and organized comparison projects that have provided substantial information to improve aerosol models (Huneeus et al., 2011; Textor and others, 2006; Dentener et al., 2006; Schulz et al., 2006; 2012; Gliß et al., 2021) or knowledge of the aerosol impacts like cloud condensation nucleation (Laj et al., 2020; Fanourgakis et al., 2019). However, most of the available data comes from North America and Europe (e.g., Szopa et al., 2021; Reddington et al., 2017). In addition, previous compilation studies have focused primarily on understanding fine aerosol particles (here defined as particles with a diameter less than 2.5 μm) and improving model simulation of these particles, because of their importance for air quality, respiratory health, cloud interactions and short-wave forcing (Collaud Coen et al., 2020; Bellouin et al., 2020; Fanourgakis et al., 2019; Reddington et al., 2017). Coarse mode particles (defined as those particles with a diameter larger than 2.5 μm) are important for long wave radiation interactions, cloud seeding and for biogeochemistry, but these interactions have received less attention (Jensen and Lee, 2008; Mahowald et al., 2011; Karydis et al., 2017; Chatziparaschos et al., 2023). In contrast to the many fine aerosol compilations and comparisons (usually considering particles with aerodynamic diameter less than 2.5 μm or $PM_{2.5}$), there are fewer studies focusing on aerosol compilations for both fine and coarse particles, and their comparison to models (Kok et al., 2014b; Albani et al., 2014b; Huneeus et al., 2011; Gliß et al., 2021; Kok et al., 2021). Nonetheless, there are many observations of the coarse particle mass with diameter less than 10 μm (PM_{10}) (e.g., Hand et al., 2017), and most climate models include these particles (e.g., Huneeus et al., 2011). Compilations of in situ data are available for dust and iron particles (Kok et al., 2014b; Albani et al., 2014b; Mahowald et al., 2009) and for sea salts (Gong et al., 1997). Other studies have focused on the important topics of wet deposition (Vet et al., 2014) or trends in aerosol properties (e.g., AOD, surface PM) (Mortier et al., 2020; Aas et al., 2019). Observations of PM_{10} or coarse and fine particles are available for many regions

and individual sites (e.g., Malm et al., 2007; Hand et al., 2019; Maenhaut and Cafmeyer, 1998; Artaxo and Maenhaut, 1990; McNeill et al., 2020) but have not previously been compiled into one database that would facilitate the evaluation of global climate models that are an important tool for projections of future climate change, air quality and their impacts upon human society. Aerosol modelers need as much information as possible about the observed composition of the particles and their transport. Thus, there is a need to compile both $PM_{2.5}$ and PM_{10} in situ concentration data into one database to make it easy for modellers to compare global model results with observations. One goal the aerosol community should work towards is making aerosol measurement datasets publicly and conveniently available, while acknowledging the principal investigators who produced these datasets, which we hope this paper serves as a step towards achieving.

The current generation of Earth system models used for the IPCC simulations tends to include the dominant aerosol species (desert dust, sea spray, black carbon (BC), organic matter (OM) and sulfate) while omitting other potentially important aerosol constituents. For example, some Earth system models ignore ammonium nitrate particles although these are known to be important for climate and biogeochemistry, and are impacted by human activities (Paulot et al., 2016; Adams et al., 1999; Thornhill et al., 2021). In this study, we use available observations to compare to a global model estimate of the total PM_{10} and $PM_{2.5}$, and deduce the importance of these often-neglected aerosol species. We also propose a method for comparing species that are often not directly measured (such as dust or sea salts) using their elemental composition. Note that we exclude super coarse (>PM_{10}) particles here because of the sparcity of available measurements, although studies have suggested their importance for climate interactions (e.g., Adebyi et al., 2023).

Climate modelers are constantly looking for multiple independent lines of evidence to verify their models, and in situ surface concentration data presents a valuable source of information about aerosols often near human society. Understanding spatial variability in aerosols, and the composition of those aerosols is key to understanding how aerosols in different regions have evolved in the past, and how they will evolve in the future. Some regions are dominated by fossil fuel derived aerosols, which may have peaked in magnitude, even as greenhouse gas concentrations continue to increase, while in other regions aerosols are driven by agriculture or by natural aerosols (Bauer et al., 2016; Turnock et al., 2020; Kok et al., 2023). In addition, different aerosol species have different impacts on climate: for example, knowing whether aerosols are scattering or absorbing changes the sign of the interaction (Li et al, 2022). Some aerosols also serve as better cloud or ice nuclei than others, while biogeochemical impacts are very sensitive to composition (Mahowald et al., 2011). Knowing even the order of magnitude in regions with aerosols (e.g., contrasting 0.1 to 0.001) is important for aerosol-cloud interactions that can be non-linear especially at low aerosol levels (Carslaw et al., 2013). Having surface concentration observational dataset with large spatial coverage based on independent data can be valuable for aerosol model comparisons, especially for models with a global domain. We focus most of this paper on the spatial distribution of climatological mean, as that is easily obtained from models, and the most important variable for many climate impacts like radiative effects or aerosol-cloud interactions, except for aerosols dispersed by large infrequent events (e.g., Clark et al., 2015; Fasullo et al., 2022). Since aerosols are thought to cause between 2 and 10

Deleted: 2020

million deaths per year (Landrigan et al., 2018; Lelieveld et al., 2019; Murray et al., 2020; Vohra et al., 2021), understanding and being able to model correctly the annual mean aerosol concentrations in the surface layer is vital and thus this dataset provides valuable information towards understanding aerosol contributions to mortality. Nonetheless, there have been trends in emissions especially of anthropogenic aerosols over the last 40 years (Quaas et al., 2022; Bauer et al., 2022), and we consider these as well.

For this study we focus on the following: a) identifying and compiling available $PM_{2.5}$ and PM_{10} aerosol data, including aerosol composition, into a new publicly available database (AERO-MAP) for the modelling community across as much of the globe as possible; b) presenting a methodology to compare the spatial distribution of the climatological mean observations to the aerosols in an Earth system model; c) briefly present some temporal trends and comparisons available from this dataset and d) identifying the measurement and modelling gaps from this comparison. While our model evaluation is not exhaustive, we hope that the convenience of this observational compilation enables an expanding and more thorough set of comparisons by future investigators.

2 Description of Methods

2.1 Observational data

PM observations are made by multiple networks, or during specific field campaigns, and for different size cut-offs, with and without a description of chemical composition. Datasets were identified by advertising at international meetings (Wiedinmyer et al., 2018), searching the literature, contacting principal investigators and accessing publicly available datasets. As expected, most of the observations are over North America or Europe, with much of the rest of the land areas and most of the ocean much more poorly observed (Fig. 1; Supplemental dataset 1). For this study, we include both $PM_{2.5}$ and PM_{10} daily (or multiple day averages) data sets that were made available by the investigators or are available from public web sites (Fig. 1; supplemental dataset 1). Some measurement sites measure $PM_{2.5}$ and coarse ($PM_{2.5}$ to PM_{10}) aerosols. For those sites, we convert the latter to PM_{10} for comparison. Some measurement sites have only a few observations of composition or mass, while others have multiple years: we included less complete datasets at sites in regions with limited data (e.g., field data: these are identified as station datasets with less than one year of data in supplemental datasets). In some poorly measured regions, we include total suspended particles (TSP) datasets (information on the size fraction measured is in the Supplemental dataset). The time period for different datasets is included in the supplemental dataset 1.

Detailed studies have shown that PM_{10} and $PM_{2.5}$ samplers can differ in the sharpness of their size cut-off (Hand et al., 2019). As an example, comparisons between data from the U.S. Environmental Protection Agency (EPA) Federal Reference Method sites and data from the Interagency Monitoring of Protected Visual Environments (IMPROVE) network show that

the coarse matter from collocated sites in both networks were offset by 28% (Hand et al., 2019). There was a bias when data were compared (slope of 0.9), but the correlation coefficient was high (0.9) suggesting overall a good agreement. We focus here on surface station measurements of PM_{10} and $PM_{2.5}$, since our model and most models only consider mass up to PM_{10}. For that reason, our model deposition is not directly comparable to observational bulk/total atmospheric deposition since larger particles may dominate the deposition close to the source areas (Kok et al., 2017; Mahowald et al., 2014; Neff et al., 2013). Measuring absolute dry and wet deposition rates is also technically more challenging (especially dry deposition, since the particles can be re-entrained into the atmosphere), but worthwhile (Heimburger et al., 2012; Prospero et al., 1996). In regions with little data (e.g., outside of North America and Europe) we include measurements of total suspended particulates (TSP) with the PM_{10}, because of the lack of size-resolved data. Data from the Japanese air quality network use a different inlet for the PM10 cutoff as well, which will include a slightly larger size fraction (https://tenbou.nies.go.jp/download/).

In addition to particulate matter in the PM_{10} and $PM_{2.5}$ size fractions, we also compile the following observations to compare to the model: black carbon (BC), elemental carbon (EC), organic carbon (OC) (or particulate organic material, OM, that is here considered to be 1.8 x OC in mass; Aiken et al., 2008; Font et al., 2024; Turpin & Lim, 2001), sulfate, nitrate, aluminum, sodium and chloride. To include both BC (based on light absorption measurements) and EC (based on thermal oxidation induced combustion measurements) data are also a source of uncertainty, both are proxies of the soot combustion particles since they are based on different measurements techniques, and there is no accepted equivalence between them (Mbengue et al., 2021). Details on the measurement methods and types are shown in Table 1 and vary between measurements of fine and coarse, versus $PM_{2.5}$ and PM_{10}, with different measurement types for elemental and chemical analysis (Table 1). Details on how the model is compared to data for different elements are in Section 2.3.

Formatted: Justified, Space Before: 0 pt

Formatted: Font color: Black

For this paper, we focus on the climatological means for 1986-2023 and decadal means for 2010-2019. The first period is chosen as the full duration of the individual data sets comprising the compilation are available; the second is chosen to recognize decadal variations in anthropogenic emission within the longer period and isolate a particular decade when data is most plentiful. In addition, annual means for each year the data is available is also calculated, as well as the climatological monthly means. The temporal means are calculated for all values at each station that are above the detection limit and reported here. At some stations or times, concentrations can be below the detection limit, and excluding these data or time periods could bias our average values. We focus on the stations that have more than 50% of the data above the detection limit, and exclude other sites. For those included stations, if the values were reported as below the detection limit, we include in the average one-third of the minimum detection limit. The reported detection limits should bound the upper limit of aerosol mass and allow us to include sites, whose observations were otherwise too low to include, while reducing the potential biasing of our compilation towards higher values (Supplemental dataset 1).

Our goal is to create easy-to-use datasets for model-data comparisons. Included in this dataset are several files with different levels of description and analysis. One file provides traceability information, including a detailed citation, type and number

of measurements included, as well as time period, climatological and decadal (2010-2019) means and standard deviations for each time period (Supplemental dataset 1). For each station dataset included in the database, there will be one line in this file. This means that for some stations (for example K-puszta), there are multiple lines in the supplemental file indicating the two different time periods where measurements were made as well as the two sizes that are measured during each time period. For each station dataset, there are latitude, longitudes, annual mean values, number of observations, year extent of the observations, standard deviations, etc, as well as the citation and where to obtain the data. There are also several netcdf files available at https://zenodo.org/records/11391232 for this dataset. The most useful is likely to be the Allobservation.AEROMAP.nc file, which contains the same quantitative data for each station dataset as the supplement, except that the data is processed to be only $PM_{2.5}$ and PM_{10} (with some TSP data in places with little data, as discussed above). That means $PM_{2.5}$ and coarse aerosol mass are added together if the station datasets are collocated to create a PM10 dataset (e.g., see Table 1). In addition, this file contains climatological monthly means, and annual means for each year for each station dataset, so that temporal information is also easily available. Another file includes the climatological mean observations averaged up to a 2°×2° grid that is used for plotting the figures shown in the paper (Allobservation.AEROMAP.2x2.nc). As indicated in the data availability, only the time-means are available and the underlying data for some datasets cannot be openly published, but please contact the authors (identified by the citation) if other time periods are desired.

The location of each site is as accurate as possible and for most sites is accurate to less than 1km. Some datasets provided more limited information and those locations are accurate only to less than 10km (data downloaded from the following air quality networks: Mexico City: http://www.aire.cdmx.gob.mx/default.php?opc=%27aKBh%27, South Africa https://saaqis.environment.gov.za/, India: https://app.cpcbccr.com/ccr/#/caaqm-dashboard-all/caaqm-landing/data and Chile: https://sinca.mma.gob.cl/index.php/).

2.2 Model description

Most of the simulations of aerosol particles were conducted using the aerosol parameterizations within the Community Atmosphere Model, version 6 (CAM6), the atmospheric component of the Community Earth System Model (CESM) developed at the National Center for Atmospheric Research (NCAR) (Hurrell et al., 2013; Scanza et al., 2015; Liu et al., 2012). The aerosol module in this version is closely related to the module used in the Energy Exascale Earth System Model (Golaz et al., 2019; Caldwell et al., 2019). Simulations were conducted at approximately 1°×1° horizontal resolution with 56 vertical layers for four years, with the last three years (2013-2015) used for the analysis (Computational and Information Systems Laboratory, 2019). The model simulates three-dimensional transport and wet and dry deposition for gases and particles by nudging toward MERRA2 winds (Gelaro et al., 2017).

The model included prognostic dust, sea salts, BC, OM, and sulfate particles in the default version, using a modal scheme based on monthly mean emissions for the year 2010 (Liu et al., 2012, 2016; Li et al., 2021). The model includes separate primary and secondary organic species which are both emitted directly, but the primary organic and black carbon aerosols are allowed to age in the model from hydrophobic to hydroscopic, and their optical properties also change (Liu et al., 2016). The coarse mode is included for sulfate, dust and sea salts. For this study, the coarse size mode (mode 3) was returned to the size parameters used in the previous version of the model: CAM5 (geometric standard deviation of 1.8) to better simulate coarse mode particles, and improve the dry deposition scheme and optics used in the model for simulating coarse mode particles like dust as described in Li et al. (2022).

Desert dust is entrained into the atmosphere in dry, sparsely vegetated regions subject to strong winds. We use the Dust Entrainment and Deposition scheme (Zender et al., 2003) with the emitted size distribution given by the updated Brittle Fragmentation Theory (Kok et al., 2014b, a) with improved incorporation of aspherical particles for optics and deposition (Li et al., 2022; Huang et al., 2021; Kok et al., 2017). Anthropogenic emissions of sulfate, OM, and BC follow the Climate Model Intercomparison Project 6 historical data for 2010 (Gidden et al., 2019). Emissions and mean concentrations for each of these constituents are included in Table 2.

2.2.1 Modelling of additional aerosol sources and types

Ammonium nitrate aerosol particles are not included in the standard CAM6, but are thought to be important for aerosol optical depth and surface concentrations (Paulot et al., 2016; Adams et al., 1999; Thornhill et al., 2021; Bauer et al., 2007, 2016), so they are included in this study. Nitrate can also react with dust particles, for example, but that is ignored in this study (Dentener et al., 1996). Ammonium nitrate particles require tropospheric chemistry interactions because the nitrogen-containing particles are both a source and a sink for gaseous nitrogen species, which are key elements of tropospheric photochemistry and the particles are in chemical equilibrium with the gas phase (e.g., Nenes et al., 2021; Baker et al., 2021; Bauer et al., 2007; 2016), so simulations using the CAM-CHEM model with tropospheric photochemistry are used covering the same time period (Vira et al., 2022). Simulations with chemistry were conducted at 2°×2° resolution and are linearly interpolated to 1°×1° resolution used for the other modelled particles. Sulfate in the CAM6 is assumed to be in the form of ammonium sulfate and the nitrate is assumed to be in the form of ammonium nitrate for these studies, so as a rough approximation only the model ammonium nitrate is compared to the observed nitrogenous aerosol optical depth. Ammonium nitrate is assumed to only form when there is surplus ammonium (and nitrate) after the ammonium sulfate is formed. While aerosol amounts are simulated, ammonium nitrate aerosol optical depth is not calculated within the model but offline. The model does calculate sulfate aerosol optical depth, which has a roughly similar increase in size with humidity compared to nitrates, and similar optical properties as long as the nitrates and sulfates are in similar size fractions (Paulot et al., 2016; Bellouin et al., 2020). Therefore the aerosol optical depth from ammonium nitrate (per unit mass) is assumed to be proportional to the sulfate aerosol optical depth per unit mass in each grid box at each time interval. Detailed

Deleted: 2020

comparison of the nitrate and ammonia particles, and other species was conducted in Vira et al. (2022). Overall, the model can simulate some of the spatial distribution, but overestimates the nitrate aerosol amounts (Vira et al. 2022).

2.3 Model-observation comparison methodology

Comparisons of the observations to model concentrations were done using BC, OC, SO_4^{2-}, Al, NO_3^-, NH_4^+, and Na composition measurements. Some of these elements/compounds map directly onto model constituents (BC, OC, SO_4^{2-}, NO_3^-, and NH_4^+), while others serve as proxies for modelled constituents (Al for dust, Na for sea salts, S for sulfate, etc.). We summarize the relationships used to obtain the values from the model (Table S1), and what observations are combined to include as much information as possible from the observations. (Table S2). We use non-sea-salt sulfate in ocean regions for estimating sulfate. We use the mean Na amounts in sea salt (31%; Schlesinger, 1997) to characterize the Na amounts and include the soluble Na measurements as well (Na^+) if available when Na measurements are not available. Note that Cl cannot be used to evaluate sea salts as the Cl is degassed from aerosols, primarily due to sulfate interactions (e.g.,Pio and Lopes, 1998). Some observing networks like IMPROVE use a composite of elements to deduce dust amounts (e.g., Hand et al., 2017). We do not choose to do this for two reasons: 1) at some sites not all the elements are available, and 2) because these elements derive not only from desert dust, but also from industrial sources. Note that model values come from the midpoint of the bottom level of the model (~30 m) while the observations are usually taken at 2 or 10 m high. There are several sources of measurement differences between different networks as well as between model and observations. Modelled values of PM content, which assume dry particles, are used here, while gravimetric measurements in some networks are equilibrated at 50% relative humidity, thus 5-25% of the mass of measured PM can be water (Prank et al., 2016; Burgos et al., 2020). In addition, comparisons of coarse mode composition at co-located sites in the US show that the inlet type can cause ~30% difference in measured mass (Hand et al., 2017). We include these differences in our error estimate in Section 3.2.

For the most part, we use model output for which there is a one- to-one relationship with what is being measured (BC, sulfate, etc). However, for dust this is not straightforward, as dust is composed of multiple elements. Here we use Al as a proxy for dust, as it is relatively constant (~7%) in dust (as opposed to Ca, which varies highly, or Fe which varies moderately) (Zhang et al., 2015). Al sources are primarily from dust (Mahowald et al., 2018). Assumptions about the model composition and how they are compared to observations are summarized in Table S1. For example, OM is assumed to be 1.8 times OC if OC measurements are available but not OM measurements. Different ratios of OM to OC appear in the literature, but 1.8 appears to be the best average for a mixture of aged and fresh plumes (Aiken et al., 2008; Font et al., 2024; Turpin & Lim, 2001).

Harmonizing models with different types of measurements is critical, and yet a difficult task (Huang et al., 2021). Models operate with the geometric or aerodynamic particle diameter, whereas in practise the measurements are done with a variety

of particle equivalent diameter, e.g., optical, volume equivalent, projected-area equivalent or aerodynamic diameter, depending on the instrument used (Hinds, 1999; Reid et al., 2003; Rodríguez et al., 2012). In the inlets of the samplers used for the mass-measurements and collection of $PM_{2.5}$ and PM_{10} particles for subsequent chemical analysis, such size cut-off at 2.5 µm and 10 µm is defined in terms of aerodynamic diameter (i.e., Stokes diameter (involving size and shape) weighed by the square root of the particle density; Hinds, 1999). The sharpness of the cut-off of such inlets influences the $PM_{2.5}$ and PM_{10} mass concentration (Hand et al., 2019; Wilson et al., 2002). The PM_{10} size cut-off aerodynamic diameter is equivalent to $PM_{6.3}$ geometric diameter for spherical dust particles (Hinds, 1999; Rodríguez et al., 2012) and to $PM_{6.9}$ in the case of dust elliptical particles (Huang et al., 2021). Similarly, for dust, $PM_{2.5}$ (aerodynamic diameter) is equivalent to $PM_{1.6}$ (geometric diameter). These differences are important to keep in mind, but the information is not available for all networks, so we include the size cutoff as an uncertainty in the model/data comparisons as described in Section 3.2.

For ease of viewing the data in this paper in the densely sampled regions as well as to compare model output to more representative spatial scales, observational records from different sites were combined into a mean within a grid cell that is two times the model resolution, or approximately 2° × 2°. This process averages the observations over a spatial scale appropriate for comparison with the chemistry model (Schutgens et al., 2016). We provide both the climatological annual average data at each site as well as the 2° × 2° grid-averaged data (with the modelled data at doi: 10.5281/zenodo.10459654, Mahowald et al., 2024). In this dataset, the number of station datasets included in the average is included (stations) and the number of observations add up across all the station datasets included.

Notice that we include both urban regions and rural or remote sites into the same dataset. Some of the original metadata did not include the resolution of the location to better than 0.1 degrees, so that the coordinates of the locations here provided with the gridded data should not be used for finer resolution studies. Because of the importance and size of megacities, which cross multiple grid boxes, as well as the difficulty in separating urban vs. rural sites, we include urban and rural air quality data in the same dataset, and previous studies show the expected differences between urban and rural concentrations and trends (e.g., Hand et al., 2019).

Statistical comparison across the globe and different regions are included in the supplemental tables. These include model and observational averages, Kendall correlation coefficients (rank correlations), linear regression slopes and uncertainties, as well as root mean squared differences. We also include the fraction of the model/data comparison which is outside the error bounds defined in Section 3.2. These results are included in tables in the supplement and referred to in the text as appropriate.

There are multiple sources of uncertainties in the observations used in the model-data comparisons of PM concentrations at the global model grid scale: errors in the measurements, differences in measurement methods, variability in aerosol concentrations during events versus background conditions, spatial variability within a model grid box, and interannual

variability. To assess the size of these uncertainties, we look at the normalized standard deviation (defined as the standard deviation over the mean) due to these factors in the observations for within year, within a 2°×2° degree grid and for interannual variability. To evaluate within year and between year variability, we focus on stations that have more than 10 years of data. To evaluate spatial variability within grid boxes, we use grid boxes that have more than 10 stations within them. Notice that these grid boxes are likely to lie close to cities and fossil fuel source regions, because the measurement network is more dense there, perhaps exaggerating the importance of spatial variability. In addition, different measurement methods (dry vs. moist aerosol mass, different inlet geometries) complicate the comparison of data. We assume here a measurement method uncertainty of 30% that is on the high side of previous studies (Prank et al., 2016; Burgos et al., 2020; Hand et al., 2017). Many of the measurements also include an assessment of their uncertainty or of the minimum detected limit: we use that to assess the average uncertainty of individual measurements (measurement errors).

2.4 Temporal aerosol variability

While the main goal of this study is to highlight and compile in one place the many surface concentration observational datasets available to compare against models, and we focus on the climatological annual mean, the datasets also include temporal variability. Annual means, standard deviations and the number of observations for each station for each year are included to allow for analysis of interannual variability or trends. In addition, the climatological monthly mean, standard deviation and number of observations is also available in order to assess the seasonal cycle. These values are all available in the Allobservvations.AEROMAP.nc file available at doi: 10.5281/zenodo.10459654.

To illustrate the included data, the trends in the $PM_{2.5}$ and PM_{10} aerosols are calculated over 2000-2023, over 8 different regions: North America, South America, Africa, Europe and Asia. Only data after 2000 is included because there is much more data after 2000 than prior (see Section 3.1). All station datasets with more than 8 years of data are included in the calculation. In order to decrease the bias and uncertainty due to the large temporal and spatial variability (similar to Hand et al., 2024), we divide the annual mean at each station by the climatological annual mean over the two time periods, and average this with the other stations within the region. We then use a Theil regression which calculates the slopes excluding different datapoints and takes the median slope to reduce dependence on outliers (Hand et al., 2024). Median, 33 and 66 percentile slopes are calculated to show the median and 1-sigma uncertainties for each region.

The seasonal cycle of aerosols can provide important information about the source strength and variability, as well as meteorological constraints (Gui et al., 2021; Rasch et al., 2000). To illustrate the value of the evaluation of the seasonal cycle in models, we calculate the climatological monthly mean in the observations and model and compare the correlation of these values, as well as the standard deviation of the 12 month means in the model versus the observations. This method

allows us to separately evaluate the seasonal cycle from the spatial distribution. The correlation is only calculated at stations where the seasonal cycle is large enough: in math terms our criteria is where the observed standard deviation across months is larger than half of the average observed within month variability.

3 Results

3.1 AEROMAP observational data set

First, we assessed the amount of data and the number of station datasets within each ~ 2° × 2° gridded area (Fig. 1). The observational dataset provides coverage predominately over North America and Europe for $PM_{2.5}$ and PM_{10}, as noted by previous studies (e.g., Szopa et al., 2021), but in addition we provide here a synthesis of more air quality data in other regions, especially Asia (Fig. 1). This compilation data set comprises most of the individual observations (at daily or longer time periods) of total $PM_{2.5}$ (Fig. 1a, 1e: blue bars) and most of the observing stations (Fig. 1e and blue line). Approximately 15,000 stations and over 20 million observations are included in this compilation.

Notice that there are two to three orders of magnitude more individual observations for the total mass (PM) of particles compared to information about the composition of particles (Fig. 1e), which is shown also by contrasting the spatial distribution of measurements between $PM_{2.5}$ and measured amounts of OM (Fig. 1a versus 1b), as well as a large difference between the number of station datasets measuring the total mass versus the speciated aerosol particles like OM (Fig. 1c versus 1d). While this dataset presents a huge increase in the amount of data available to the aerosol modelling community (for example, an eight-fold increase compared to the datasets included in Reddington et al., 2017), still the dominant proportion of the total $PM_{2.5}$ or PM_{10} data are clustered over a few industrialized land regions, and there is little composition information over most of the globe (Fig. 1).

3.2 Uncertainties in model-data comparisons

Our goal in this study was to identify observational datasets and compile them together into one easy-to-use dataset for climate and air quality modelers. To do that we collect all available datasets, prioritizing long-term stations with composition data, but in regions with few measurements, we include only PM data, or data collected during field campaigns, which may last only a month or two. Previous studies have shown that even a 1-day average aerosol measurements, carried out on cruises, can constrain aerosol concentrations within a order of magnitude (1-sigma) for phosphorus in dust, which varies spatially by 4 orders of magnitude (Mahowald et al., 2008). Other studies have highlighted that even for particles that have highly variable sources, such as dust, that only a few months of observations are enough to characterize the mean and standard deviation in most places across the globe (Smith et al., 2017). However, that study highlighted that for places where dust events do not occur every year or occur with varying number, like near South America, several years are required to characterize the mean (Smith et al., 2017).

Uncertainties in the observation-model comparisons can include both uncertainties in the observations, as well as interannual variability in both the model and observations that are temporally averaged. Uncertainties used in the comparisons of aerosols at the global model grid scale come from multiple sources: errors in the measurements, differences in measurement methods, variability in aerosol concentrations during events versus background conditions, spatial variability within a model grid box, and interannual variability, as discussed in Section 2.3. To assess the size of the variability contribution to the uncertainties, we look at the normalized standard deviation (defined as the standard deviation over the mean) due to these factors in the observations for within year, within grid and interannual variability. Nonetheless, our estimate of spatial variability will underestimate the true value in the absence of sufficient spatial coverage. In addition, different measurement methods (dry vs. moist aerosol mass, different inlet geometries) complicate the comparison of data (Section 2.3 discusses sources of uncertainties in more detail). We assume here a measurement method uncertainty of 30% that is on the high side used in previous studies (Prank et al., 2016; Burgos et al., 2020; Hand et al., 2017). Many of the measurements also include an assessment of their uncertainty: we use that to assess the average uncertainty of individual measurements due to measurement errors.

We focus on the uncertainties in the PM2.5 measurements first. The largest uncertainties are associated with within-year variability (0.53) (Figure 1f; Table S3). This is because most of the aerosol mass can sometimes come in a few pollution events. Uncertainty due to combining different measurement methods (0.3) and from spatial variability within a model grid cell (0.24) are also important (Figure 1g). Both interannual variability (0.18) and measurement errors (0.08) are smaller but important contributions to uncertainty. The importance of within year variability (which is similar to within month variability: see Table S4) is consistent with studies showing that in most places, there are a few pollution events carrying much of the mass, and with otherwise much lower background concentrations (Luo et al., 2003; Fiore et al., 2022). Obviously, interannual variability is important for secular trends (Gupta et al., 2022; Watson-Parris et al., 2020; Mahowald et al, 2010), but in this compilation the interannual variability is much smaller than the 2-4 orders of magnitude of the spatial variability across the globe, and thus can be neglected for understanding global spatial distributions (Figure 1f).

These sources of uncertainties occur simultaneously and if we sum them assuming orthogonality, we obtain an normalized uncertainty of ~0.68 (Table S3), which was interpreted as meaning that model/data comparisons within a factor or three should be considered adequate. To ease the visual evaluation of the comparison we show in the following scatter plots both the 1:1 line and the range within a factor of 3. We discuss an example of uncertainties in more detail in Section 3.3. Notice that if we use the same metric (normalized standard deviation) to evaluate the variability across the climatological concentrations measured in the observations at different locations (Figure 3a) or across the grid averages in the model we obtain 1.0 and 2.2, respectively, much larger than the uncertainties (0.6): there is much more variability across different grid boxes (4-5 orders of magnitude: see Figure 2d) than across different years (up to 50% normalized standard deviation; Figure 2f). As expected, the model contains more spatial variability than the observations, as the model reports concentrations in very high (North Africa)

and very low (Antarctica) aerosol regions where we have no data, although where we have data, the model simulates a similar range (Figure 3a). For composition measurements, there is larger uncertainty in some individual species (e.g., BC and Al) than for PM. However there are many fewer composition observations (Table S3). Since the statistics of the uncertainty calculations are likely more robust with the bulk PM measurements, as there are an order of magnitude more data for the bulk PM data, we use the uncertainty estimate derived for PM for all of the composition data in this paper.

There is time variation in how much data is available for both $PM_{2.5}$ and PM_{10} data (Figure 2a and 2b), with the most data available between 2010 and 2020. Different regions have slightly different trends in the amount of data (Figure 2). For much of this paper we will discuss global and regional comparisons, and the regions we focus on are Africa, Asia, Australia, Europe, North America, South America and the high latitudes (Figure 2c).

Trends in aerosols are an important scientific question, although for most of this paper we use the climatological annual mean. What if there were strong trends in the aerosols; would that lead to differences between our climatological means and what we expect for some decades? In order to assess this, we look at the individual annual means for each station with more than 8 years of data and see if the individual annual mean is ever outside of the 3x uncertainty calculated here. Out of the 13320 station datasets for $PM_{2.5}$ or PM_{10} which have more than 8 years of data, only 175 (1.3%) have an annual average outside the uncertainty estimated here. Of those with a value outside the uncertainty, only 10 (<0.01%) have a statistically significant trend. This suggests that for the temporal interval we have chosen for the climatology, long term trends are not a significant source of differences in the spatial climatological dataset presented here. Nonetheless, we acknowledge that in regions where aerosol emissions increase and then decrease over our multi-decadal observational record (e.g. China), our test for trends will not reveal where the climatology over the full period is less representative of individual decades. We also supply in the compiled dataset a decadal mean for the time period of 2010-2019, which is made publicly available. A comparison of the climatological mean versus the decadal mean for the $PM_{2.5}$ and PM_{10} concentrations show that for almost all locations, there is a small difference between the two values, and they lie on a one-to-one line (Figure 2d and 2e; Table S4). There are a few station datasets (<5%) which have a difference between the climatological mean and the decadal mean that is larger than 20%, and very few (<0.05%) have a difference which is larger than the uncertainties described in this section (factor of 3; Table S4). The biggest difference between the climatological and decadal average values is the number of station datasets and observations and thus spatial coverage: we lose between 20% and 100% of the station datasets, depending on the size and composition, when we use the decadal means (Table S5). This is because even though this is the most observed decade, still some datasets are outside this time period. In order to emphasize the spatial distribution of the datasets, and because the climatological values are so similar to the decadal means, we will show just the climatological values in the next few sections, although both are available (Supplemental dataset 1 and https://zenodo.org/records/10459654).

3.3 $PM_{2.5}$ model-data comparison

Modelled concentrations of $PM_{2.5}$ are more often compared against observations than for PM_{10} or other size fractions, and comprise an important portion of the particulate matter associated with human activities. Therefore, we describe first the observational synthesis and comparison to model results for $PM_{2.5}$. Because the high number of observations in some parts of the world would make the figures unreadable, the observations are gridded onto an approximately 2°×2° grid for comparisons with the model, although individual data points are still difficult to read (Fig. 3a). The maps illustrate where the observational comparison in the scatter plot is made, and focused maps of each major region are available in the supplement (Figure S1) as well as global and regional statistics (Table S5). As expected, in the model the highest concentrations are over the desert dust regions, such as North Africa, and over heavily industrialized regions in Asia. For the heavily industrialized regions in Asia, these high values are consistent with the observations, but the regions in North Africa with the highest modelled values do not have similar observational validation for high concentration values due to a lack of data (Fig. 3a).

Overall, the model is able to simulate much of the spatial variability in $PM_{2.5}$ over two orders of magnitude (Fig. 3a and 3c), however there is a tendency to overestimate in the $PM_{2.5}$ over India and China (Fig. 3b), although the mean over all the regions is within the 3x uncertainty (Fig. 3c: bold symbols). In addition, there are some observations (globally ~6% Table S6) that are outside the 3x uncertainty estimates (Figure 3c and 3d). The scatterplots show the comparisons of the model to the observations using the gridded data (Fig. 3c) and all original data (Fig. 3d), and the correlation coefficients are similar (0.60 vs. 0.67 in Fig 3c and Fig 3d, respectively). It is interesting that the correlation using the ungridded data (Fig 3d) is slightly higher, perhaps because the model does better in regions with more data, although this is not a statistically significant result. The averages over different regions show that on average, the model is simulating the regions within the uncertainty (bold black symbols in Fig 3d; Table S5).

As an example of the source of the uncertainties discussed in Section 3.2, we discuss the differences over India and China in the Asia region in more detail. It seems likely that at least some of these errors are due to an overestimate in the emission databases, since satellite based remote sensing has suggested that models overestimate in SO_2 over China (Luo et al., 2020). In addition, these discrepancies could be due to an error in the aerosol transport or chemical modelling, such as incorrect reaction rates or deposition rates or the alternatively due to differences in the time period: the observations are more recent while the assumptions for the emissions are for the year 2010 (Quass et al., 2021). The comparison using the decadal averages (2010-2019) show similar biases (Figure S2) as expected since the decadal averages are so similar to the climatological averages (Figure 2d), which suggests the time differences may not be the most important factor. In addition, notice that once averaged over the 2°×2° grids more observations are within a factor of 3, our uncertainty bound (contrast 3c and 3d). However, there could also be methodological and analytical differences due to which group or network did the observations or the exact locations of the different monitors. Much of the data in those regions are not usually included in routinely used previous compilations of data (e.g., Reddington et al., 2017), so the fact that previous model studies have not

Deleted: or

been able to assess emission datasets in these regions could also partially explain this discrepancy. Comparison between different observations in some cities (Fig. 4) shows that in these grid boxes there can be very large differences (~factor of 3) between the annually averaged values reported at nearby stations within 1° distance radially. Notice that the AirNow measurements (**https://www.airnow.gov/international/us-embassies-and-consulates/** on the US embassies) tend to be higher than those reported from government air quality networks. The sites compared are in large cities and thus are likely to have strong local sources and intense gradients in pollutants. For now, we keep in mind this large difference, but continue to use the observations. As indicated below, in these regions we do not have measurements of composition so we do not know which constituents are poorly simulated in our emissions or transport modelling. More statistics describing the model data comparisons are shown in Table S5.

Next, we consider the composition of the $PM_{2.5}$ aerosol in the model versus the observations. The model simulates high and low values of sulfate observed with a correlation coefficient of 0.64. Sulfate particles concentration are on the high side in the model in several regions: more so in North America, Africa, but less so for Europe and other regions (Fig. 5a and b; Figure S3; Table S5), although all of the regional means are within the 3x uncertainty (bold symbols in Fig. 5b). Previous studies have compared SO_4^{2-} aerosol observations to some model simulations and have not noted this bias (e.g., Barrie et al., 2001; Aas et al., 2019) but this bias was seen in this model and attributed to the simple chemistry included in the model (Liu et al., 2012; Yang et al., 2018). About 18% of the climatological mean model values are outside the 3x uncertainty, and a larger fraction is outside for Africa, Australia and South America, where there is less data (Table S5).

BC comparisons suggest the model results are roughly able (r=0.63, within the 3x uncertainty) to capture the spatial dynamics of this aerosol across more than 2 orders of magnitude, although in some regions model values are on the low side (Europe and Asia) (Fig. 5c and d; Fig. S4; Table S5). This is similar to previous model intercomparisons (Koch et al., 2009; Bond et al., 2004, 2013; Liu et al., 2012, 2016). About 18% of the model values are outside the uncertainty bounds, and many of these values come from Europe, where 36% of the values in Europe are outside the uncertainty bounds (Table S5). Simulations of OM in the default model (Fig. 5e) suggest that the model is within the uncertainty of most of the data, and the regional averages are close to the 1:1 line (Fig. 5f). Correctly modelling organic material is very difficult both due to the sparsity of data for comparison, as well as the importance of both primary and secondary OM in PM (Heald et al., 2010; Kanakidou et al., 2005; Olson et al., 1997; Tsigaridis et al., 2014), and previous studies with this model have noted an overestimate in comparison with surface observations (Liu et al., 2012).

As a proxy for sea salts, we use the elemental data of the major component, Na, and we see the highest values over oceans and lower values over land, as expected and seen in the observations (Fig. 5g). Although most of the data is within the uncertainties (30% is outside the uncertainties; Table S5), the model tends to be too high at low Na and too low at high Na in North America, where much of the data are available (Fig. 5g and h; also seen in slopes Table S5), which has been seen

previously with this model (Liu et al., 2012). Notice that we do not include industrial emissions of Na, but the concentrations far inland include some Na, suggesting land-based natural or industrial sources. As a proxy for dust, we use Al amounts (Fig. 5i and j), which globally and over dust regions are dominated by dust, although there are few observational datasets in high dust regions. The comparisons suggest the model is able to simulate dust (correlation coefficient=0.5, Table S5) across 4 orders of magnitude, similar to previous studies (Liu et al., 2012; Albani et al., 2014a; Li et al., 2022; Huneeus et al., 2011) although there is a tendency for a high bias in the models over low dust regions and a low bias in high dust regions, similar to sea salts (Fig. 5i and 5j; also seen in the slopes in Table S5). One reason for this overestimate of $PM_{2.5}$ aerosol mass for constituents like sea salt and dust that are predominantly in the coarse mode, is that the coarse mode in this model has a wide enough standard deviation that it contributes significantly to the $PM_{2.5}$ size fraction (Ke et al., 2022; Li et al., in prep.). Better resolution of the coarse mode aerosol may be required to better simulate these aerosols (Ke et al., 2022; Li et al., in prep.).

Next, we consider the ammonium nitrate that requires complicated gas-aerosol phase equilibrium to correctly simulate (e.g., Bauer et al., 2007; Thornhill et al., 2021; Adams et al., 2001; Regayre et al., 2018; Seinfeld and Pandis, 2006; Wolff, 1984). To summarize these complicated interactions, because SO_4^{2-} is a stronger acid than NO_3^- in the atmosphere, the basic NH_4^+ is preferentially found with SO_4^{2-}. Thus NO_3^- particles will only form if there is sufficient NH_4^+ available. As described in the methods, to include these particles we added to the aerosol mass simulations from a different version of the same model which include chemistry (Vira et al., 2022), and a more process-based source of ammonia (Vira et al., 2020) since the default CESM2 version used here does not include chemistry. Note that even in the chemistry version of the model for CESM2 the complicated gas-aerosol phase thermodynamic equilibrium calculations are not included, which causes errors in the simulation of the amounts of nitrogen aerosol (e.g., Bauer et al., 2007; Thornhill et al., 2021; Adams et al., 2001; Regayre et al., 2018; Nenes et al., 2021). Thus while the NH_3 agricultural emission scheme used in this model is state-of-the-art, the lack of an adequate gas-aerosol phase separation may lead to biases as discussed in Vira et al. (2022). In addition, recent studies have suggested that emissions of NH4 from vehicles should be 1.8x higher than previously estimated (Toro et al., 2024), highlighting the difficulty of adequate emission datasets for nitrogenous aerosol precursors. NO_3^- particles compared against available observations show that over 2 orders of magnitude, the model results are able to simulate the spatial variability (correlation coefficient=0.55), but the model tends to overestimate the observations by about a factor of 2 (except in South America), similar to what was seen in Vira et al., (2022) (Fig. 5k, 5l, Table S5). The model surface concentration NO_3 values are with most of the data within the uncertainties (Fig. 5k and l; 46% are outside the uncertainty bounds in Table S6). The model and data distribution of NH_4^+ show the high values of NH_4^+ over agricultural regions especially (e.g., Vira et al., 2022), like the mid-western US or central Europe (Fig. 5m and Fig. 5n; correlation coefficient=0.52). The NH_4^+ in the simulation used here compares well to available observations across the different regions by having the regional averages being close to the 1:1 line (Fig. 5n), most of the individual model-data comparisons being within the uncertainties at most observational sites (Fig. 5m and n; and 16% of the data is outside the uncertainty bounds in Table S5).

How would these comparisons change if we used the decadal 2010-2019 averages instead of the climatological averages of the observations? As expected from the similarity between the observations averaged over these two time periods (Section 3.2; Table S4) the results do not substantially change (>20%) in most regions where there is a similar amount of data (Fig. S2a; Table S6). But for some regions and composition datasets, there is much less data (>25% less data), and in those cases, there can be large differences between using the decadal averages versus the climatological averages (Table S6). This suggests that using the climatological averages for our comparisons for $PM_{2.5}$ allows us to include more data and evaluate more regions, without including much bias, since interannual variability is a small source of uncertainty compared to other uncertainties (Table S4).

3.4 PM_{10} model-data comparison

PM_{10} was the first size selective standard for particulate air quality until more studies showed that smaller particles ($PM_{2.5}$ or PM_1) were more relevant for health impacts and $PM_{2.5}$ standards were added (e.g., https://www.epa.gov/pm-pollution/timeline-particulate-matter-pm-national-ambient-air-quality-standards-naaqs, accessed October 4, 2023). However, there are still many PM_{10} measurements routinely made (Fig 1d; Fig. 7a). The model is able to simulate PM_{10} concentrations across 2 orders of magnitude with some skill (correlation=0.55; Fig. 7a and 6b), as most of the data is within the uncertainties (Fig. 5a, b and c; 8% of data is outside the uncertainty Table S7). Gridding the data before comparing to the model results in a slightly higher correlation across space as including all data (0.55 vs. 0.72; Fig 5b vs. c). More statistical comparisons are shown in Table S7. The regional averages are all within the uncertainty bounds for all regions.

There are fewer comparisons with PM_{10} composition data available in the literature: usually only sea salts and dust are compared to observations that include the coarse mode (Gong et al., 2003; Ginoux et al., 2001; Albani et al., 2014b; Mahowald et al., 2006). Comparisons for SO_4^{2-} suggest that the model can estimate the distribution of the high and low concentrations (correlation coefficient=0.43), but tends to over predict PM_{10} values across most regions (Africa, Australia, Europe, North America and South America), as many observations are too high and outside the uncertainty bounds (Fig. 7a and b.; Table S7 indicates 48% of the model values are outside the uncertainty bounds). For BC, the PM_{10} simulation captures the range of values (correlation coefficient of 0.47), with most of the model results within the uncertainty bounds of the observations across all the regions (Fig. 7c and d; 16% outside the uncertainty bounds in Table S7). There is suggestion in the observations that there may be some fraction of BC in the coarse model, since there is more BC in PM_{10} than in $PM_{2.5}$, but in the simulations used here there is no mass in the coarse mode (compare Fig. 7c versus 5c). The model-data comparisons simulations for OM suggest a good spatial distribution of OM (correlation coefficient=0.43) and the modelled regional averages are similar to the observations. Again, the model does not simulate coarse mode OM currently, and does not include primary biogenics (Jaenicke, 1979; Mahowald et al., 2008), and yet can match the observations. The limited Na (indicating sea salt) data suggest the model can simulate the spatial distribution (correlation coefficient=0.49), but tends to overestimate and has many observations outside the error bound (Fig. 7g and h; 50% of the observations are outside the

uncertainty bounds in Table S7), as was seen previously (Liu et al., 2012). Most of the regional averages, however, are just on the line of the uncertainty bounds (Fig. 7h). Comparisons with Al (used here as a proxy for dust) show that the spatial variability is correlated between model and observations (correlation coefficient of 0.46), but the model overpredicts the concentrations in high dust regions and underestimates in low dust region (Fig 7i and 7j; 54% of the observations are outside the uncertainty bounds in Table S7). The largest overestimates are in Asia and Africa (Fig 7i and 7j). Dust models are compared against aerosol optical depth, deposition and surface concentrations and it is currently not possible to simulate all of these different types of measurements at the same time, consistent with previous studies with this model (Li et al., 2022; Kok et al., 2014b; Albani et al., 2014a; Matsui and Mahowald, 2017; Zhao et al., 2022), and indeed across most dust models (Huneeus et al., 2011).

The model simulations of NO_3^- suggest too high values in high NO_3^- areas, and too low in low NO_3^- regions, especially in the limited data for the South American region (Fig. 7k and l; Table S7 shows 69% of the data is outside the uncertainty bounds). NH_4^+ shows a slightly better comparison to the limited available data (Fig. 7m and n) as seen in Vira et al. (2022). As discussed earlier, the model does not include other forms of nitrate aerosols which may be important, such as the reaction of nitrate with dust aerosols (Wolff, 1984; Dentener et al., 1996; Xu and Penner, 2012).

If we compared instead to the decadal averages rather than the climatological averages, we would obtain similar results in many cases (Fig. 2b; Table S8), but being limited to decadal averages reduces substantially the amount of observations available for comparison. The few regions which lose less than 25% of the data sets when we temporally limit our comparison have similar statistics similar as in the $PM_{2.5}$ comparisons. Again, this suggests that using the climatological averages includes more regions in the comparisons without evidence that it increases bias, because of the small amount of interannual variability in this data set (Section 3.2).

3.5 Temporal variability

This paper emphasizes the expanded spatial coverage in this compiled dataset with the spatial comparisons in Section 3.2-3.5, but the dataset also contains temporal variability as well. To illustrate the type of temporal data within this dataset we present briefly some common metrics. First, we consider what trends this data suggests in the surface concentrations for $PM_{2.5}$ and PM_{10}. Because most of this data comes from after 2000 (Figure 2a and 2b), we focus on the trends between 2000-2023. We also average by region in order to obtain a large-scale trend in surface concentrations (see details of methods in Section 2.5). Overall, the observations suggest that there is a statistically significant (1-sigma) decrease in aerosols over this time period of about 1% per year for $PM_{2.5}$ for North America, South America, Africa, and Europe, but not a statistically significant change over Asia and Australia (Figure 8a). These downward trends are similar to those seen in other studies including North America and Europe (Hand et al., 2024; Gui et al., 2021; Gupta et al., 2020; Mortier et al., 2020) and South America (Mortier et al., 2020), and the more ambivalent signals over Asia and Australia have also been seen (Gui et al.,

2021; Gupta et al., 2020; Mortier et al., 2020). For PM10, there are different trends: North America and Europe have a statistically significant downward trend of about 1%/year while Asia has a larger downward trend of about 3% per year, but the error bar overlaps the 0 line for the south American, Africa and Australian regions, indicating that those regions do not have statistically significant downward trends. There are no other studies we know of that looked at trends in PM10 specifically. Note that we do not compare against the model results here, as our example model simulation does not include emission trends, but these datasets include each station's annual average so that more detailed comparisons could be conducted. In addition, apparently these trends do occur long enough to cause a large bias in the climatology (Section 3.2)

Next, we use the climatological monthly mean data for $PM_{2.5}$ and PM_{10} and compare against the model to see how well the models simulate the seasonal cycle. There are many ways to evaluate the seasonality in the literature (Gleckler et al., 2008; Henriksson et al., 2011; Huneeus et al., 2011; Rasch et al., 2000). We chose one way here, but this dataset could be used in other ways as well. The models can simulate the timing of the seasonal cycle well across most regions as seen in correlations between the climatological monthly mean in the model and observation (Figure 9a and 9b), but there are several regions where the model is not capturing the timing of the seasonal cycle (e.g., northern India, Turkey, New Zealand). The spatial distribution of the size of the seasonal cycle (defined here as the standard deviation in the climatological monthly mean) is less well simulated than the annual mean (contrast Fig. 8d with Fig. 3c and 8f with 6c: the correlation coefficients are smaller and there is more spread in the comparisons with the scatter plot). Examining whether this is a model-specific result or more generally occurs in the models would help discriminate between errors in the input emission datasets or meteorological errors in the model (e.g., Huneeus et al., 2011).

3.6 Data and model coverage

The compilation shown here is the most comprehensive currently available for describing the spatial variability of the total mass and composition of in situ particulate surface concentration data, and yet it highlights the lack of sufficient data to constrain the current global distribution of particles and their composition (Fig. 10a and b). Only 3% of the grid boxes (2°×2°) have $PM_{2.5}$ data (about 10% of land grid boxes), and only 0.3% have sufficient data to constrain most of the composition (defined as having 90% of the variables considered here: total mass, SO_4^{2-}, BC, OM, Na or Cl, Al or dust, NO_3^- and NH_4^+). There are even less data available to characterize PM_{10} (Fig. 10b), which is less important for air quality and aerosol-cloud interactions but more important for aerosol-biogeochemistry interactions and long wave interactions (Mahowald et al., 2011; Li et al., 2022a; Lim et al., 2012; Kanakidou et al., 2018). Because of the high spatial and temporal variability of coarse aerosols and the lack of satellite or other remote sensing data to characterize coarse sizes, this lack of data is a severe handicap in constraining aerosol radiative forcing, its uncertainties and other impacts of particles in the climate system. Indeed, many of these regions have also been identified as regions lacking sufficient remote sensing data for climate and air quality purposes (Millet et al., 2024).

In this paper, we included nitrate aerosols, which are not included in the default CESM simulations conducted for climate, and represent about 10% of the globally averaged surface concentration mass (Table 2; Fig. S18 and S19). When we look spatially, the default particles are the dominant particles over most of the planet (Fig. 11), but in many regions for both $PM_{2.5}$ and PM_{10}, the default aerosol scheme includes less than 50% of the aerosol particles (Fig. 10a and c), with substantial contributions from the nitrate particles that we add to the simulation (Fig. 10b and d). The CESM2 (and some other climate models) do not include nitrogen particles (NO_3^- and NH_4^+), because of the substantial complexity and computation load of chemistry and gas-aerosol equilibrium (Bauer et al., 2007; Thornhill et al., 2021; Adams et al., 2001; Regayre et al., 2018)). Previous studies have highlighted the importance of nitrogen particles for climate, air quality and ecosystem impacts (e.g., Adams et al., 2001; Bauer et al., 2007, 2016; Kanakidou et al., 2016; Baker et al., 2021). Changes in nitrogen aerosol precursor emissions are likely to follow different future trajectories than SO_4^{2-}, BC or OC, whose anthropogenic sources are mostly fossil fuel derived and should decrease in the future as renewable energy resources expand (Gidden et al., 2019). Ammonia has substantial sources from agriculture, which will likely to stay constant or expand (Gidden et al., 2019; Klimont et al., 2017; Bauer et al., 2016). This suggests there could be a substantial bias, especially regionally, in both historical and future aerosol forcings due to the exclusion of these important sources (e.g., Bauer et al., 2007; Thornhill et al., 2021; Adams et al., 2001; Regayre et al., 2018).

4. Conclusions

In this study, we collect aerosol surface concentration datasets and present a new aerosol compilation (AERO-MAP) designed to evaluate the spatial and temporal variability of particulate matter in Earth system and air quality models. The in situ surface measurements complement the column totals typically retrieved by satellites. This dataset includes both total mass and composition, where available, including 15,000 station datasets and over 20 million daily to weekly averaged measurements. Climatological and decadal averages (2010-2019) are presented, and we recommend that the climatological averages be used, because they include more datasets, and multi-decadal and decadal means are extremely similar when compared (Section 3.2). Spatial variability of aerosols (Figure 1f and Section 3.2) is important to simulate accurately in models, as a prerequisite to identifying their human impacts. In addition, we make available annual means across time, and the climatological monthly means so that temporal trends can be assessed. Here we expand beyond the usual limited coverage of North America and Europe to present a more global view for observations of both $PM_{2.5}$ and PM_{10} (Fig. 1). Unfortunately, there are still very limited data characterizing both the surface concentration, size and composition of aerosol particles (Fig. 10), and the locations where we lack data have also been identified as lacking sufficient remote sensing data as well (Millet et al., 2024). While satellite remote sensing can indicate the total atmospheric loading during cloud free conditions, it cannot yet provide information about the size or composition of particles (Kahn et al., 2005; Tanré et al., 1997; Remer et al., 2005). Surface based remote sensing may provide more information about size and absorption properties (Holben et al., 2001; Dubovik et al., 2002; Schuster et al., 2016; Gonçalves Ageitos et al., 2023; Obiso et al., 2023), but

single scattering albedo, for example, is only available under very high (>0.4 AOD) aerosol loading conditions, and thus is not available most of the time and space (Dubovik et al, 2002). Knowing the size and the composition of aerosols is key to their impacts on air quality and climate (Mahowald et al., 2011). Knowing what particles are dominant in a region is required, as fossil fuel derived aerosols will likely be reduced, while agriculturally based aerosols may well increase (Gidden et al., 2019). We also present a method that is generalizable to other models that use this dataset to evaluate both mass and composition for intercomparison projects and improvements in air quality and Earth system models. The novel aspect of this paper is to present this compilation in an easy to use netcdf format and some example comparisons that can be used in the future to evaluate and improve model simulations for individual models or for AEROCOM intercomparisons. The underlying data could also be used for data assimilation efforts or for estimating from the observations what the contributions are from different aerosols (e.g., similar to Prank et al., 2016).

This study has highlighted the value of surface concentration data by showing that it can identify where models do well or poorly not just for total mass, but also for different compositions and size, complimenting other data sources, such as remote sensing. A recent, independent and complementary effort collects all atmospheric composition data (not just aerosols) from many networks into one easy to use framework called GHOST (Globally harmonised dataset of surface atmospheric composition measurements; Bowdalo et al., 2024). The approach used in GHOST includes presenting the data in netcdf format, at the original resolution, with meta data about measurement type, etc. included, and is an important step forward (Bowdalo et al., 2024). At this point GHOST only includes a subset of the data available in this study: we hope that the GHOST effort can be expanded to include more spatial variability and be maintained into the future.

This study also highlights the importance of including all aerosol components into the models, and shows that in the CESM2 approximately 10% is missing. In many places, there is 50% of the particulate mass missing, due to lack of the nitrate particles (Fig. 10; Paulot et al., 2016; Adams et al., 1999; Thornhill et al., 2021). Because these particles are largely driven by agricultural sources and not fossil fuels, their concentrations will be hardly affected by the transition to renewable energy and may increase if agricultural production expands with population. Therefore, these nitrate aerosol particles represent important air quality and climate impacts that should be represented more accurately in future studies.

Deleted: 2020

Data availability: The data compiled here is available as a csv table with citations as a supplemental data 1. This same file is available as well as gridded datasets with the compiled observations and modelled data in netcdf format at

https://zenodo.org/records/10459654, **10.5281/zenodo.11391232** Mahowald et al., 2024. Additional underlying datasets available by request to mahowald@cornell.edu.

Code availability: The model used here is a version of the Community Earth System Model, and the modifications and input files to that code are available at https://zenodo.org/records/10459654, Mahowald et al., 2024.

Author contributions: NMM designed and oversaw the implementation of the approach with the advice of HL, CW, RVM and JL, and wrote the first draft of the manuscript. JV, PH, LLi, ZK, CD, SR, TB and DH assisted in the version of the model and emission datasets used. EA, DM, HM and LLu authors assisted in the compilation and conversion of the data, CH, ZKl contributed emission datasets, XL and XZ contributed model code, MGA, CA, AA, PA,AB, FB, SB, GC, SC, YC, PC, DC, CC, ED, GD, JE, KE, CG-L, CG, DG, YGR, HH, RH, CH, BH, PH, CH, MK, ZKe, KK, FL XL, RL, RL, WM, BM, RLM, RVM, NM, YM-G, AP, JP, SR, PS, DV, BW authors contributed data. All authors edited the manuscript.

Competing interests: The authors declare that the only conflict of interest is that Maria Kanakidou, Xiaohong Liu, Willy Maenhaut, and Sergio Rodriguez are editors at Atmospheric Chemistry and Physics.

Acknowledgments

NMM and LL would like to acknowledge support from DOE (DE-SC0021302), as well as from Paul Ekhart (EBAS), the many freely available air quality websites acknowledged in the paper: EBAS (https://ebas.nilu.no/)--including data affiliated with ACTRIS (Aerosol Clouds and Trace gas Research Infrastructure), EMEP (European Monitoring and Evaluation Programme), GAW-WDCA (Global Atmosphere Watch-World Data Centre for Aerosols), EANET Acid Deposition Monitoring Network in (East Asian)--All Indian Air Quality Management data (https://app.cpcbccr.com/ccr/#/caaqm-dashboard-all/caaqm-landing/data), Australian National Air Pollution Monitoring Database (https://osf.io/jxd98/), South African Air Quality Information System (https://saaqis.environment.gov.za/), Mexico City Air quality data (http://www.aire.cdmx.gob.mx/default.php?opc=%27aKBh%27), Chile (Sistema de Informacion Nacional de Calidad del Aire--https://sinca.mma.gob.cl/index.php/), Japan's NIES (National Institute for Environmental studies-https://tenbou.nies.go.jp/download/), Turkey Air Quality Monitoring Network, Israel Air Quality Monitoring website, US EPA CASNET and IMPROVE, US AIRNOW, New Zealand Stats now website, Chilean (https://www.stats.govt.nz/indicators), Chinese Air Quality data collected together (https://osf.io/jxd98/) and Canadian

National Air Quality Surveillence (https://data.ec.gc.ca/data/air/monitor/national-air-pollution-surveillance-naps-program/Data-Donnees). FB and FL would like to acknowledge support from the Ministerio del Medio Ambiente de Chile (https://mma.gob.cl) and Fondecyt 1231682. SC is grateful for financial support from the Texas Air Research Center and the Texas Commission on Environmental Quality. PA acknowledges funding from Fundação de Amparo à Pesquisa do Estado de São Paulo (FAPESP), grants number 2017-17047-0 and 2023/04358-9. RVM acknowledges funding from NSF Grant 2020673. MK and NM acknowledge support by Greece and the European Union (European Regional Development Fund) via the project PANhellenic infrastructure for Atmospheric Composition and climatE chAnge (PANACEA, MIS 5021516). CGL and BM acknowledge support of CNRS, IRD and ACTRIS-France to the International Network to study Atmospheric Deposition and Atmospheric chemistry in AFrica programe (INDAAF). HM acknowledges support by the MEXT/JSPS KAKENHI Grant Numbers JP19H05699, JP19KK0265, JP20H00196, JP22H03722, JP22F22092, JP23H00515, JP23H00523, JP23K18519, JP23K24976, and JP24H02225, the MEXT Arctic Challenge for Sustainability phase II (ArCS II; JPMXD1420318865) project, and by the Environment Research and Technology Development Fund 2–2301 (JPMEERF20232001) of the Environmental Restoration and Conservation Agency. RLM acknowledges support from the NASA Modeling, Analysis and Prediction Program. We acknowledge contributions from Sagar Rathod, Tami Bond, Giles Bergametti, Javier Miranda Martin del Campo, and Xavier Querol. The support to CESAM by FCT/MCTES (UIDP/50017/2020+UIDB/50017/2020+ LA/P/0094/2020) is also acknowledged.

References

Aas, W., Mortier, A., Bowersox, V., Cherian, R., Faluvegi, G., Fagerli, H., Hand, J., Klimont, Z., Galy-Lacaux, C., Lehmann, C. M. B., Myhre, C. L., Myhre, G., Olivié, D., Sato, K., Quaas, J., Rao, P. S. P., Schulz, M., Shindell, D., Skeie, R. B., Stein, A., Takemura, T., Tsyro, S., Vet, R., and Xu, X.: Global and regional trends of atmospheric sulfur, Sci Rep, 9, https://doi.org/10.1038/s41598-018-37304-0, 2019.

Adams, P., Seinfeld, J., and Koch, D.: Global concentrations of tropospheric sulfate, nitrate and ammonium aerosol simulated in a general circulation model, J. Geophysical Research, 104, 13791–13823, 1999.

Adams, P., Seinfeld, J., Koch, D., Mickley, L., and Jacob, D.: General circulation model assessment of direct radiative forcing by sulfate-nitrate-ammonium-water inorganic aerosol system, J Geophys Res, 106, 1097–1111, 2001.

Adebiyi, A., Kok, J. F., Murray, B. J., Ryder, C. L., Stuut, J.-B. W., Kahn, R. A., Knippertz, P., Formenti, P., Mahowald, N. M., Pérez García-Pando, C., Klose, M., Ansmann, A., Samset, B. H., Ito, A., Balkanski, Y., Di Biagio, C., Romanias, M. N., Huang, Y., and Meng, J.: A review of coarse mineral dust in the Earth system, Aeolian Res, 60, 100849, https://doi.org/10.1016/j.aeolia.2022.100849, 2023.

Aiken, A. C., Decarlo, P. F., Kroll, J. H., Worsnop, D. R., Huffman, J. A., Docherty, K. S., et al. (2008). O/C and OM/OC ratios of primary, secondary, and ambient organic aerosols with high-resolution time-of-flight aerosol mass spectrometry. *Environmental Science and Technology*, *42*(12), 4478–4485. https://doi.org/10.1021/es703009q

Alastuey, A., Querol, X., Aas, W., Lucarelli, F., Pérez, N., Moreno, T., Cavalli, F., Areskoug, H., Balan, V., Catrambone, M., Ceburnis, D., Cerro, J. C., Conil, S., Gevorgyan, L., Hueglin, C., Imre, K., Jaffrezo, J. L., Leeson, S. R., Mihalopoulos, N., Mitosinkova, M., O'Dowd, C. D., Pey, J., Putaud, J. P., Riffault, V., Ripoll, A., Sciare, J., Sellegri, K., Spindler, G., and Yttri, K. E.: Geochemistry of PM10 over Europe during the EMEP intensive measurement periods in summer 2012 and winter 2013, Atmos Chem Phys, 16, 6107–6129, https://doi.org/10.5194/acp-16-6107-2016, 2016.

Albani, S., Mahowald, N. M., Perry, A. T., Scanza, R. A., Zender, C. S., Heavens, N. G., Maggi, V., Kok, J. F., and Otto-Bliesner, B. L.: Improved dust representation in the Community Atmosphere Model, J Adv Model Earth Syst, 6, 541–570, https://doi.org/10.1002/2013MS000279, 2014a.

Albani, S., Mahowald, N., Perry, A., Scanza, R., Zender, C., and Flanner, M. G.: Improved representation of dust size and optics in the CESM, Journal of Advances in Modeling of Earth Systems, 6, doi:10.1002/2013MS000279, 2014b.

Almeida, S. M., Pio, C. A., Freitas, M. C., Reis, M. A., and Trancoso, M. A.: Source apportionment of fine and coarse particulate matter in a sub-urban area at the Western European Coast, Atmos Environ, 39, 3127–3138, https://doi.org/10.1016/j.atmosenv.2005.01.048, 2005.

Amato, F., Alastuey, A., Karanasiou, A., Lucarelli, F., Nava, S., Calzolai, G., Severi, M., Becagli, S., Gianelle, V. L., Colombi, C., Alves, C., Custódio, D., Nunes, T., Cerqueira, M., Pio, C., Eleftheriadis, K., Diapouli, E., Reche, C., Minguillón, M. C., Manousakas, M. I., Maggos, T., Vratolis, S., Harrison, R. M., and Querol, X.: AIRUSE-LIFE+: A harmonized PM speciation and source apportionment in five southern European cities, Atmos Chem Phys, 16, 3289–3309, https://doi.org/10.5194/acp-16-3289-2016, 2016.

Andreae, T. W., Andreae, M. O., Ichoku, C., Maenhaut, W., Cafmeyer, J., Karnieli, A., and Orlovsky, L.: Light scattering by dust and anthropogenic aerosol at a remote site in the Negev desert, Israel, Journal Geophysical Research, 107, https://doi.org/10.1029/2001JD900252., 2002.

Arimoto, R., Duce, R. A., Ray, B. J., and Tomza, U.: Dry deposition of trace elements to the western North Atlantic, Global Biogeochem Cycles, 17, https://doi.org/10.1029/2001GB001406, 2003.

Artaxo, P. and Maenhaut, W.: Aerosol characteristics and sources for the Amazon Basin during the west season, J Geophys Res, 95, 16971–16985, 1990.

Moved (insertion) [1]

Moved (insertion) [2]

Moved (insertion) [3]

Moved (insertion) [4]

Moved (insertion) [5]

Artaxo, P., Martins, J. V., Yamasoe, M. A., Procopio, A. S., Pauliquevis, T. M., Andrae, M. O., Guyon, P., Gatti, L. V, and Leal, A. M. C.: Physical and chemical properties of aerosol particles in the wet and dry seasons in Rondonia, Amazonia, J Geophys Res, 107, 8081, doi: 10.1029/2001JD0000666, 2002.

Baker, A.R., Kanakidou, M., Nenes, A., Myriokefalitakis, S., Croot, P. L., Duce, R.A., Yuan Gao, Y., Guieu, C, Ito, A., Jickells, T.D., Mahowald, M.A, Middag, R., Perron, M.M.G., Sarin, MM., Shelley, R., Turner D.R: Changing atmospheric acidity as a modulator of nutrient deposition and ocean biogeochemistry, Science Advances, 2021 (7) eabd8800, 2021

Barkley, A. E., Prospero, J. M., Mahowald, N., Hamilton, D. S., Popendorf, K. J., Oehlert, A. M., Pourmand, A., Gatineau, A., Panechou-Pulcherie, K., Blackwelder, P., and Gaston, C. J.: African biomass burning is a substantial source of phosphorus deposition to the Amazon, Tropical Atlantic Ocean, and Southern Ocean, Proceedings of the National Academy of Sciences, 116, 16216–16221, https://doi.org/10.1073/pnas.1906091116, 2019.

Barraza, F., Lambert, F., Jorquera, H., Villalobos, A. M., and Gallardo, L.: Temporal evolution of main ambient PM2.5 sources in Santiago, Chile, from 1998 to 2012, Atmos Chem Phys, 17, 10093–10107, https://doi.org/10.5194/acp-17-10093-2017, 2017.

Barrie, L. A., Yi, Y., Leaitch, W. R., Lohmann, U., Kasibhatla, P., Roelofs, G. J., Wilson, J., McGovern, F., Benkovitz, C., Mélières, M. A., Law, K., Prospero, J., Kritz, M., Bergmann, D., Bridgeman, C., Chin, M., Christensen, J., Easter, R., Feichter, J., Land, C., Jeuken, A., Kjellström, E., Koch, D., and Rasch, P.: A comparison of large-scale atmospheric sulphate aerosol models (COSAM): Overview and highlights, Tellus B Chem Phys Meteorol, 53, 615–645, https://doi.org/10.3402/tellusb.v53i5.16642, 2001.

Bauer, S. E., Koch, D., Unger, N., Metzger, S. M., Shindell, D. T., and Streets, D. G.: Nitrate aerosols today and in 2030: a global simulation including aerosols and tropospheric ozone, Atmos. Chem. Phys., 7, 5043–5059, https://doi.org/10.5194/acp-7-5043-2007, 2007.

Bauer, S. E., Tsigaridis, K., and Miller, R.: Significant atmospheric aerosol pollution caused by world food cultivation, Geophys. Res. Lett., 43, 5394–5400, doi:10.1002/2016GL068354, 2016.

Bauer, S.E., Tsigaridis, K., Faluvegi, G., Nazarenko, L., Miller, R.L., Kelley, M., and Schmidt, G.: The turning point of the aerosol era. J. Adv. Model. Earth Syst., 14, no. 12, e2022MS003070, doi:10.1029/2022MS003070, 2022.

Bellouin, N., Quaas, J., Gryspeerdt, E., Kinne, S., Stier, P., Watson-Parris, D., Boucher, O., Carslaw, K. S., Christensen, M., Daniau, A. L., Dufresne, J. L., Feingold, G., Fiedler, S., Forster, P., Gettelman, A., Haywood, J. M., Lohmann, U., Malavelle, F., Mauritsen, T., McCoy, D. T., Myhre, G., Mülmenstädt, J., Neubauer, D., Possner, A., Rugenstein, M., Sato, Y., Schulz, M., Schwartz, S. E., Sourdeval, O., Storelvmo, T., Toll, V., Winker, D., and Stevens, B.: Bounding Global Aerosol Radiative Forcing of Climate Change, https://doi.org/10.1029/2019RG000660, 1 March 2020.

Bergametti, G., Gomes, L., Doude-Gaussen, G., Rognon, P., and Le Coustumer, M. N: African dust observed over the Canary Islands: source-regions identification and the transport pattern for some summer situations, J Geophys Res, 94, 14855–14864, 1989.

Bond, T., Doherty, S. J., Fahey, D., Forster, P., Bernsten, T., DeAngelo, B., Flanner, M., Ghan, S., Karcher, B., Koch, D., Kinne, S., Kondo, Y., Quinn, P. K., Sarofim, M., Schultz, M., Venkataraman, C., Zhang, H., Zhang, S., Bellouin, N., Guttikunda, S., Hopke, P., Jacobson, M., Kaiser, J. W., Klimont, Z., Lohman, U., Schwartz, J., Shindel, D., Storelvmo, T., Warren, S., and Zender, C.: Bounding the role of black carbon in the climate system: A scientific assessment, J Geophys Res, D118, 5380–5552; doi:10.1002/jgrd_50171, 2013.

Bond, T. C., Streets, D. G., Yarber, K. F., Nelson, S. M., Woo, J.-H., and Klimont, Z.: A technology-based global inventory of black and organic carbon emissions from combustion, J Geophys Res, 109, doi:10.1029/2003JD003697, 2004.

Bouet, C., Labiadh, M. T., Rajot, J. L., Bergametti, G., Marticorena, B., des Tureaux, T. H., Ltifi, M., Sekrafi, S., and Féron, A.: Impact of desert dust on air quality: What is the meaningfulness of daily PM standards in regions close to the sources? The example of Southern Tunisia, Atmosphere (Basel), 10, https://doi.org/10.3390/atmos10080452, 2019.

Bowdalo, D., Basart, S., Guevara, M., Jorba, O., Pérez García-Pando, C., Jaimes Palomera, M., et al. (2024), GHOST: a globally harmonised dataset of surface atmospheric composition measurements, *Earth System Science Data*, *16*(10), 4417–4495. https://doi.org/10.5194/essd-16-4417-2024

Bozlaker, A., Buzcu-Güven, B., Fraser, M. P., and Chellam, S.: Insights into PM10 sources in Houston, Texas: Role of petroleum refineries in enriching lanthanoid metals during episodic emission events, Atmos Environ, 69, 109–117, https://doi.org/10.1016/j.atmosenv.2012.11.068, 2013.

Bullard, J., Baddock, M., McTainsh, G., and Leys, J.: Sub-basin scale dust source geomorphology detected using MODIS, Geophys Res Lett, 35, https://doi.org/10.1029/2008GL033928, 2008.

Burnett, R., Chen, H., Szyszkowicz, M., Fann, N., Hubbell, B., Pope, C. A., Apte, J. S., Brauer, M., Cohen, A., Weichenthal, S., Coggins, J., Di, Q., Brunekreef, B., Frostad, J., Lim, S. S., Kan, H., Walker, K. D., Thurston, G. D., Hayes, R. B., Lim, C. C., Turner, M. C., Jerrett, M., Krewski, D., Gapstur, S. M., Diver, W. R., Ostro, B., Goldberg, D., Crouse, D. L., Martin, R. v., Peters, P., Pinault, L., Tjepkema, M., van Donkelaar, A., Villeneuve, P. J., Miller, A. B., Yin, P., Zhou, M., Wang, L., Janssen, N. A. H., Marra, M., Atkinson, R. W., Tsang, H., Thach, T. Q., Cannon, J. B., Allen, R. T., Hart, J. E., Laden, F., Cesaroni, G., Forastiere, F., Weinmayr, G., Jaensch, A., Nagel, G., Concin, H., and Spadaro, J. v.: Global estimates of mortality associated with longterm exposure to outdoor fine particulate matter, Proc Natl Acad Sci U S A, 115, 9592–9597, https://doi.org/10.1073/pnas.1803222115, 2018.

Burgos, M. A., E. Andrews, G. Titos, A. Benedetti, H. Bian, V. Buchard, G. Curci, Z. Kipling, A. Kirkevåg, H. Kokkola, A. Laakso, J. Letertre-Danczak, M. T. Lund, H. Matsui, G. Myhre, C. Randles, M. Schulz, T. van Noije, K. Zhang, L. Alados-Arboledas, U. Baltensperger, A. Jefferson, J. Sherman, J. Sun, E. Weingartner, and P. Zieger (2020), A global model-measurement evaluation of particle light scattering coefficients at elevated relative humidity, Atmospheric Chemistry and Physics, 20, 10231-10258, doi:10.5194/acp-20-10231-2020.

Moved up [5]: S.,

Deleted: . J., Rivera Hernandez, O., Puchalski, M., Gay, D., Klausen, J., Moreno,

Deleted: Netcheva, S., and Tarasova, O.:

Deleted: A

Formatted: Justified

Deleted: ,

Deleted: Syst Sci

Deleted: 1–37,

Formatted: Font: Italic

Formatted: Font: Italic

Deleted: 5281/zenodo.10637449,

Deleted: .

Formatted: Font color: Auto

898 Caldwell, P. M., Mametjanov, A., Tang, Q., van Roekel, L. P., Golaz, J. C., Lin, W., Bader, D. C., Keen, N. D., Feng, Y.,
899 Jacob, R., Maltrud, M. E., Roberts, A. F., Taylor, M. A., Veneziani, M., Wang, H., Wolfe, J. D., Balaguru, K.,
900 Cameron-Smith, P., Dong, L., Klein, S. A., Leung, L. R., Li, H. Y., Li, Q., Liu, X., Neale, R. B., Pinheiro, M., Qian,
901 Y., Ullrich, P. A., Xie, S., Yang, Y., Zhang, Y., Zhang, K., and Zhou, T.: The DOE E3SM Coupled Model Version
902 1: Description and Results at High Resolution, J Adv Model Earth Syst, https://doi.org/10.1029/2019MS001870,
903 2019.
904 Carslaw, K. S., Lee, L., Reddington, C., Pringle, K., Rap, A., Forster, P., Mann, G., Spracklen, D., Woodhouse, M., Regayre,
905 L., and Pierce, J.: Large contribution of natural aerosols to uncertainty in indirect forcing, Nature, 503, 67–71, 2013.
906 Castellanos, P., Colarco, P., Espinosa, W. R., Guzewich, S. D., Levy, R. C., Miller, R. L., et al. (2024, March 15). Mineral
907 dust optical properties for remote sensing and global modeling: A review. *Remote Sensing of Environment*. Elsevier
908 Inc. https://doi.org/10.1016/j.rse.2023.113982
909 Chatziparaschos, M., Daskalakis, N., Myriokefalitakis, S., Kalivitis, N., Nenes, A., Gonçalves Ageitos, M., Costa-Surós, M.,
910 Pérez García-Pando, C., Zanoli, M., Vrekoussis, M., and Kanakidou, M.: Role of K-feldspar and quartz in global
911 ice nucleation by mineral dust in mixed-phase clouds, Atmos. Chem. Phys., 23, 1785–1801,
912 https://doi.org/10.5194/acp-23-1785-2023, 2023.
913 Chen, Y., Street, J., and Paytan, A.: Comparison between pure-water- and seawater-soluble nutrient concentrations of
914 aerosol particles from the {Gulf} of {Aqaba}, Mar Chem, 101, 141–152,
915 https://doi.org/10.1016/j.marchem.2006.02.002, 2006.
916 Chuang, P., Duvall, R., Shafer, M., and Schauer, J.: The origin of water soluble particulate iron in the Asian atmospheric
917 outflow, Geophys Res Lett, 32, doi:10.1029/2004GL021946, 2005.
918 Cipoli, Y. A., Alves, C., Rapuano, M., Evtyugina, M., Rienda, I. C., Kováts, N., Vicente, A., Giardi, F., Furst, L., Nunes, T.,
919 and Feliciano, M.: Nighttime–daytime PM10 source apportionment and toxicity in a remoteness inland city of the
920 Iberian Peninsula, Atmos Environ, 303, https://doi.org/10.1016/j.atmosenv.2023.119771, 2023.
921 Clark, S. K., Ward, D. S., and Mahowald, N. M.: The sensitivity of global climate to the episodicity of fire aerosol emissions,
922 Journal of Geophysical Research: Atmospheres, 120, https://doi.org/10.1002/2015JD024068, 2015.
923 Cohen, D., Garton, D., Stelcer, E., Hawas, O., Wang, T., Pon, S., Kim, J., Choi, B., Oh, S., Shin, H.-J., Ko, M., and
924 Uematsu, M.: Multielemental analysis and characterization of fine aerosols at several key ACE-Asia sites, 109,
925 doi:10.1029/2003JD003569, 2004.
926 Collaud Coen, M., Andrews, E., Lastuey, A., Petkov Arsov, T., Backman, J., Brem, B. T., Bukowiecki, N., Couret, C.,
927 Eleftheriadis, K., Flentje, H., Fiebig, M., Gysel-Beer, M., Hand, J. L., Hoffer, A., Hooda, R., Hueglin, C., Joubert,
928 W., Keywood, M., Eun Kim, J., Kim, S. W., Labuschagne, C., Lin, N. H., Lin, Y., Lund Myhre, C., Luoma, K.,
929 Lyamani, H., Marinoni, A., Mayol-Bracero, O. L., Mihalopoulos, N., Pandolfi, M., Prats, N., Prenni, A. J., Putaud,
930 J. P., Ries, L., Reisen, F., Sellegri, K., Sharma, S., Sheridan, P., Patrick Sherman, J., Sun, J., Titos, G., Torres, E.,
931 Tuch, T., Weller, R., Wiedensohler, A., Zieger, P., and Laj, P.: Multidecadal trend analysis of in situ aerosol

radiative properties around the world, Atmos Chem Phys, 20, 8867–8908, https://doi.org/10.5194/acp-20-8867-2020, 2020.

Computational and Information Systems Laboratory: Cheyenne: HPE/SGI ICE XA System (NCAR Community Computing)., https://doi.org/10.5065/D6RX99HX, 2019.

da Silva, L. I. D., de Souza Sarkis, J. E., Zotin, F. M. Z., Carneiro, M. C., Neto, A. A., da Silva, A. dos S. A. G., Cardoso, M. J. B., and Monteiro, M. I. C.: Traffic and catalytic converter - Related atmospheric contamination in the metropolitan region of the city of Rio de Janeiro, Brazil, Chemosphere, 71, 677–684, https://doi.org/10.1016/j.chemosphere.2007.10.057, 2008.

Dentener, F. J., Carmichael, G. R., Zhang, Y., Lelieveld, J., and Crutzen, P. J.: Role of mineral aerosol as a reactive surface in the global troposphere, J Geophys Res, 101, 22,822-869,889, 1996.

Dentener, F., Kinne, S., Bond, T., Boucher, O., Cofala, J., Generoso, S., Ginoux, P., Gong, S., Hoelzemann, J. J., Ito, A., Marelli, L., Penner, J., Putaud, J.-P., Textor, C., Schulz, M., van der Werf, G. R., and Wilson, J.: Emissions of primary aerosol and precursor gases in the years 2000 and 1750: prescribed data-sets for AeroCom, Atmos Chem Phys, 6, 4321–4344, 2006.

Dongarrà, G., Manno, E., Varrica, D., and Vultaggio, M.: Mass levels, crustal component and trace elements in PM10 in Palermo, Italy, Atmos Environ, 41, 7977–7986, https://doi.org/10.1016/j.atmosenv.2007.09.015, 2007.

Dongarrà, G., Manno, E., Varrica, D., Lombardo, M., and Vultaggio, M.: Study on ambient concentrations of PM10, PM10-2.5, PM2.5 and gaseous pollutants. Trace elements and chemical speciation of atmospheric particulates, Atmos Environ, 44, 5244–5257, https://doi.org/10.1016/j.atmosenv.2010.08.041, 2010.

Dubovik, O., Smirnov, A., Holben, B. N., King, M. D., Kaufman, Y. J., ECK, T. F., and Slutsker, I.: Accuracy assessments of aerosol optical properties retrieved from Aerosol Robotic Network (AERONET) Sun and sky radiance measurments, J Geophys Res, 105, 9791–9806, 2000.

Dubovik, O., Holben, B., Eck, T. F., Smirnov, A., et al.: Variability of absorption and optical properties of key aerosol types observed in worldwide locations, Journal of Atmospheric Science, 590–608, 2002.

Engelbrecht, Johann, Eric V. McDonald, John A. Gillies, R. K. M. Jayanty, Gary Casuccio & Alan W. Gertler (2009) Characterizing Mineral Dusts and Other Aerosols from the Middle East, Part 1: Ambient Sampling, Inhalation Toxicology, 21:4, 297-326, DOI: 10.1080/08958370802464273, 2009.

Fanourgakis, G. S., Kanakidou, M., Nenes, A., Bauer, S. E., Bergman, T., Carslaw, K. S., Grini, A., Hamilton, D. S., Johnson, J. S., Karydis, V. A., Kirkeväg, A., Kodros, J. K., Lohmann, U., Luo, G., Makkonen, R., Matsui, H., Neubauer, D., Pierce, J. R., Schmale, J., Stier, P., Tsigaridis, K., Van Noije, T., Wang, H., Watson-Parris, D., Westervelt, D. M., Yang, Y., Yoshioka, M., Daskalakis, N., Decesari, S., Gysel-Beer, M., Kalivitis, N., Liu, X., Mahowald, N. M., Myriokefalitakis, S., Schrödner, R., Sfakianaki, M., Tsimpidi, A. P., Wu, M., and Yu, F.: Evaluation of global simulations of aerosol particle and cloud condensation nuclei number, with implications for cloud droplet formation, Atmos Chem Phys, 19, 8591–8617, https://doi.org/10.5194/acp-19-8591-2019, 2019.

966 Fasullo, J. T., Lamarque, J. F., Hannay, C., Rosenbloom, N., Tilmes, S., DeRepentigny, P., Jahn, A., and Deser, C.: Spurious
967 Late Historical-Era Warming in CESM2 Driven by Prescribed Biomass Burning Emissions, Geophyical Research
968 Letters, 49, https://doi.org/10.1029/2021GL097420, 28 January 2022.
969 Fiore, A. M., Milly, G. P., Hancock, S. E., Quiñones, L., Bowden, J. H., Helstrom, E., Lamarque, J. F., Schnell, J., West, J.
970 J., and Xu, Y.: Characterizing Changes in Eastern U.S. Pollution Events in a Warming World, Journal of
971 Geophysical Research: Atmospheres, 127, https://doi.org/10.1029/2021JD035985, 2022.
972 Font, A., F. de Brito, J., Riffault, V., Conil, S., Jaffrezo, J. L., & Bourin, A. (2024). Calculations of the conversion factor
973 from organic carbon to organic matter for aerosol mass balance. *Atmospheric Pollution Research*, *15*(12).
974 https://doi.org/10.1016/j.apr.2024.102301
975 Formenti, P., Elbert, W., Maenhaut, W., Haywood, J., and Andreae, M. O.: Chemical composition of mineral dust aerosol
976 during the Saharan Dust Experiment (SHADE) airborne campaign in the Cape Verde region, September 2000, J.
977 Geophys. Res., 108, 8576, doi:10.1029/2002JD002648, 2003.
978 Furu, E., Katona-Szabo, I., Angyal, A., Szoboszlai, Z., Török, Z., and Kertész, Z.: The effect of the tramway track construction
979 on the aerosol pollution in Debrecen, Hungary, in: Nuclear Instruments and Methods in Physics Research, Section B:
980 Beam Interactions with Materials and Atoms, 124–130, https://doi.org/10.1016/j.nimb.2015.08.014, 2015.
981 Furu, E., Angyal, A., Szoboszlai, Z., Papp, E., Török, Z., and Kertész, Z.: Characterization of Aerosol Pollution in Two
982 Hungarian Cities in Winter 2009–2010, Atmosphere (Basel), 13, https://doi.org/10.3390/atmos13040554, 2022.
983 Fuzzi, S., Decesari, S., Facchini, M., Cavalli, F., Emblico, L., Mircea, M., Andreae, M., Trebs, I., Hoffer, A., Guyon, P.,
984 Artaxo, P., Rizzo, L., Lara, L., Pauliquevis, T., Maenhaut, W., et al.: Overview of the inorganic and organic
985 composition of size-segregated aerosol in Rondonia, Brazil from the biomass-burning period to the onset of the wet
986 season., J Geophys Res, 112, doi:10.1029/2005JD006741, 2007.
987 García, M. I., Rodríguez, S., and Alastuey, A.: Impact of North America on the aerosol composition in the North Atlantic
988 free troposphere, Atmos Chem Phys, 17, 7387–7404, https://doi.org/10.5194/acp-17-7387-2017, 2017.
989 Gelaro, R., McCarty, W., Suárez, M. J., Todling, R., Molod, A., Takacs, L., Randles, C. A., Darmenov, A., Bosilovich, M.
990 G., and Reichle, R.: The modern-era retrospective analysis for research and applications, version 2 (MERRA-2), J
991 Clim, 30, 5419–5454, 2017.
992 Gianini, M. F. D., Gehrig, R., Fischer, A., Ulrich, A., Wichser, A., and Hueglin, C.: Chemical composition of PM10 in
993 Switzerland: An analysis for 2008/2009 and changes since 1998/1999, Atmos Environ, 54, 97–106,
994 https://doi.org/10.1016/j.atmosenv.2012.02.037, 2012a.
995 Gianini, M. F. D., Fischer, A., Gehrig, R., Ulrich, A., Wichser, A., Piot, C., Besombes, J. L., and Hueglin, C.: Comparative
996 source apportionment of PM10 in Switzerland for 2008/2009 and 1998/1999 by Positive Matrix Factorisation,
997 Atmos Environ, 54, 149–158, https://doi.org/10.1016/j.atmosenv.2012.02.036, 2012b.
998 Gidden, M. J., Riahi, K., Smith, S. J., Fujimori, S., Luderer, G., Kriegler, E., Van Vuuren, D. P., Van Den Berg, M., Feng,
999 L., Klein, D., Calvin, K., Doelman, J. C., Frank, S., Fricko, O., Harmsen, M., Hasegawa, T., Havlik, P., Hilaire, J.,

Hoesly, R., Horing, J., Popp, A., Stehfest, E., and Takahashi, K.: Global emissions pathways under different socioeconomic scenarios for use in CMIP6: A dataset of harmonized emissions trajectories through the end of the century, Geosci Model Dev, 12, 1443–1475, https://doi.org/10.5194/gmd-12-1443-2019, 2019.

Ginoux, P., Chin, M., Tegen, I., Prospero, J. M., Holben, B. N., Dubovik, O., and Lin, S.-J.: Sources and distribution of dust aerosol particles with the GOCART model, J Geophys Res, 106, 20255–20273, 2001.

Gleckler, P., Taylor, K. E., and Doutriaux, C.: Performance metrics for climate models, J Geophys Res, 113, D06104, doi:10.1029/2007JD008972, 2008.

Gliß, J., Mortier, A., Schulz, M., Andrews, E., Balkanski, Y., Bauer, S. E., Benedictow, A. M. K., Bian, H., Checa-Garcia, R., Chin, M., Ginoux, P., Griesfeller, J. J., Heckel, A., Kipling, Z., Kirkeväg, A., Kokkola, H., Laj, P., Le Sager, P., Lund, T. M., Lund Myhre, C., Matsui, H., Myhre, G., Neubauer, D., Van Noije, T., North, P., Olivié, D. J. L., Rémy, S., Sogacheva, L., Takemura, T., Tsigaridis, K., and Tsyro, S. G.: AeroCom phase III multi-model evaluation of the aerosol life cycle and optical properties using ground- And space-based remote sensing as well as surface in situ observations, Atmos Chem Phys, 21, 87–128, https://doi.org/10.5194/acp-21-87-2021, 2021.

Golaz, J. C., Caldwell, P. M., van Roekel, L. P., Petersen, M. R., Tang, Q., Wolfe, J. D., Abeshu, G., Anantharaj, V., Asay-Davis, X. S., Bader, D. C., Baldwin, S. A., Bisht, G., Bogenschutz, P. A., Branstetter, M., Brunke, M. A., Brus, S. R., Burrows, S. M., Cameron-Smith, P. J., Donahue, A. S., Deakin, M., Easter, R. C., Evans, K. J., Feng, Y., Flanner, M., Foucar, J. G., Fyke, J. G., Griffin, B. M., Hannay, C., Harrop, B. E., Hoffman, M. J., Hunke, E. C., Jacob, R. L., Jacobsen, D. W., Jeffery, N., Jones, P. W., Keen, N. D., Klein, S. A., Larson, V. E., Leung, L. R., Li, H. Y., Lin, W., Lipscomb, W. H., Ma, P. L., Mahajan, S., Maltrud, M. E., Mametjanov, A., McClean, J. L., McCoy, R. B., Neale, R. B., Price, S. F., Qian, Y., Rasch, P. J., Reeves Eyre, J. E. J., Riley, W. J., Ringler, T. D., Roberts, A. F., Roesler, E. L., Salinger, A. G., Shaheen, Z., Shi, X., Singh, B., Tang, J., Taylor, M. A., Thornton, P. E., Turner, A. K., Veneziani, M., Wan, H., Wang, H., Wang, S., Williams, D. N., Wolfram, P. J., Worley, P. H., Xie, S., Yang, Y., Yoon, J. H., Zelinka, M. D., Zender, C. S., Zeng, X., Zhang, C., Zhang, K., Zhang, Y., Zheng, X., Zhou, T., and Zhu, Q.: The DOE E3SM Coupled Model Version 1: Overview and Evaluation at Standard Resolution, J Adv Model Earth Syst, 11, 2089–2129, https://doi.org/10.1029/2018MS001603, 2019.

Gonçalves Ageitos, M., Obiso, V., Miller, R. L., Jorba, O., Klose, M., Dawson, M., Balkanski, Y., Perlwitz, J., Basart, S., Di Tomaso, E., Escribano, J., Macchia, F.,. Montané, G., Mahowald,N., Green, R. O., Thompson, D. R., and Pérez García-Pando, C.: Modeling dust mineralogical composition: sensitivity to soil mineralogy atlases and their expected climate impacts. Atmos. Chem. Phys., 23, no. 15, 8623-8657, doi:10.5194/acp-23-8623-2023, 2023.

Gong, S. L., Barrie, L. A., Prospero, J. M., Savoie, D. L., Ayers, G. P., Blanchet, J.-P., and Spacek, L.: Modeling sea-salt aerosol particles in the atmosphere 2. Atmospheric concentrations and fluxes, J Geophys Res, 102, 3819–3830, 1997.

Gong, S. L., Zhang, X. Y., Zhao, T. L., McKendry, I. G., Jaffe, D. A., and Lu, N. M.: Characterization of soil dust aerosol in China and its transport and distribution during 2001 ACE-Asia: 2. Model simulation and validation, J Geophys Res, 108, 4262, 2003.

Gui, K., Che, H., Zheng, Y., Wang, Y., Zhang, L., Zhao, H., et al. (2021). Seasonal variability and trends in global type-segregated aerosol optical depth as revealed by MISR satellite observations. *Science of the Total Environment*, *787*. https://doi.org/10.1016/j.scitotenv.2021.147543

Gulev, S. K., Thorne, P. W., Ahn, J., Dentener, F. J., Domingues, C. M., Gerland, S., Gong, D., Kaufman, D. S., Nnamchi, H. C., Quaas, J., Rivera, J. A., Sathyendranath, S., Smith, S. L., Trewin, B., von Schuckmann, K., and Vose, R. ,S.: Chapter 2: Changing State of the Climate System., in: Climate Change 2021: The Physical Science Basis. Contribution of Working Group I to the Sixth Assessment Report of the Intergovernmental Panel on Climate Change, edited by: Masson-Delmotte, V. , Zhai, P., Pirani, A., Connors, S. L., Péan, C., Berger, S., Caud, N., Chen, Y., Goldfarb, L., Gomis, M. I., Huang, M., Leitzell, K., Lonnoy, E., Matthews, J. B. R., Maycock, T. K., Waterfield, T., Yelekçi, O., Yu, R., and Zhou, B. Cambridge University Press, Cambridge, United Kingdom and New York, NY, USA, 287–422, https://doi.org/10.1017/9781009157896.004, 2021.

Gupta, G., Venkat Ratnam, M., Madhavan, B. L., and Narayanamurthy, C. S.: Long-term trends in Aerosol Optical Depth obtained across the globe using multi-satellite measurements, Atmos Environ, 273, https://doi.org/10.1016/j.atmosenv.2022.118953, 2022.

Hand, J. L., Gill, T. E., and Schichtel, B. A.: Spatial and seasonal variability in fine mineral dust and coarse aerosol mass at remote sites across the United States, J Geophys Res, 122, 3080–3097, https://doi.org/10.1002/2016JD026290, 2017.

Hand, J. L., Gill, T. E., and Schichtel, B. A.: Urban and rural coarse aerosol mass across the United States: Spatial and seasonal variability and long-term trends, Atmos Environ, 218, 117025, https://doi.org/10.1016/j.atmosenv.2019.117025, 2019.

Hand, J. L., Prenni, A. J., & Schichtel, B. A. (2024). Trends in Seasonal Mean Speciated Aerosol Composition in Remote Areas of the United States From 2000 Through 2021. *Journal of Geophysical Research: Atmospheres*, *129*(2). https://doi.org/10.1029/2023JD039902

Hansen, J. and Nazarenko, L.: Soot climate forcing via snow and ice albedos, PNAS, 101, 423–428, doi/10.1073/pnas.ss37157100, 2004.

Heald, C., Ridley, D., Kreidenweis, S., and Drury, E.: Satellite observations cap the atmospheric organic aerosol budget, Geophys Res Lett, 37, L24808; doi:10.1029/2010GL045095, 2010.

Heimburger, A., Losno, R., Triquet, S., Dulac, F., and Mahowald, N.: Direct measurement of atmospheric iron, cobalt and aluminum-derived dust deposition at Kerguelen Islands, Global Biogeochem Cycles, 26, doi:10.1029/2012GB004301, https://doi.org/10.1029/2012GB004301, 2012.

Henriksson, S. V., Laaksonen, A., Kerminen, V. M., Räisänen, P., Järvinen, H., Sundstr̈om, A. M., and De Leeuw, G.: Spatial distributions and seasonal cycles of aerosols in India and China seen in global climate-aerosol model, Atmos Chem Phys, 11, 7975–7990, https://doi.org/10.5194/acp-11-7975-2011, 2011.

Herut, B. and Krom, M.: Atmospheric input of nutrients and dust to the SE Mediterranean, in: The Impact of Desert Dust Across the Mediterranean , edited by: Guerzoni, S. and Chester, R., 349–360, 1996.

Herut, B., Nimmo, M., Medway, A., Chester, R., and Krom, M.D.: Dry atmospheric inputs of trace metals at the Mediterranean coast of Israel (SE Mediterranean): sources and fluxes. Atmos. Environ., 35, 803-813, 2001.

Hinds, W. C., Aerosol Technology, Properties, Behavior and Measurement of Airborne Particles, John Wiley, New York, 1999.

Holben, B. N., Tanre, D., Smirnov, A., ECK, T. F., Slutsker, I., Abuhassan, N., et al. (2001). An emerging ground-based aerosol climatology:Aerosol optical depth from AERONET. *Journal of Geophysical Research*, *106*(D11), 12067–12097.

Hsu, C. Y., Chiang, H. C., Lin, S. L., Chen, M. J., Lin, T. Y., and Chen, Y. C.: Elemental characterization and source apportionment of PM10 and PM2.5 in the western coastal area of central Taiwan, Science of the Total Environment, 541, 1139–1150, https://doi.org/10.1016/j.scitotenv.2015.09.122, 2016.

Huang, Y., Adebiyi, A. A., Formenti, P., and Kok, J. F.: Linking the Different Diameter Types of Aspherical Desert Dust Indicates That Models Underestimate Coarse Dust Emission, Geophys Res Lett, 48, https://doi.org/10.1029/2020GL092054, 2021.

Hueglin, C., Gehrig, R., Baltensperger, U., Gysel, M., Monn, C., and Vonmont, H.: Chemical characterisation of PM2.5, PM10 and coarse particles at urban, near-city and rural sites in Switzerland, Atmos Environ, 39, 637–651, https://doi.org/10.1016/j.atmosenv.2004.10.027, 2005.

Huneeus, N., Schulz, M., Balkanski, Y., Griesfeller, J., Prospero, J., Kinne, S., Bauer, S., Boucher, O., Chin, M., Dentener, F., Diehl, T., Easter, R., Fillmore, D., Ghan, S., Ginoux, P., Grini, A., Horowitz, L., Koch, D., Krol, M. C., Landing, W., Liu, X., Mahowald, N., Miller, R., Morcrette, J.-J., Myhre, G., Penner, J., Perlwitz, J., Stier, P., Takemura, T., and Zender, C. S.: Global dust model intercomparison in AeroCom phase i, Atmos Chem Phys, 11, https://doi.org/10.5194/acp-11-7781-2011, 2011.

Hurrell, J. W., Holland, M. M., Gent, P. R., Ghan, S., Kay, J. E., Kushner, P. J., Lamarque, J.-F., Large, W. G., Lawrence, D., Lindsay, K., Lipscomb, W. H., Long, M. C., Mahowald, N., Marsh, D. R., Neale, R. B., Rasch, P., Vavrus, S., Vertenstein, M., Bader, D., Collins, W. D., Hack, J. J., Kiehl, J., and Marshall, S.: The community earth system model: A framework for collaborative research, Bull Am Meteorol Soc, 94, https://doi.org/10.1175/BAMS-D-12-00121.1, 2013.

IPCC: Summary for Policymakers, in: Climate Change 2021: The Physical Science Basis. Contribution of Working Group I to the Sixth Assessment Report of the Intergovernmental Panel on Climate Change, edited by: Masson-Delmotte, V. , P., Zhai, A., Pirani, S.L., Connors, C., Péan, S., Berger, N., Caud, Y,. Chen, L., Goldfarb, M. I., Gomis, M.,

Huang, K., Leitzell, E., Lonnoy, J. B. R., Matthews, T. B. R., Maycock, T. K., Waterfield, T., Yelekçi, O.., Yu, R., and Zhou B., Cambridge University Press, Cambridge, UK, 3–32, https://doi.org/10.1017/9781009157896.001, 2021.

Jaenicke, R.: Abundance of cellular material and proteins in the atmosphere, Science (1979), 308, 73, https://doi.org/10.1126/science.1106335, 2005.

Jensen, J. B. and Lee, S.: Giant sea-salt aerosols and warm rain formation in marine stratocumulus, J Atmos Sci, 65, 3678–3694, https://doi.org/10.1175/2008JAS2617.1, 2008.

Kahn, R. A., Gaitley, B., Martonchik, J., Diner, D. J., Crean, K., and Holben, B.: MISR global aerosol optical depth validation based on two years of coincident AERONET observations, J Geophys Res, 110, doi:10.1029/2004JD004706, 2005.

Kalivitis, N., E. Gerasopoulos, M. Vrekoussis, G. Kouvarakis, N. Kubilay, N. Hatzianastassiou, I. Vardavas, and N. Mihalopoulos (2007), Dust transport over the eastern Mediterranean derived from Total Ozone Mapping Spectrometer, Aerosol Robotic Network, and surface measurements, J. Geophys. Res., 112, D03202, doi:10.1029/2006JD007510, 2007.

Kaly, F., Marticorena, B., Chatenet, B., Rajot, J. L., Janicot, S., Niang, A., Yahi, H., Thiria, S., Maman, A., Zakou, A., Coulibaly, B. S., Coulibaly, M., Koné, I., Traoré, S., Diallo, A., and Ndiaye, T.: Variability of mineral dust concentrations over West Africa monitored by the Sahelian Dust Transect, Atmos Res, 164–165, 226–241, https://doi.org/10.1016/j.atmosres.2015.05.011, 2015

Kanakidou, M., Seinfeld, J., Pandis, S., Barnes, I., Dentener, F., Facchini, M., et al.: Organic aerosol and global climate modeling: a review, Atmos Chem Phys, 5, 1053–1123, 2005.

Kanakidou M., Myriokefalitakis S., Tsigaridis K.: Aerosols in atmospheric chemistry and biogeochemical cycles of nutrients, Environ. Res. Lett. 13 063004, 2018. https://doi.org/10.1088/1748-9326/aabcdb

Kanakidou, M., Myriokefalitakis, S., Daskalakis, N., Fanourgakis, G., Nenes, A., Baker, A., et al. (2016). Past, present and future atmospheric nitrogen deposition. *Journal of Atmospheric Science*, *73*, 2039–2047; DOI: 10.1175/JAS-D-15-0278.1.

Karydis, V. A., Tsimpidi, A. P., Bacer, S., Pozzer, A., Nenes, A., and Lelieveld, J.: Global impact of mineral dust on cloud droplet number concentration, Atmos. Chem. Phys., 17, 5601–5621, https://doi.org/10.5194/acp-17-5601-2017, 2017.

Ke, Z., Liu, X., Wu, M., Shan, Y., and Shi, Y.: Improved Dust Representation and Impacts on Dust Transport and Radiative Effect in CAM5, J Adv Model Earth Syst, 14, https://doi.org/10.1029/2021MS002845, 2022.

Klimont, Z., Kupiainen, K., Heyes, C., Purohit, P., Cofala, J., Rafaj, P., Borken-Kleefeld, J., and Schöpp, W.: Global anthropogenic emissions of particulate matter including black carbon, Atmos Chem Phys, 17, 8681–8723, https://doi.org/10.5194/acp-17-8681-2017, 2017.

Koch, D., Schulz, M., Kinne, S., McNaughton, C., et al.: Evaluation of black carbon estimations in global aerosol models, Atmos Chem Phys, 9, 9001–9026, 2009.

Kok, J. F., Mahowald, N. M., Fratini, G., Gillies, J. A., Ishizuka, M., Leys, J. F., Mikami, M., Park, M.-S., Park, S.-U., van Pelt, R. S., and Zobeck, T. M.: An improved dust emission model - Part 1: Model description and comparison against measurements, Atmos Chem Phys, 14, https://doi.org/10.5194/acp-14-13023-2014, 2014a.

Kok, J. F., Albani, S., Mahowald, N. M., and Ward, D. S.: An improved dust emission model - Part 2: Evaluation in the Community Earth System Model, with implications for the use of dust source functions, Atmos Chem Phys, 14, https://doi.org/10.5194/acp-14-13043-2014, 2014b.

Kok, J. F., Ridley, D. A., Zhou, Q., Miller, R. L., Zhao, C., Heald, C. L., Ward, D. S., Albani, S., and Haustein, K.: Smaller desert dust cooling effect estimated from analysis of dust size and abundance, Nat Geosci, 10, 274–278, https://doi.org/10.1038/ngeo2912, 2017.

Kok, J. F., Adebiyi, A. A., Albani, S., Balkanski, Y., Checa-Garcia, R., Chin, M., Colarco, P. R., Hamilton, D. S., Huang, Y., Ito, A., Klose, M., Leung, D. M., Li, L., Mahowald, N. M., Miller, R. L., Obiso, V., Pérez García-Pando, C., Rocha-Lima, A., Wan, J. S., and Whicker, C. A.: Improved representation of the global dust cycle using observational constraints on dust properties and abundance, Atmos Chem Phys, 21, 8127–8167, https://doi.org/10.5194/acp-21-8127-2021, 2021.

Kok, J. F., Storelvmo, T., Karydis, V. A., Adebiyi, A. A., Mahowald, N. M., Evan, A. T., He, C., and Leung, D. M.: Mineral dust aerosol impacts on global climate and climate change, Nature Reviews Earth and Environment, 4, 71-86, https://doi.org/10.1038/s43017-022-00379-5, 2023.

Kubilay, N., Nickovic, S., Moulin, C., and Dulac, F.: An illustration of the transport and deposition of mineral dust onto the eastern Mediterranean, Atmos Environ, 34, 1293–1303, 2000.

Kyllönen, K., Vestenius, M., Anttila, P., Makkonen, U., Aurela, M., Wängberg, I., Nerentorp Mastromonaco, M., and Hakola, H.: Trends and source apportionment of atmospheric heavy metals at a subarctic site during 1996–2018, Atmos Environ, 236, https://doi.org/10.1016/j.atmosenv.2020.117644, 2020.

Laing, J. R., Hopke, P. K., Hopke, E. F., Husain, L., Dutkiewicz, V. A., Paatero, J., and Viisanen, Y.: Long-term particle measurements in finnish arctic: Part I - Chemical composition and trace metal solubility, Atmos Environ, 88, 275–284, https://doi.org/10.1016/j.atmosenv.2014.03.002, 2014a.

Laing, J. R., Hopke, P. K., Hopke, E. F., Husain, L., Dutkiewicz, V. A., Paatero, J., and Viisanen, Y.: Long-term particle measurements in finnish arctic: Part II - trend analysis and source location identification, Atmos Environ, 88, 285–296, https://doi.org/10.1016/j.atmosenv.2014.01.015, 2014b.

Laj, P., Bigi, A., Rose, C., Andrews, E., Lund Myhre, C., Collaud Coen, M., Lin, Y., Wiedensohler, A., Schulz, M., A. Ogren, J., Fiebig, M., Gliß, J., Mortier, A., Pandolfi, M., Petäja, T., Kim, S. W., Aas, W., Putaud, J. P., Mayol-Bracero, O., Keywood, M., Labrador, L., Aalto, P., Ahlberg, E., Alados Arboledas, L., Alastuey, A., Andrade, M.,

Artinano, B., Ausmeel, S., Arsov, T., Asmi, E., Backman, J., Baltensperger, U., Bastian, S., Bath, O., Paul Beukes, J., T. Brem, B., Bukowiecki, N., Conil, S., Couret, C., Day, D., Dayantolis, W., Degorska, A., Eleftheriadis, K., Fetfatzis, P., Favez, O., Flentje, H., I. Gini, M., Gregorič, A., Gysel-Beer, M., Gannet Hallar, A., Hand, J., Hoffer, A., Hueglin, C., K. Hooda, R., Hyvärinen, A., Kalapov, I., Kalivitis, N., Kasper-Giebl, A., Eun Kim, J., Kouvarakis, G., Kranjc, I., Krejci, R., Kulmala, M., Labuschagne, C., Lee, H. J., Lihavainen, H., Lin, N. H., Löschau, G., Luoma, K., Marinoni, A., Martins Dos Santos, S., Meinhardt, F., Merkel, M., Metzger, J. M., Mihalopoulos, N., Anh Nguyen, N., Ondracek, J., Pérez, N., Rita Perrone, M., Pichon, J. M., Picard, D., Pichon, J. M., Pont, V., Prats, N., Prenni, A., Reisen, F., Romano, S., Sellegri, K., Sharma, S., Schauer, G., Sheridan, P., Patrick Sherman, J., Schütze, M., Schwerin, A., Sohmer, R., Sorribas, M., Steinbacher, M., Sun, J., Titos, G., et al.: A global analysis of climate-relevant aerosol properties retrieved from the network of Global Atmosphere Watch (GAW) near-surface observatories, Atmos Meas Tech, 13, 4353–4392, https://doi.org/10.5194/amt-13-4353-2020, 2020.

Landrigan, P. J., Fuller, R., Acosta, N. J. R., Adeyi, O., Arnold, R., Basu, N. (Nil), et al. (2018, February 3). The Lancet Commission on pollution and health. *The Lancet*. Lancet Publishing Group. https://doi.org/10.1016/S0140-6736(17)32345-0

Lelieveld, J., Klingmüller, K., Pozzer, A., Burnett, R. T., Haines, A., & Ramanathan, V. (2019). Effects of fossil fuel and total anthropogenic emission removal on public health and climate. *Proceedings of the National Academy of Sciences of the United States of America*, *116*(15), 7192–7197. https://doi.org/10.1073/pnas.1819989116

Li, J., Carlson, B. E., Yung, Y. L., Lv, D., Hansen, J., Penner, J. E., Liao, H., Ramaswamy, V., Kahn, R. A., Zhang, P., Dubovik, O., Ding, A., Lacis, A. A., Zhang, L., and Dong, Y.: Scattering and absorbing aerosols in the climate system, https://doi.org/10.1038/s43017-022-00296-7, 1 June 2022a.

Li, L., Mahowald, N. M., Miller, R. L., Pérez Garciá-Pando, C., Klose, M., Hamilton, D. S., Gonçalves Ageitos, M., Ginoux, P., Balkanski, Y., Green, R. O., Kalashnikova, O., Kok, J. F., Obiso, V., Paynter, D., and Thompson, D. R.: Quantifying the range of the dust direct radiative effect due to source mineralogy uncertainty, Atmos Chem Phys, 21, 3973–4005, https://doi.org/10.5194/acp-21-3973-2021, 2021.

Li, L., Mahowald, N. M., Kok, J. F., Liu, X., Wu, M., Leung, D. M., et al. (2022). Importance of different parameterization changes for the updated dust cycle modeling in the Community Atmosphere Model (version 6.1). *Geoscientific Model Development*, *15*(22), 8181–8219. https://doi.org/10.5194/gmd-15-8181-2022

Li, L., Mahowald, N. M., Liu, X., Ke, Z., Leung, D. M., Kok, F., Gonçalves Ageitos, M., Pérez García-Pando, C., Miller, R. L., Obiso, V., Formenti, P., Albani, S., Adebiyi, A. A., Di, C., Brodrick, P. G., Thompson, D. R., Green, R. O., and Clark, R. N.: Modeling Large Dust Aerosols in the Community Earth System Model, Journal of Advances in the Modeling of the Earth System, in prep.

Lim, S. S., Vos, T., Flaxman, A. D., Danaei, G., Shibuya, K., Adair-Rohani, H., and AlMazroa, M. ; A comparative risk assessment of burden of disease and injury attributable to 67 risk factors and risk factor clusters in 21 regions, 1990−2010: A systematic analysis for the Global Burden of Disease Study 2010., Lancet, 380, 2224–2260, 2012.

Deleted: Hamilton, D. S., Emmons, L. K., Huang, Y., Meng, J., Sexton, N., and Wan, J.:

Formatted: Font color: Black

Formatted: Font color: Black

Deleted: modelling

Deleted:),

Formatted: Font color: Black

Formatted: Font color: Black

Formatted: Font: Italic, Font color: Black

Deleted: Discussion,

Deleted: 2022-31,

Deleted: .

Formatted: Font color: Black

Formatted: Font color: Black

Formatted: Font: Times New Roman

Liu, X., Easter, R. C., Ghan, S. J., Zaveri, R., Rasch, P., Shi, X., Lamarque, J.-F., Gettelman, A., Morrison, H., Vitt, F., Conley, A., Park, S., Neale, R., Hannay, C., Ekman, A., Hess, P., Mahowald, N., Collins, W., Iacono, M., Bretherton, C., Flanner, M., and Mitchell, D: Toward a minimal representation of aerosols in climate models: Description and evaluation in the Community Atmosphere Model CAM5, Geoscientific Model Development, 5, 709-739, doi:10.5194/gmd-5-709-2012, 2012.

Liu, X., Ma, P. L., Wang, H., Tilmes, S., Singh, B., Easter, R. C., Ghan, S. J., and Rasch, P. J.: Description and evaluation of a new four-mode version of the Modal Aerosol Module (MAM4) within version 5.3 of the Community Atmosphere Model, Geosci Model Dev, 9, 505–522, https://doi.org/10.5194/gmd-9-505-2016, 2016.

Lucarelli, F., Calzolai, G., Chiari, M., Giannoni, M., Mochi, D., Nava, S., and Carraresi, L.: The upgraded external-beam PIXE/PIGE set-up at LABEC for very fast measurements on aerosol samples, Nucl Instrum Methods Phys Res B, 318, 55–59, https://doi.org/10.1016/j.nimb.2013.05.099, 2014.

Lucarelli, F., Barrera, V., Becagli, S., Chiari, M., Giannoni, M., Nava, S., Traversi, R., and Calzolai, G.: Combined use of daily and hourly data sets for the source apportionment of particulate matter near a waste incinerator plant, Environmental Pollution, 247, 802–811, https://doi.org/10.1016/j.envpol.2018.11.107, 2019.

Luo, C., Mahowald, N. M., and del Corral, J.: Sensitivity study of meteorological parameters on mineral aerosol mobilization, transport, and distribution, Journal of Geophysical Research D: Atmospheres, 108, 2003.

Luo, J., Han, Y., Zhao, Y., Liu, X., Huang, Y., Wang, L., Chen, K., Tao, S., Liu, J., and Ma, J.: An inter-comparative evaluation of PKU-FUEL global SO2 emission inventory, Science of the Total Environment, 722, https://doi.org/10.1016/j.scitotenv.2020.137755, 2020.

Mackey, K. R. M., Hunter, D., Fischer, E. V, Jiang, Y., Allen, B., Chen, Y., Liston, A., Reuter, J., Schladow, G., and Paytan, A.: Aerosol-nutrient-induced picoplankton growth in Lake Tahoe, J Geophys Res Biogeosci, 118, 1054–1067, https://doi.org/10.1002/jgrg.20084, 2013.

Maenhaut, W., Cafmeyer, J.., Ptasinski, J., Andreae, M. O., Andreae, T. W., Elbert, W., Meixner, F. X., Karnieli, A., and Ichoku, C.: Chemical composition and light scattering of the atmospheric aerosol at a remote site in the Negev desert, Israel, J. Aerosol Sci., 28 (suppl.), 73–74, 1997b.

Maenhaut, W. and Cafmeyer, J.: Long-Term Atmospheric Aerosol Study at Urban and Rural Sites in Belgium Using Multi-Elemental Analysis by Particle-Induced X-Ray Emission Spectrometry and Short-Irradiation Instrumental Neutron Activation Analysis, X-Ray Spectrometry, 27, 236–246, https://doi.org/10.1002/(SICI)1097-4539(199807/08)27:4<236::AID-XRS292>3.0.CO;2-F, 1998.

Maenhaut, W., Salomonovic, R., Cafmeyer, J., Ichoku, C., Karnieli, A., and Andreae, M. O.: Anthropogenic and natural radiatively active aerosol types at Sede Boker, Israel, J. Aerosol Sci., 27 (suppl., 47–48, https://doi.org/10.1016/0021-8502(96)00096-1, 1996a.

Maenhaut, W., Koppen, G., and Artaxo, P.: Long-term atmospheric aerosol study in Cuiaba´, Brazil: Multielemental composition, sources, and impact of biomass burning, in: Biomass Burning and Global Change, vol. 2, Biomass

Deleted: REaster

Burning in South America, Southeast Asia, and Temperate and Boreal Ecosystems, and the Oil Fires of Kuwait, edited by: Levine, J. S., MIT Press, Cambridge Massachusetts, 637–652, 1996b.

Maenhaut, W., Salma, I., Cafmeyer, J., Annegard, H., and Andreae, M.: Regional atmospheric aerosol composition and sources in the eastern Transvaal, South Africa and impact of biomass burning, J Geophys Res, 101, 23631–23650, 1996c.

Maenhaut, W., Francois, F., Cafmeyer, J., Gilot, C., and Hanssen, J. E.: Long-term aerosol study in southern Norway, and the relationship of aerosol components to source, in: Proceedings of EUROTRAC Symposium '96, vol. 1, Clouds, Aerosols, Modelling and Photo-oxidants, edited by: Borrell, P. M., Comput. Mech. Publ., South Hampton, UK), 277–280, 1997a.

Maenhaut, W., Fernandez-Jimenez, M.-T., and Artaxo, P.: Long-term study of atmospheric aerosols in Cuiaba, Brazil: Multielemental composition, sources and source apportionment, J. Aerosol Sci., 30 (suppl., 259–260, 1999.

Maenhaut, W., Fernandez-Jimenez, M.-T., Vanderzalm, J. L., Hooper, B., Hooper, M. A., and Tapper, N. J.: Aerosol composition at Jabiru, Australia, and impact of biomass burning, J. Aerosol Sci., 31 (suppl., 745–746, https://doi.org/10.1016/S0021-8502(00)90755-9, 2000a.

Maenhaut, W., Fernandez-Jimenez, M.-T., Rajta, I., Dubtsov, S., Meixner, F. X., Andreae, M. O., Torr, S., Hargrove, J. W., Chimanga, P., and Mlambo, J.: Long-term aerosol composition measurements and source apportionment at Rukomechi, Zimbabwe, J. Aerosol Sci., 31 (suppl., 228–229, https://doi.org/10.1016/S0021-8502(00)90237-4., 2000b.

Maenhaut, W., De Ridder, D. J. A., Fernandez-Jimenez, M.-T., Hooper, M. A., Hooper, B., and Nurhayati, M.: Long-term observations of regional aerosol composition at two sites in Indonesia, Nucl. Instrum. Methods Phys. Res., Sect. B., 189, 259–265, https://doi.org/10.1016/S0168- 583X(01)01054-0., 2002a.

Maenhaut, W., Fernandez-Jimenez, M.-T., Rajta, I., and Artaxo, P.: Two-year study of atmospheric aerosol particles in Alta Floresta, Brazil: Multielemental composition and source apportionment, Nuclear Instruments and Methods in Physics Research B, 189, 243–248, 2002b.

Maenhaut, W., Raes, N., Chi, X., Cafmeyer, J., Wang, W., and Salma, I.: Chemical composition and mass closure for fine and coarse aerosols at a kerbside in Budapest, Hungary, in spring 2002, X-Ray Spectrometry, 34, 290–296, https://doi.org/10.1002/xrs.820, 2005.

Maenhaut, W., Raes, N., Chi, X., Cafmeyer, J., and Wang, W.: Chemical composition and mass closure for PM2.5 and PM 10 aerosols at K-puszta, Hungary, in summer 2006, in: X-Ray Spectrometry, 193–197, https://doi.org/10.1002/xrs.1062, 2008.

Maenhaut, W., Nava, S., Lucarelli, F., Wang, W., Chi, X., and Kulmala, M.: Chemical composition, impact from biomass burning, and mass closure for PM2.5 and PM10 aerosols at Hyytiälä, Finland, in summer 2007, X-Ray Spectrometry, 40, 168–171, https://doi.org/10.1002/xrs.1302, 2011.

Mahowald, N., Li, L., Vira, J., Prank, M., Hamilton, D. S., Matsui, H., Miller, R. L., Lu, L., Akyuz, E. A., Daphne, M., Hess, P., Lihavainen, H., Wiedinmyer, C., Hand, J., Alaimo, M. G., Alves, C., Alastuey, A., Artaxo, P., Barreto, A., Barraza, F., Becagli, S., Calzolai, G., Chellam., S., Chen, Y., Chuang, P., Cohen, D. Colombi, C., Diapouli, E. Dongarra, G., Eleftheriadis, K., Galy-Lacaux, C., Gaston, C., Gomez, D., Gonzalez Ramos, Y., Hakola, H., Harrison, R., Heyes, C., Herut, B., Hopke, P., Huglin, C., Kanakidou, M., Kertesz, Z., Klimont, Z., Kyllonen, K., Lambert, F., Liu, X., Losno, R., Lucarelli, F., Maenhaut, W., Marticorena, B., Martin, R., Mihalopoulos, N., Morera-Gomez, Y. Paytan, A., Prospero, J., Rodriguez, S., Smichowski, P., Varrica, D., Walsh, B. Weagle, C., Zhao, X. (2024). Datasets for: AERO-MAP: A data compilation and modelling approach to understand the fine and coarse mode aerosol composition (January 4, 2024 version) [Data set]. Zenodo. https://doi.org/10.5281/zenodo.10459654

Mahowald, N., Lamarque, J.-F., Tie, X., and Wolff, E.: Sea salt aerosol response to climate change: last glacial maximum, pre-industrial, and doubled-carbon dioxide climates, J Geophys Res, 111, D05303; doi:10.1029/2005JD006459, 2006.

Mahowald, N., Jickells, T. D., Baker, A. R., Artaxo, P., Benitez-Nelson, C. R., Bergametti, G., Bond, T. C., Chen, Y., Cohen, D. D., Herut, B., Kubilay, N., Losno, R., Luo, C., Maenhaut, W., McGee, K. A., Okin, G. S., Siefert, R. L., and Tsukuda, S.: Global distribution of atmospheric phosphorus sources, concentrations and deposition rates, and anthropogenic impacts, Global Biogeochem Cycles, 22, https://doi.org/10.1029/2008GB003240, 2008.

Mahowald, N. M., Kloster, S., Engelstaedter, S., Moore, J. K. K., Mukhopadhyay, S., McConnell, J. R. R., et al. (2010). Observed 20th century desert dust variability: impact on climate and biogeochemistry. *Atmospheric Chemistry and Physics*, *10*(22), 10875–10893. https://doi.org/10.5194/acp-10-10875-2010

Mahowald, N., Ward, D. S., Kloster, S., Flanner, M. G., Heald, C. L., Heavens, N. G., Hess, P. G., Lamarque, J.-F., and Chuang, P. Y.: Aerosol Impacts on Climate and Biogeochemistry, Annu Rev Environ Resour, 36, 45–74, https://doi.org/10.1146/annurev-environ-042009-094507, 2011.

Mahowald, N. M., Engelstaedter, S., Luo, C., Sealy, A., Artaxo, P., Benitez-Nelson, C., Bonnet, S., Chen, Y., Chuang, P. Y., Cohen, D., Dulac, F., Herut, B., Johansen, A. M., Kubilay, N., Losno, R., Maenhaut, W., Paytan, A., Prospero, J. M., Shank, L. M., and Siefert, R. L.: Atmospheric Iron Deposition: Global Distribution, Variability, and Human Perturbations, Annual Review of Marine Science of Marine Science, 1, 245–278, https://doi.org/10.1146/annurev.marine.010908.163727, 2009.

Mahowald, N. M., Scanza, R., Brahney, J., Goodale, C. L., Hess, P. G., Moore, J. K., and Neff, J.: Aerosol Deposition Impacts on Land and Ocean Carbon Cycles, Curr Clim Change Rep, 3, 16–31, https://doi.org/10.1007/s40641-017-0056-z, 2017.

Mahowald, N. M., Hamilton, D. S., Mackey, K. R. M., Moore, J. K., Baker, A. R., Scanza, R., and Zhang, Y.: Aerosol trace metal deposition dissolution and impacts on marine microorganisms and biogeochemistry, Nature Communication, 81, 1–15, https://doi.org/10.1038/s41467-018-04970-7, 2018.

Malm, W., Pitchford, M., McDade, C., and Ashbaugh, L.: Coarse particle speciation at selected locations in the rural continental United States, Atmos Environ, 41, 225–2239, 2007.

Marshak, A., Ackerman, A., da Silva, A. M., Eck, T., Holben, B., Kahn, R., et al. (2021, November 1). Aerosol properties in cloudy environments from remote sensing observations. A review of the current state of knowledge. *Bulletin of the American Meteorological Society*. American Meteorological Society. https://doi.org/10.1175/BAMS-D-20-0225.1

Mbengue, S., Zikova, N., Schwarz, J., Vodička, P., Šmejkalová, A. H., and Holoubek, I.: Mass absorption cross-section and absorption enhancement from long term black and elemental carbon measurements: A rural background station in Central Europe, Science of the Total Environment, 794, https://doi.org/10.1016/j.scitotenv.2021.148365, 2021.

Marticorena, B., Chatenet, B., Rajot, J., Traore, S., Diallo, A., Kone, I., Maman, A., NDiaye, T., and Zakou, A.: Temporal variability of mineral dust concentrations over West Africa: analyses of a pluriannual monitoring from the AMMA Sahelian Dust Transect, Atmos. Chem. Phys., 10, 2010–8899, 2010.

Matsui, H. and N. Mahowald (2017), Development of a global aerosol model using a two-dimensional sectional method: 2. Evaluation and sensitivity simulations, Journal of Advances in Modeling Earth Systems, 9, 1887-1920, doi:10.1002/2017MS000937.

McNeill, J., Snider, G., Weagle, C. L., Walsh, B., Bissonnette, P., Stone, E., Abboud, I., Akoshile, C., Anh, N. X., Balasubramanian, R., Brook, J. R., Coburn, C., Cohen, A., Dong, J., Gagnon, G., Garland, R. M., He, K., Holben, B. N., Kahn, R., Kim, J. S., Lagrosas, N., Lestari, P., Liu, Y., Jeba, F., Joy, K. S., Martins, J. V., Misra, A., Norford, L. K., Quel, E. J., Salam, A., Schichtel, B., Tripathi, S. N., Wang, C., Zhang, Q., Brauer, M., Gibson, M. D., Rudich, Y., and Martin, R. V.: Large global variations in measured airborne metal concentrations driven by anthropogenic sources, Sci Rep, 10, https://doi.org/10.1038/s41598-020-78789-y, 2020.

Mihalopoulos N., E. Stephanou, M. Kanakidou, S. Pilitsidis and P. Bousquet, Tropospheric aerosol ionic composition above the Eastern Mediterranean Area, Tellus B, 49B, 314-326, 1997.

Millet, D. B., Palmer, P. I., Levelt, P. F., Gallardo, L., & Shikwambana, L. (2024, October 1). Coordinated Geostationary, Multispectral Satellite Observations Are Critical for Climate and Air Quality Progress. *AGU Advances*. John Wiley and Sons Inc. https://doi.org/10.1029/2024AV001322

Mirante F., Oliveira C., Martins N., Pio C., Caseiro A., Cerqueira M., Alves C., Oliveira C., Oliveira J., Camões F., Matos M., and Silva H.: Carbonaceous content of atmospheric aerosols in Lisbon urban atmosphere. European Geophysical Union General Assembly, 2-7 May, Vienna, Austria, 2010.

Mirante, F., Alves, C., Pio, C., Pindado, O., Perez, R., Revuelta, M. A., and Artiñano, B.: Organic composition of size segregated atmospheric particulate matter, during summer and winter sampling campaigns at representative sites in Madrid, Spain, Atmos Res, 132–133, 345–361, https://doi.org/10.1016/j.atmosres.2013.07.005, 2013.

Mkoma, S. L.: Physico-chemical characterisation of atmospheric aerosols in Tanzania, with emphasis on the carbonaceous aerosol components and on chemical mass closure, Ghent University, Ghent, Belgium, 2008.

Mkoma, S. L., Maenhaut, W., Chi, X., Wang, W., and Raes, N.: Characterisation of PM10 atmospheric aerosols for the wet season 2005 at two sites in East Africa, Atmos Environ, 43, 631–639, https://doi.org/10.1016/j.atmosenv.2008.10.008, 2009.

Morera-Gómez, Y., Elustondo, D., Lasheras, E., Alonso-Hernández, C. M., and Santamaría, J. M.: Chemical characterization of PM10 samples collected simultaneously at a rural and an urban site in the Caribbean coast: Local and long-range source apportionment, Atmos Environ, 192, 182–192, https://doi.org/10.1016/j.atmosenv.2018.08.058, 2018.

Morera-Gómez, Y., Santamaría, J. M., Elustondo, D., Lasheras, E., and Alonso-Hernández, C. M.: Determination and source apportionment of major and trace elements in atmospheric bulk deposition in a Caribbean rural area, Atmos Environ, 202, 93–104, https://doi.org/10.1016/j.atmosenv.2019.01.019, 2019.

Mortier, A., Gliß, J., Schulz, M., Aas, W., Andrews, E., Bian, H., Chin, M., Ginoux, P., Hand, J., Holben, B., Zhang, H., Kipling, Z., Kirkevåg, A., Laj, P., Lurton, T., Myhre, G., Neubauer, D., Olivié, D., von Salzen, K., Skeie, R. B., Takemura, T., and Tilmes, S.: Evaluation of climate model aerosol trends with ground-based observations over the last 2 decades - an AeroCom and CMIP6 analysis, Atmos Chem Phys, 20, 13355–13378, https://doi.org/10.5194/acp-20-13355-2020, 2020.

Murray, C. J. L., Aravkin, A. Y., Zheng, P., Abbafati, C., Abbas, K. M., Abbasi-Kangevari, M., et al. (2020). Global burden of 87 risk factors in 204 countries and territories, 1990–2019: a systematic analysis for the Global Burden of Disease Study 2019. *The Lancet*, *396*(10258), 1223–1249. https://doi.org/https://doi.org/10.1016/S0140-6736(20)30752-2

Nava, S., Lucarelli, F., Amato, F., Becagli, S., Calzolai, G., Chiari, M., Giannoni, M., Traversi, R., and Udisti, R.: Biomass burning contributions estimated by synergistic coupling of daily and hourly aerosol composition records, Science of the Total Environment, 511, 11–20, https://doi.org/10.1016/j.scitotenv.2014.11.034, 2015.

Nava, S., Calzolai, G., Chiari, M., Giannoni, M., Giardi, F., Becagli, S., Severi, M., Traversi, R., and Lucarelli, F.: Source apportionment of PM2.5 in Florence (Italy) by PMF analysis of aerosol composition records, Atmosphere (Basel), 11, https://doi.org/10.3390/ATMOS11050484, 2020.

Neff, J., Reynolds, M. P., Munson, S., Fernandez, D., and Belnap, J.: The role of dust storms in total atmospheric particle concentration at two sites in the western U.S., J Geophys Res, 118, 11,201–11,212, 2013.

Nenes, A., Pandis, S. N., Kanakidou, M., Russell, A., Song, S., Vasilakos, P., and Weber, R. J.: Aerosol acidity and liquid water content regulate the dry deposition of inorganic reactive nitrogen, Atmos. Chem. Phys., 21, 6023–6033, https://doi.org/10.5194/acp-21-6023-2021, 2021.

Nyanganyura, D., Maenhaut, W., Mathutu, M., Makarau, A., and Meixner, F. X.: The chemical composition of tropospheric aerosol particles and their contributing sources to a continental background site in northern Zimbabwe from 1994 to 2000, Atmos. Environ., 41, 2644–2659, https://doi.org/10.1016/j.atmosenv.2006.11.015, 2007.

Deleted: 1–12

Obiso, V., Gonçalves Ageitos, M., Pérez García-Pando,C., Schuster, G. L., Bauer, S. E., Di Biagio, C., Formenti, P. Perlwitz, J. P., Tsigaridis,K., and Miller, R. L., 2023: Observationally constrained regional variations of shortwave absorption by iron oxides emphasize the cooling effect of dust. Atmos. Chem. Phys., submitted.

Oliveira, C., Pio, C., Caseiro, A., Santos, P., Nunes, T., Mao, H., Luahana, L., and Sokhi, R.: Road traffic impact on urban atmospheric aerosol loading at Oporto, Portugal, Atmos Environ, 44, 3147–3158, https://doi.org/10.1016/j.atmosenv.2010.05.027, 2010.

Oliveira C., PAHLIS Team: Atmospheric pollution in Lisbon urban atmosphere. European Geosciences Union General Assembly, 19-24 Apr., Vienna, Austria, 2009.

Olson, J., Prather, M., Berntsen, T., Carmichael, G., Chatfield, R., Connell, P., Derwent, R., Horowitz, L., Jin, S., Kanakidou, M., Kasibhatla, P., Kotamarthi, R., Kuhn, M., Law, K., Penner, J., Perliski, L., Sillman, S., Stordal, F., Thompson, A., and Wild, O.: Results from the Intergovernmental Panel on Climatic Change Photochemical Model Intercomparison (PhotoComp), Journal of Geophysical Research: Atmospheres, 102, 5979–5991, https://doi.org/doi:10.1029/96JD03380, 1997.

Paulot, F., Ginoux, P., Cooke, W. F., Donner, L. J., Fan, S., Lin, M. Y., Mao, J., Naik, V., and Horowitz, L. W.: Sensitivity of nitrate aerosols to ammonia emissions and to nitrate chemistry: Implications for present and future nitrate optical depth, Atmos Chem Phys, 16, 1459–1477, https://doi.org/10.5194/acp-16-1459-2016, 2016.

Pérez, N., Pey, J., Querol, X., Alastuey, A., López, J. M., and Viana, M.: Partitioning of major and trace components in PM10-PM2.5-PM1 at an urban site in Southern Europe, Atmos Environ, 42, 1677–1691, https://doi.org/10.1016/j.atmosenv.2007.11.034, 2008.

Philip, S., Martin, R. v., Snider, G., Weagle, C. L., van Donkelaar, A., Brauer, M., Henze, D. K., Klimont, Z., Venkataraman, C., Guttikunda, S. K., and Zhang, Q.: Anthropogenic fugitive, combustion and industrial dust is a significant, underrepresented fine particulate matter source in global atmospheric models, Environmental Research Letters, 12, 1–46, 2017.

Pio, C., Rienda, I. C., Nunes, T., Gonçalves, C., Tchepel, O., Pina, N. K., Rodrigues, J., Lucarelli, F., and Alves, C. A.: Impact of biomass burning and non-exhaust vehicle emissions on PM10 levels in a mid-size non-industrial western Iberian city, Atmos Environ, 289, https://doi.org/10.1016/j.atmosenv.2022.119293, 2022.

Pio, C. A., & Lopes, D. A. (1998). Chlorine loss from marine aerosol in a coastal atmosphere. *Journal of Geophysical Research Atmospheres*, *103*(D19), 25263–25272. https://doi.org/10.1029/98JD02088

Prank, M., Sofiev, M., Tsyro, S., Hendriks, C., Semeena, V., Francis, X. V., Butler, T., Van Der Gon, H. D., Friedrich, R., Hendricks, J., Kong, X., Lawrence, M., Righi, M., Samaras, Z., Sausen, R., Kukkonen, J., and Sokhi, R.: Evaluation of the performance of four chemical transport models in predicting the aerosol chemical composition in Europe in 2005, Atmos Chem Phys, 16, 6041–6070, https://doi.org/10.5194/acp-16-6041-2016, 2016.

Prospero, J., Bullard, J., and Hodkins, R.: High-Latitude Dust Over the North Atlantic: Inputs from Icelandic Proglacial Dust Storms, Science (1979), 335, 1078–1082, 2012.

1409 Prospero, J., Barkely, A., Gaston, C., Gatineau, A., Campos y Sanasano, A., and Pulcherie, K. P.: Data From: Characterizing
1410 and quantifying African dust transport and deposition to South America: Implications for the phosphorus budget in
1411 the Amazon Basin, Miami, https://doi.org/https://doi.org/10.17604/vrsh-w974, 2020.
1412 Prospero, J. M.: Long-range transport of mineral dust in the global atmosphere: Impact of African dust on the environment
1413 of the southeastern United States, Proc. Natl. Academy Science, 96, 3396–3403, 1999.
1414 Prospero, J. M., Uematsu, M., and Savoie, D. L.: Mineral Aerosol Transport to the Pacific Ocean, in: Chemical
1415 Oceanography, vol. 10, Academic Press Limited, 187–218, 1989.
1416 Prospero, J.: The atmospheric transport of particles to the ocean, in: Particle Flux in the Ocean, edited by: Ittekkot, I.,
1417 Schaffer, P., Honjo, S., and Depetris, P. J., John Wiley, New York, 1996.
1418 Prospero, J. M., Barrett, K., Church, T., Dentener, F., Duce, R. A., Galloway, J. N., Levy, H., Moody, J., and Quinn, P.:
1419 Atmospheric deposition of nutrients to the North Atlantic Basin, Biogeochemistry, 35, 27–73,
1420 https://doi.org/10.1007/BF02179824, 1996.
1421 Putaud, J.-P., Raes, F., Dingenen, R. Van, U. Baltensperger, Bruggemann, E., Facchini, M.-C., Decesari, S., Fuzzi, S., R.
1422 Gehrig, Huglin, C., Laj, P., Lorbeer, G., Maenhaut, W., N. Mihalopoulos, Muller, K., Querol, X., Rodriguez, S.,
1423 Schneider, J., G. Spindler, ten Brink, H., Torseth, K., and Wiedensohler., A.: A European aerosol phenomenology.
1424 2: chemical characteristics of particulate matter at kerbside, urban, rural and background sites in Europe, Atmos
1425 Environ, 38, 2579–2595, 2004.
1426 Putaud, J. P., Van Dingenen, R., Alastuey, A., Bauer, H., Birmili, W., Cyrys, J., Flentje, H., Fuzzi, S., Gehrig, R., Hansson,
1427 H. C., Harrison, R. M., Herrmann, H., Hitzenberger, R., Hüglin, C., Jones, A. M., Kasper-Giebl, A., Kiss, G.,
1428 Kousa, A., Kuhlbusch, T. A. J., Löschau, G., Maenhaut, W., Molnar, A., Moreno, T., Pekkanen, J., Perrino, C., Pitz,
1429 M., Puxbaum, H., Querol, X., Rodriguez, S., Salma, I., Schwarz, J., Smolik, J., Schneider, J., Spindler, G., ten
1430 Brink, H., Tursic, J., Viana, M., Wiedensohler, A., and Raes, F.: A European aerosol phenomenology - 3: Physical
1431 and chemical characteristics of particulate matter from 60 rural, urban, and kerbside sites across Europe, Atmos
1432 Environ, 44, 1308–1320, https://doi.org/10.1016/j.atmosenv.2009.12.011, 2010.
1433 Quass, J., Jia, H., Smith, C., Albright, A. L., Aas, W., Bellouin, N., Boucher, O., Doutriaux-Boucher, M., Forster, P. M.,
1434 Grosvenor, D., Jenkins, S., Klimont, Z., Loeb, N. G., Ma, X., Naik, V., Paulot, F., Stier, P., Wild, M., Myhre, G.,
1435 and Schulz, M.: Robust evidence for reversal of the trend in aerosol effective climate forcing, Atmos. Chem. Phys.,
1436 22, 12221–12239, https://doi.org/10.5194/acp-22-12221-2022, 2022.
1437 Rasch, P. J. J., Feichter, J., Law, K., Mahowald, N., Penner, J., Benkovitz, C., Genthon, C., Giannakopoulos, C., Kasibhatla,
1438 P., Koch, D., Levy, H., Maki, T., Prather, M., Roberts, D. L. L., Roelofs, G.-J. G. J., Stevenson, D., Stockwell, Z.,
1439 Taguchi, S., Kritz, M., Chipperfield, M., Baldocchi, D., McMurry, P., Barrie, L., Balkanski, Y., Chatfield, R.,
1440 Kjellstrom, E., Lawrence, M., Lee, H. N. N., Lelieveld, J., Noone, K. J. J., Seinfeld, J., Stenchikov, G., Schwartz,
1441 S., Walcek, C., Williamson, D., Feichter, H., Law, K., Mahowald, N., Penner, J., Benkovitz, C., Genthon, C.,
1442 Giannakopoulos, C., Kasibhatla, P., Koch, D., Levy, H., Maki, T., Prather, M., Roberts, D. L. L., Roelofs, G.-J. G.

J., Stevenson, D., Stockwell, Z., Taguchi, S., Chipperfield, M., Baldocchi, D., McMurry, P., Barrie, L., Balkanski, Y., Chatfield, B., Jacob, D., Kritz, M., Lawrence, M., Lee, H. N. N., Leaitch, R., Lelieveld, J., Noone, K. J. J., Seinfeld, J., Stenchikov, G., Schwarz, S., Walcek, C., and Williamson, D.: An Assessment of Scavenging and Deposition Processes in Global Models: Results from the WCRP Cambridge Workshop of 1995, Tellus, 52B, 1025–1056, 2000.

Reddington, C. L., Carslaw, K. S., Stier, P., Schutgens, N., Coe, H., Liu, D., et al. (2017). The global aerosol synthesis and science project (GASSP): Measurements and modeling to reduce uncertainty. *Bulletin of the American Meteorological Society*, *98*(9), 1857–1877. https://doi.org/10.1175/BAMS-D-15-00317.1

Regayre, L. A., Johnson, J. S., Yoshioka, M., Pringle, K. J., Sexton, D. M. H., Booth, B. B. B., Lee, L. A., Bellouin, N., and Carslaw, K. S.: Aerosol and physical atmosphere model parameters are both important sources of uncertainty in aerosol ERF, Atmos Chem Phys, 18, 9975–10006, https://doi.org/10.5194/acp-18-9975-2018, 2018.

Reid, J. S., Jonson, H., Maring, H., Smirnov, A., Savoie, D., Cliff, S., Reid, E., Livingston, J., Meier, M., Dubovik, O., and Tsay, S.-C.: Comparison of size and morphological measurements of dust particles from Africa, J Geophys Res, 108, 8593: doi:1029/2002JD002485, 2003.

Remer, L., Kaufman, Y., Tanre, D., Mattoo, S., Chu, D., Martins, J., Li, R., Ichoku, C., Levy, R., Kleidman, R., Eck, T., Vermote, E., and Holbren, B.: The MODIS aerosol algorithm, products and validation, J Atmos Sci, 62, 947–973, 2005.

Remer, L. A., Kleidman, R. G., Levy, R. C., Kaufman, Y. J., Tanré, D., Mattoo, S., et al. (2008). Global aerosol climatology from the MODIS satellite sensors. *Journal of Geophysical Research Atmospheres*, *113*(14). https://doi.org/10.1029/2007JD009661

Rodríguez, S., Alastuey, A., Alonso-Pérez, S., Querol, X., Cuevas, E., Abreu-Afonso, J., Viana, M., Pérez, N., Pandolfi, M., and De La Rosa, J.: Transport of desert dust mixed with North African industrial pollutants in the subtropical Saharan Air Layer, Atmos Chem Phys, 11, 6663–6685, https://doi.org/10.5194/acp-11-6663-2011, 2011.

Rodríguez, S., Alastuey, A., and Querol, X.: A review of methods for long term in situ characterization of aerosol dust, https://doi.org/10.1016/j.aeolia.2012.07.004, October 2012.

Rodríguez, S., Cuevas, E., Prospero, J. M., Alastuey, A., Querol, X., López-Solano, J., García, M. I., and Alonso-Pérez, S.: Modulation of Saharan dust export by the North African dipole, Atmos Chem Phys, 15, 7471–7486, https://doi.org/10.5194/acp-15-7471-2015, 2015.

Salma, I., Maenhaut, W., Annegarn, H. J., Andreae, M. O., Meixner, F. X., and Garstang., M.: Combined application of INAA and PIXE for studying the regional aerosol composition in Southern Africa, Journal of Geophysical Research, 101, 2361–23650, 1997.

Savoie, D. L., Prospero, J. M., Larsen, R. J., Huang, R., Izaguirre, M. A., Huang, T., Snowdon, T., Custals, L., and Sanderson, C.: Nitrogen and sulfur species in Antarctic aerosols at Mawson, Palmer Station, and Marsh (King George Island), J Atmos Chem, 17, 95–122, 1993.

Sayer, A. M., Govaerts, Y., Kolmonen, P., Lipponen, A., Luffarelli, M., Mielonen, T., et al. (2020). A review and framework for the evaluation of pixel-level uncertainty estimates in satellite aerosol remote sensing. *Atmospheric Measurement Techniques*, *13*(2), 373–404. https://doi.org/10.5194/amt-13-373-2020

Scanza, R., Mahowald, N., Ghan, S., Zender, C., Kok, J., Liu, X., and Zhang, Y.: Dependence of dust radiative forcing on mineralogy in the Community Atmosphere Model, Atmos Chem Phys, 15, 537–561, 2015.

Schlesinger, W. H. (1997). *Biogeochemistry: an analysis of global change* (2nd ed.). San Diego: Academic Press.

Schulz, M., Textor, C., Kinne, S., Balkanski, Y., Bauer, S., Berntsen, T., et al. (2006). Radiative forcing by aerosols as derived from the AeroCom present-day and preindustrial simulations. *Atmospheric Chemistry and Physics*, *6*(12), 2006–5225.

Schulz, M., Prospero, J. M., Baker, A. R., Dentener, F., Ickes, L., Liss, P. S., Mahowald, N. M., Nickovic, S., García-Pando, C. P., Rodríguez, S., Sarin, M., Tegen, I., and Duce, R. A.: Atmospheric transport and deposition of mineral dust to the ocean: Implications for research needs, Environ Sci Technol, 46, https://doi.org/10.1021/es300073u, 2012.

Schuster, G. L., Dubovik, O., and Arola, A.: Remote sensing of soot carbon – Part 1: Distinguishing different absorbing aerosol species, Atmos. Chem. Phys., 16, 1565–1585, https://doi.org/10.5194/acp-16-1565-2016, 2016.

Schutgens, N. A. J., Gryspeerdt, E., Weigum, N., Tsyro, S., Goto, D., Schulz, M., and Stier, P.: Will a perfect model agree with perfect observations? The impact of spatial sampling, Atmos Chem Phys, 16, 6335–6353, https://doi.org/10.5194/acp-16-6335-2016, 2016.

Seinfeld, J. H. and Pandis, S. N.: Atmospheric Chemistry and Physics: From Air Pollution to Climate Change, 2006.

Silva, H.F., Matos, M. J., Oliveira, C., Ferreira, A. F., Oliveira, J. C., Cantinho, P., Calado, M., Oliveira, C., Martins, N., Pio, C., and Camões M. F. : Effect of climate on PM concentration and size distribution in two sites in the city of Lisbon, Encontro de Jovens Químicos Portugueses, Aveiro, 21 to 23 of April, 2010.

Skiles, S. M. K., Flanner, M., Cook, J. M., Dumont, M., and Painter, T. H.: Radiative forcing by light-absorbing particles in snow, https://doi.org/10.1038/s41558-018-0296-5, 1 November 2018.

Smichowski, P., Gómez, D. R., Dawidowski, L. E., Giné, M. F., Bellato, A. C. S., and Reich, S. L.: Monitoring trace metals in urban aerosols from Buenos Aires city. Determination by plasma-based techniques, Journal of Environmental Monitoring, 6, 286–294, https://doi.org/10.1039/b312446k, 2004.

Smith, M. B., Mahowald, N. M., Albani, S., Perry, A., Losno, R., Qu, Z., Marticorena, B., Ridley, D. A., and Heald, C. L.: Sensitivity of the interannual variability of mineral aerosol simulations to meteorological forcing dataset, Atmos Chem Phys, 17, https://doi.org/10.5194/acp-17-3253-2017, 2017.

Swap, R., Garstang, M., Greco, S., Talbot, R., and Kallberg, P.: Saharan dust in the Amazon Basin, Tellus, 44B, 133–149, https://doi.org/https://doi.org/10.3402/tellusb.v44i2.15434, 1992.

Szopa, S., Naik, V., Adhikary, B., Artaxo, P., Berntsen, T., Collins, W. D., Aas, W., Akritidis, D., Allen, R. J., Kanaya, Y., Prather, M. J., Kuo, C., Zhai, P., Pirani, A., Connors, S., Péan, C., Berger, S., Caud, N., Chen, Y., Goldfarb, L., Gomis, M., Huang, M., Leitzell, K., Lonnoy, E., Matthews, J., Maycock, T., Waterfield, T., Yelekçi, O., Yu, R., and

Zhou, B.: Chapter 6: Short-lived Climate Forcers, in: Climate Change 2021: The Physical Science Basis. Contribution of Working Group I to the Sixth Assessment Report of the Intergovernmental Panel on Climate Change, edited by: Masson-Delmotte, V. , Zhai, P., A. Pirani, A., Connors, S. L., Péan, C. S., Berger, S., Caud, N., Chen, Y., Goldfarb, L., Gomis, M. I., Huang, M., Leitzell, K., Lonnoy, E., Matthews, J. B. R., Maycock, T. K., Waterfield, T., Yelekçi, O., Yu, R., and Zhou, B., Cambridge University Press, , Cambridge, United Kingdom and New York, NY, USA, 816–921, https://doi.org/10.1017/9781009157896.008, 2021.

Tanré, D., Kaufman, Y. J., Herman, M., and Mattoo, S.: Remote sensing of aerosol properties over oceans using the MODIS/EOS spectral radiances, J Geophys Res, 102, 16,916-971,988, 1997.

Textor, C. and others: Analysis and quantification of the diversities of aerosol life cycles within AeroCOM, Atmos Chem Phys, 6, 1777–1813, 2006.

Thornhill, G., Collins, W., Olivié, D., B. Skeie, R., Archibald, A., Bauer, S., Checa-Garcia, R., Fiedler, S., Folberth, G., Gjermundsen, A., Horowitz, L., Lamarque, J. F., Michou, M., Mulcahy, J., Nabat, P., Naik, V., M. O'Connor, F., Paulot, F., Schulz, M., E. Scott, C., Séférian, R., Smith, C., Takemura, T., Tilmes, S., Tsigaridis, K., and Weber, J.: Climate-driven chemistry and aerosol feedbacks in CMIP6 Earth system models, Atmos Chem Phys, 21, 1105–1126, https://doi.org/10.5194/acp-21-1105-2021, 2021.

Toro, C., Sonntag, D., Bash, J., Burke, G., Murphy, B. N., Seltzer, K. M., Simon, H., Shephard, M. W., and Cady-Pereira, K. E.: Sensitivity of air quality to vehicle ammonia emissions in the United States, Atmos Environ, 327, https://doi.org/10.1016/j.atmosenv.2024.120484, 2024.

Tørseth, K., Aas, W., Breivik, K., Fjeraa, A. M., Fiebig, M., Hjellbrekke, A. G., Lund Myhre, C., Solberg, S., and Yttri, K. E.: Introduction to the European Monitoring and Evaluation Programme (EMEP) and observed atmospheric composition change during 1972-2009, https://doi.org/10.5194/acp-12-5447-2012, 2012.

Tsigaridis K., N. Daskalakis, M. Kanakidou, P. J. Adams, P. Artaxo, R. Bahadur, Y. Balkanski, S. E. Bauer, N. Bellouin, A. Benedetti, T. Bergman, T. K. Berntsen, J. P. Beukes, H. Bian, K. S. Carslaw, M. Chin, G. Curci, T. Diehl, R. C. Easter, S. J. Ghan, S. L. Gong, A. Hodzic, C. R. Hoyle, T. Iversen, S. Jathar, J. L. Jimenez, J. W. Kaiser, A. Kirkevag, D. Koch, H. Kokkola, Y. H Lee, G. Lin, X. Liu, G. Luo, X. Ma, G. W. Mann, N. Mihalopoulos, J.-J. Morcrette, J.-F. Muller, G. Myhre, S. Myriokefalitakis, N. L. Ng, D. O'Donnell, J. E. Penner, L. Pozzoli, K. J. Pringle, L. M. Russell, M. Schulz, J. Sciare, O. Seland, D. T. Shindell, S. Sillman, R. B. Skeie, D. Spracklen, T. Stavrakou, S. D. Steenrod, T. Takemura, P. Tiitta, S. Tilmes, H. Tost, T. van Noije, P. G. van Zyl, K. von Salzen, F. Yu, Z. Wang, Z. Wang, R. A. Zaveri, H. Zhang, K. Zhang, Q. Zhang, and X. Zhang, The AeroCom evaluation and intercomparison of organic aerosol in global models, Atmospheric Chemistry and Physics, 14, pp. 10845-10895, 2014.

Turnock, S. T., Allen, R. J., Andrews, M., Bauer, S. E., Deushi, M., Emmons, L., Good, P., Horowitz, L., John, J. G., Michou, M., Nabat, P., Naik, V., Neubauer, D., O'Connor, F. M., Olivié, D., Oshima, N., Schulz, M., Sellar, A., Shim, S., Takemura, T., Tilmes, S., Tsigaridis, K., Wu, T., and Zhang, J.: Historical and future changes in air pollutants from CMIP6 models, Atmos Chem Phys, 20, 14547–14579, https://doi.org/10.5194/acp-20-14547-2020, 2020.

Moved up [4]: A.,

Moved up [3]: R.,

Moved up [2]: F.,

Moved up [1]: C.,

Deleted: Archibald,

Deleted: Bauer, S., Checa-Garcia,

Deleted: Fiedler, S., Folberth, G., Gjermundsen, A., Horowitz, L., Lamarque, J.-

Deleted: Michou, M., Mulcahy, J., Nabat, P., Naik, V., O'Connor, F., Paulot, F., Schulz, M., Scott,

Deleted: Seferian, R., Smith, C., Takemura, T., Tilmes, S., and Weber, J.: Climate-driven chemistry and aerosol feedbacks in CMIP6 Earth system models, Atmos Chem Phys, 1–36, https://doi.org/10.5194/acp-2019-1207, 2020.¶ Thornhill, G., Collins, W., Olivié, D.,

Turpin, B. J., & Lim, H. J. (2001). Species contributions to pm2.5 mass concentrations: Revisiting common assumptions for estimating organic mass. *Aerosol Science and Technology*, *35*(1), 602–610. https://doi.org/10.1080/02786820119445

Uematsu, M., Duce, R. A., Prospero, J. M., Chen, L., Merrill, J. T., & McDonald, R. L. (1983). Transport of Mineral Aerosol From Asia Over the North Pacific Ocean. *Journal of Geophysical Research*, *88*(C9), 5343–5352.

Vanderzalm, J. L., Hooper, M. A., Ryan, B., Maenhaut, W., P. Martin, P. R., Rayment, and Hooper, B. M.: Impact of seasonal biomass burning on air quality in the '"Top End"' of regional northern Australia, Clean Air Environ. Qual., 37, 28–34, 2003.

Vet, R., Artz, R. S. R. S., Carou, S., Shaw, M., Ro, C.-U. C.-U., Aas, W., Baker, A., Bowersox, V. C., Dentener, F., Galy-Lacaux, C., Hou, A., Pienaar, J. J., Gillett, R., Forti, M. C. C., Gromov, S., Hara, H., Khodzher, T., Mahowald, N. M. N. M., Nickovic, S., Rao, P. S. P., Reid, N. W. N. W., Dentener, F., Galy-Lacaux, C., Hou, A., Gillett, R., Forti, M. C. C., Gromov, S., Hara, H., Khodzher, T., Mahowald, N. M. N. M., Nickovic, S., Reid, N. W. N. W., Vet, R., Artz, R. S., Carou, S., Shaw, M., Ro, C.-U., Aas, W., Baker, A., Bowersox, V. C., Dentener, F., Galy-Lacaux, C., Hou, A., Pienaar, J. J., Gillett, R., Forti, M. C., Gromov, S., Hara, H., Khodzher, T.,. Mahowald, N. M., Nickovic, S., Rao, P. S. P.., and Reid, N. W. N. W.: A global assessment of precipitation chemistry and depositoin of sulfur, nitrogen, sea salt , base cations, organic acids, acidity and pH and phosphorus, Atmospheric Enviroment, 93, 3–100, 2014.

Vira, J., Hess, P., Melkonian, J., and Wieder, W. R.: An improved mechanistic model for ammonia volatilization in Earth system models: Flow of Agricultural Nitrogen version 2 (FANv2), Geosci Model Dev, 13, 4459–4490, https://doi.org/10.5194/gmd-13-4459-2020, 2020.

Vira, J., Hess, P., Ossohou, M., and Galy-Lacaux, C.: Evaluation of interactive and prescribed agricultural ammonia emissions for simulating atmospheric composition in CAM-chem, Atmos Chem Phys, 22, 1883–1904, https://doi.org/10.5194/acp-22-1883-2022, 2022.

Virkkula, A., Aurela, M., Hillamo, R., Makela, T., Pakkanen, T., Kerminen, V. M., Maenhaut, W., Francois, F., and Cafmeyer, J.: Chemical composition of atmospheric aerosol in the European subarctic: Contribution of the Kola Peninsula smelter areas, central Europe and the Arctic Ocean, Journal Geophysical Research, 104, 23,681–23,696, https://doi.org/10.1029/ 1999JD900426, 1999.

Vogel, A., Alessa, G., Scheele, R., Weber, L., Dubovik, O., North, P., & Fiedler, S. (2022). Uncertainty in Aerosol Optical Depth From Modern Aerosol-Climate Models, Reanalyses, and Satellite Products. *Journal of Geophysical Research: Atmospheres*, *127*(2). https://doi.org/10.1029/2021JD035483

Vohra, K., Vodonos, A., Schwartz, J., Marais, E. A., Sulprizio, M. P., & Mickley, L. J. (2021). Global mortality from outdoor fine particle pollution generated by fossil fuel combustion: Results from GEOS-Chem. *Environmental Research*, *195*. https://doi.org/10.1016/j.envres.2021.110754

Watson-Parris, D., Bellouin, N., Deaconu, L. T., Schutgens, N. A. J., Yoshioka, M., Regayre, L. A., Pringle, K. J., Johnson, J. S., Smith, C. J., Carslaw, K. S., and Stier, P.: Constraining Uncertainty in Aerosol Direct Forcing, Geophys Res Lett, 47, https://doi.org/10.1029/2020GL087141, 2020.

Wiedinmyer, C., Lihavainen, H., Mahowald, N., Alastuey, A., Albani, S., Artaxo, P., Bergametti, G., Batterman, S., Brahney, J., Duce, R., Feng, Y., Buck, C., Ginoux, P., Chen, Y., Guieu, C., Cohen, D., Hand, J., Harrison, R., Herut, B., and Zhang, Y.: COARSEMAP: synthesis of observations and models for coarse-mode aerosols, Fall American Geophysical Union, 2018.

Wilson, W. E., Chow, J. C., Claiborn, C., Fusheng, W., Engelbrecht, J., and Watson, J. G.: Monitoring of particulate matter outdoors, 1009–1043 pp., 2002.

Winker, D., Hunt, W., & McGill, M. (2007). Initial performance assessment of CALIOP. *Geophysical Research Letters*, *34*(L19803), doi:10.1029/2007GL030135.

Wolff, G. T. (1984), On the nature of nitrate in coarse continental aerosols, Atmospheric Environment, 977–981 pp., 1984.

Xiao, Y. H., Liu, S. R., Tong, F. C., Kuang, Y. W., Chen, B. F., and Guo, Y. D.: Characteristics and sources of metals in TSP and PM2.5 in an urban forest park at Guangzhou, Atmosphere (Basel), 5, 775–787, https://doi.org/10.3390/atmos5040775, 2014.

Xu, L. and Penner, J. E.: Global simulations of nitrate and ammonium aerosols and their radiative effects, Atmos Chem Phys, 12, 9479–9504, https://doi.org/10.5194/acp-12-9479-2012, 2012.

Yang, Y., Wang, H., Smith, S. J., Zhang, R., Lou, S., Yu, H., Li, C., and Rasch, P. J.: Source Apportionments of Aerosols and Their Direct Radiative Forcing and Long-Term Trends Over Continental United States, Earths Future, 6, 793–808, https://doi.org/10.1029/2018EF000859, 2018.

Zender, C., Bian, H., and Newman, D.: Mineral Dust Entrainment and Deposition (DEAD) model: Description and 1990s dust climatology, J Geophys Res, 108, 4416, doi:10.1029/2002JD002775, 2003.

Zhang, J., & Christopher, S. (2003). Long wave radiative forcing of Saharan dust aerosols estimated from MODIS, MISR and CERES observations on TERRA. *Geophysical Research Letters*, *30*(23), 2188, doi:10.1029/2003GL018479.

Zhang, Y., Mahowald, N., Scanza, R. A., Journet, E., Desboeufs, K., Albani, S., Kok, J. F., Zhuang, G., Chen, Y., Cohen, D. D., Paytan, A., Patey, M. D., Achterberg, E. P., Engelbrecht, J. P., and Fomba, K. W.: Modeling the global emission, transport and deposition of trace elements associated with mineral dust, Biogeosciences, 12, https://doi.org/10.5194/bg-12-5771-2015, 2015.

Zhao, A., Ryder, C. L., and Wilcox, L. J.: How well do the CMIP6 models simulate dust aerosols?, Atmos Chem Phys, 22, 2095–2119, https://doi.org/10.5194/acp-22-2095-2022, 2022.

Zihan, Q. and Losno, R.: Chemical properties of continental aerosol transported over the Southern Ocean: Patagonian and Namibian sources, Paris, France, 215 pp., 2016.

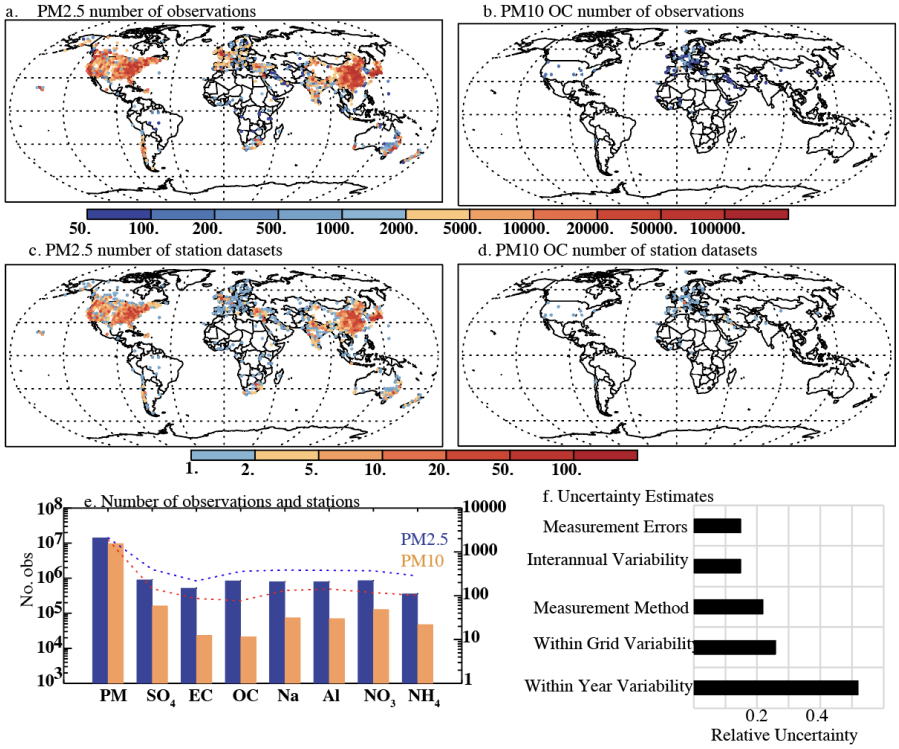

Figure 1: Distribution of observations in the data base, showing the number of observations of $PM_{2.5}$ (a) and PM_{10} organic carbon (OC) (b) (with the colors indicating different numbers using the top color bar), as well as the number of stations within each 2x2 grid locations for $PM_{2.5}$ (c) and PM_{10} OC (d) (using the second color bar), showing that there is much more $PM_{2.5}$ or PM_{10} data, in contrast to speciated data. e) The number of observations (bars) for total particulate matter (PM) or speciated data is summarized for the $PM_{2.5}$ (blue) and PM_{10} (orange) fraction using the left-hand side y-axis. The number of stations included in the study is shown as a dotted line (e) and uses the right-hand size y-axis. f) Normalized (1 standard deviation over the mean) observational uncertainty for $PM_{2.5}$ from measurement errors, interannual variability, measurement method, within grid variability and

within year variability at the same station. Interannual variability and within grid uncertainty are defined as the normalized standard deviation in the variability for stations that have more than 10 years of data. Within grid variability is the normalized standard deviation of 2x2 grid cells that have more than 10 stations. Measurement errors are the normalized standard deviation of the reported measurement errors for $PM_{2.5}$. Measurement method error derives from differences between different measurement methods (e.g., Prank et al., 2016; Burgos et al., 2020; Hand et al., 2017). The stations included derive from the following sources (see supplemental dataset for more details): Alastuey et al., 2016; Almeida et al., 2005; Amato et al., 2016; Andreae et al., 2002; Arimoto et al., 2003; Artaxo et al., 2002; Barkley et al., 2019; Barraza et al., 2017; Bergametti et al., 1989; Bouet et al., 2019; Bozlaker et al., 2013; Chen et al., 2006; Chuang et al., 2005; Cipoli et al., 2023; Cohen et al., 2004; da Silva et al., 2008; Dongarrà et al., 2007, 2010; Engelbrecht et al., 2009; Formenti et al., 2003; Fuzzi et al., 2007; Hand et al., 2017; Heimburger et al., 2012; Herut and Krom, 1996; Herut et al., 2001; Hsu et al., 2016; Hueglin et al., 2005; Furu et al., 2022, 2015; Gianini et al., 2012a, b; Kalivitis et al., 2007; Kaly et al., 2015; Kubilay et al., 2000; Kyllönen et al., 2020; Laing et al., 2014b, a; Lucarelli et al., 2014, 2019; Mackey et al., 2013; Maenhaut et al., 1996c, a, b, 1997a, b, 1999, 2000a, 2000b, 2002a, b, 2005, 2008, 2011; Maenhaut and Cafmeyer, 1998; Malm et al., 2007; Marticorena et al., 2010; Mihalopoulos et al., 1997; Mirante et al., 2010 , 2013; Mkoma, 2008; Mkoma et al, 2009; Morera-Gómez et al., 2018, 2019; Nava et al., 2015, 2020; Nyanganyura et al., 2007; Oliveira, 2009; Oliveira et al., 2010; Pérez et al., 2008; Pio et al., 2022; Prospero et al., 1989, 2012, 2020; Prospero, 1996, 1999; Putaud et al., 2004, 2010; Rodríguez et al., 2011, 2015; Salma et al., 1997; Savoie et al., 1993; Silva et al., 2010; Smichowski et al., 2004; Swap et al., 1992; Tørseth et al., 2012; Uematsu et al., 1983; Vanderzalm et al., 2003; Virkkula et al., 1999; Xiao et al., 2014; Zihan and Losno, 2016. Data from several online networks are also included (e.g., https://www.airnow.gov/international/us-embassies-and-consulates/, https://quotsoft.net/air/, https://app.cpcbccr.com/ccr/#/caaqm-dashboard-all/caaqm-landing/data, https://sinca.mma.gob.cl/index.php/. https://tenbou.nies.go.jp/download/). See the supplemental data set for more details and the doi links for the datasets.

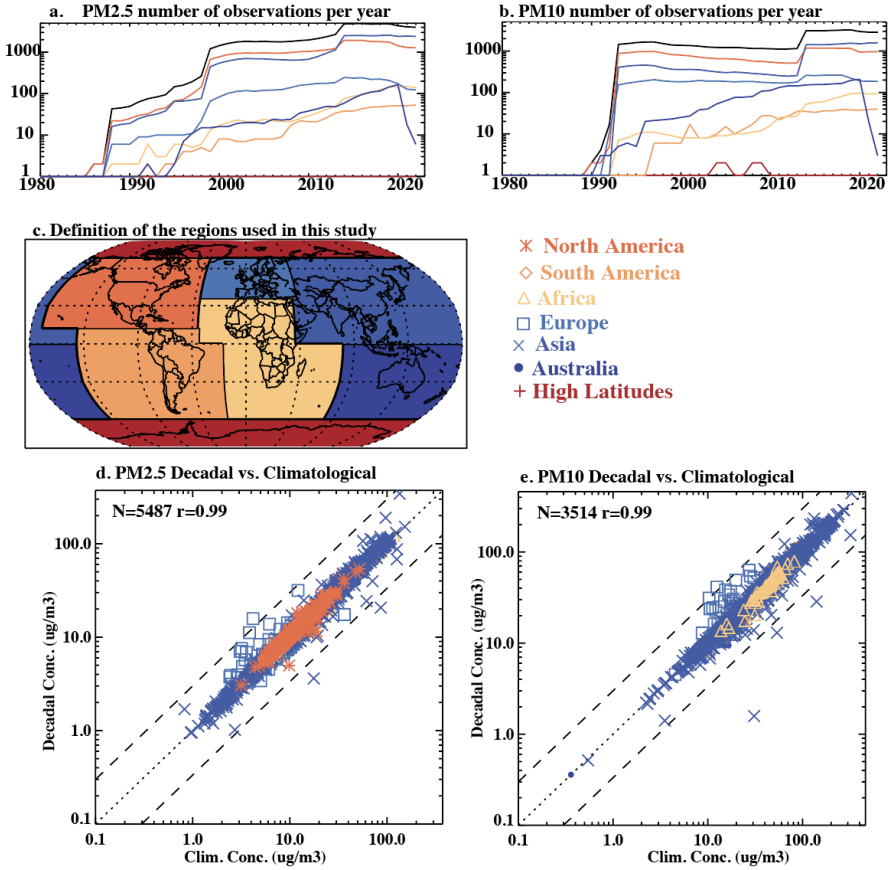

Figure 2: The temporal change in the number of observations of PM2.5 (a) and PM10 (b) available in this study (black) and by region: Dark blue: Australia, Blue: Asia, Light Blue: Europe, Yellow: Africa, Orange: South America, Red/orange: North America and Red: High latitudes; the regions are shown in (c), and are used throughout this study. Scatterplots comparing the climatological mean versus the decadal (2010-2019) mean surface concentration for PM2.5 (d) and PM10 (e), using symbols which indicate the region of the dataset point plotted.

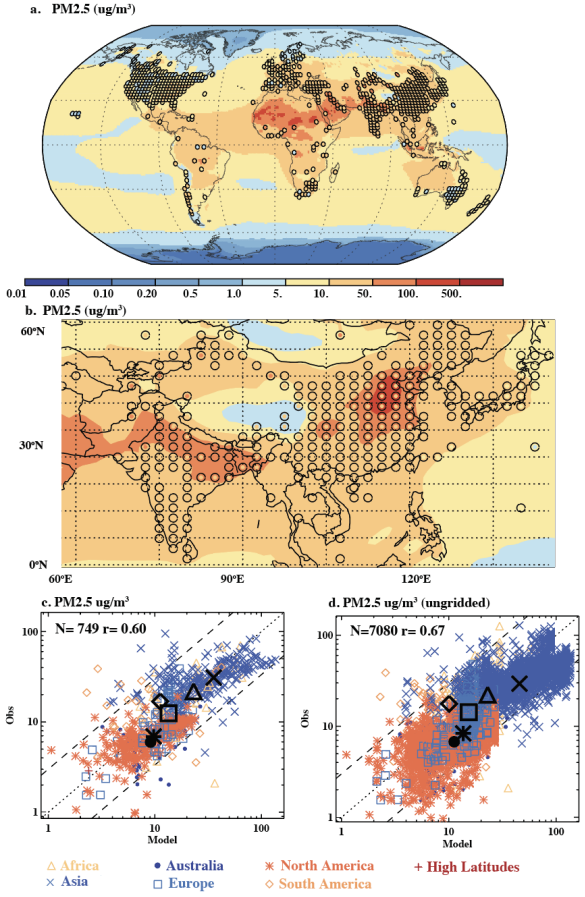

Figure 3: Model results and gridded observations for $PM_{2.5}$ in $\mu g/m^3$ spatially mapped globally (a) and focused on just Asia (b) where the model is plotted as the background and the observations are circles with the colors indicating the amount of $PM_{2.5}$ using the same scale. A comparison of the model (x-axis) to the observations (y-axis) is shown for the gridded data (c) and including all stations (d). In the scatter plots, the color and symbols indicate the regions, the bold black symbols are the average across each region (indicated by the symbol), the

dotted line is the 1:1 line and the dashed lines are the factor of 3 uncertainty estimates. More statistics are shown in Table S7, and maps focused on different regions are available in Figure S1.

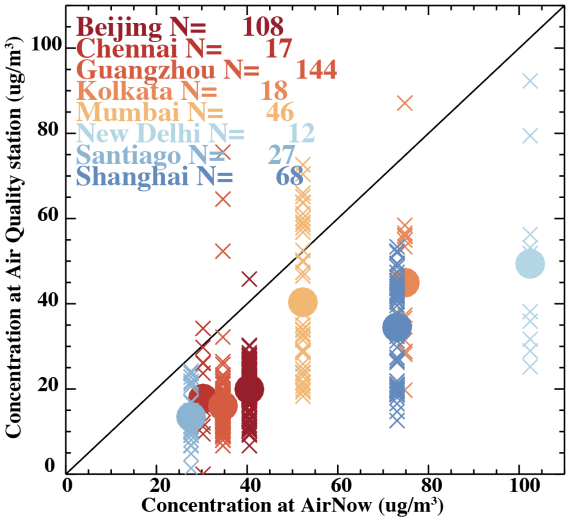

Figure 4: Comparison of $PM_{2.5}$ observations from the US Embassy's AirNow network (**https://www.airnow.gov/international/us-embassies-and-consulates/**) versus observations from the Chinese air quality network (downloaded from **https://quotsoft.net/air/**) (Beijing 39.9N 116.4E, Guangzhou 23N 113E, Shanghai 31N 121E) and the Indian (Chennai 13N 80E, Kolkata 23N 88E, New Delhi 27N 77E) network (**https://app.cpcbccr.com/ccr/#/caaqm-dashboard-all/caaqm-landing/data**); and observations (Barraza et al., 2017) from Santiago, Chile (23.7S 70.4W) against the Chilean air quality network (https://sinca.mma.gob.cl/index.php/). The numbers after each city name are the number of stations found within 1° distance of the AirNow (or Chile observations) station.

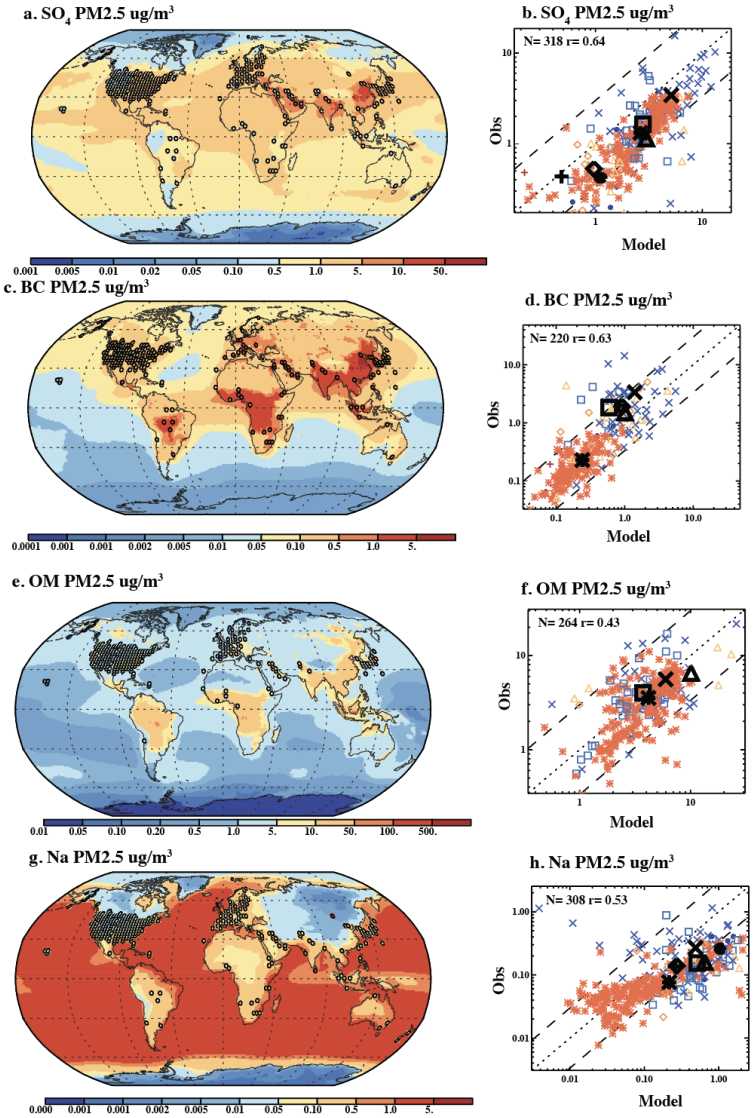
a. SO4 PM2.5 ug/m3
0.001 0.005 0.01 0.02 0.05 0.10 0.5 1.0 5. 10. 50.
b. SO4 PM2.5 ug/m3
N= 318 r= 0.64
Obs
Model
c. BC PM2.5 ug/m3
0.0001 0.001 0.001 0.002 0.005 0.01 0.05 0.10 0.5 1.0 5.
d. BC PM2.5 ug/m3
N= 220 r= 0.63
Obs
Model
e. OM PM2.5 ug/m3
0.01 0.05 0.10 0.20 0.5 1.0 5. 10. 50. 100. 500.
f. OM PM2.5 ug/m3
N= 264 r= 0.43
Obs
Model
g. Na PM2.5 ug/m3
0.000 0.001 0.001 0.002 0.005 0.01 0.05 0.10 0.5 1.0 5.
h. Na PM2.5 ug/m3
N= 308 r= 0.53
Obs
Model

1687

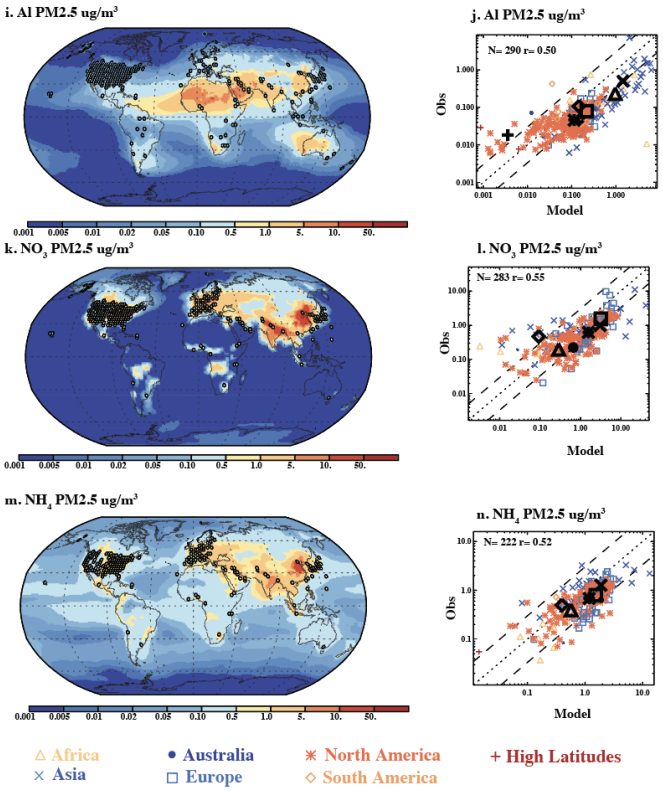

Figure 5: Model results and gridded observations for different types of $PM_{2.5}$ in $\mu g/m^3$ spatially mapped globally where the model is plotted as the background and the observations are circles with the colors indicating the amount $PM_{2.5}$ using the same scale for (a) SO_4^{2-}, (c) BC (black carbon), (e) OM (organic material=1.8 times organic carbon (OC)), (g) Na, (i) Al, (k) NO_3^-, (m) NH_4^+. A scatter plot comparison of the model (x-axis) to the

observations (y-axis) is shown for the gridded observational data for for (b) SO_4^{2-}, (d) BC (f) OM, (h) Na, (j) Al, (l) NO_3^-, (n) NH_4^+. In the scatter plots, the colors and symbols indicate the regions, the bold black symbols are the average across each region (indicated by the symbol), the dotted line is the 1:1 line and the dashed lines are the factor of 3 uncertainty estimates. More statistics are shown in Table S5, and the maps focused on specific regions are available in Figure S3-S9 for SO_4^{2-}, BC, OM, Na, Al, NO_3^-, and NH_4^+, respectively.

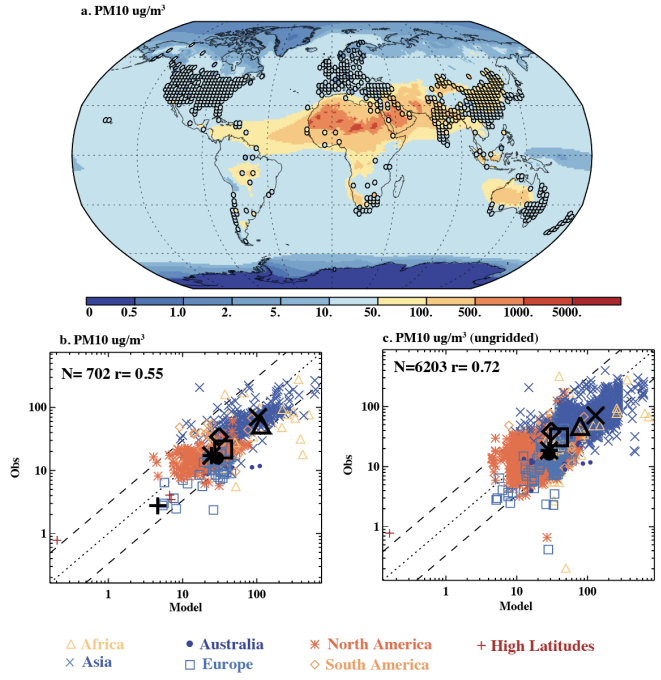

Figure 6: Model results and gridded observations for PM_{10} in $\mu g/m^3$ spatially mapped globally (a). A comparison of the model (x-axis) to the obsevations (y-axis) is shown for the gridded data (b) and including all stations (c). In the scatter plots, the colors and symbols indicate the regions, the bold black symbols are the average across each region (indicated by the symbol), the dotted line is the 1:1 line and dashed lines are the factor of 3 uncertainty estimates. More statistics are shown in Table S7, and maps focused on different regions are shown in Fig. S10

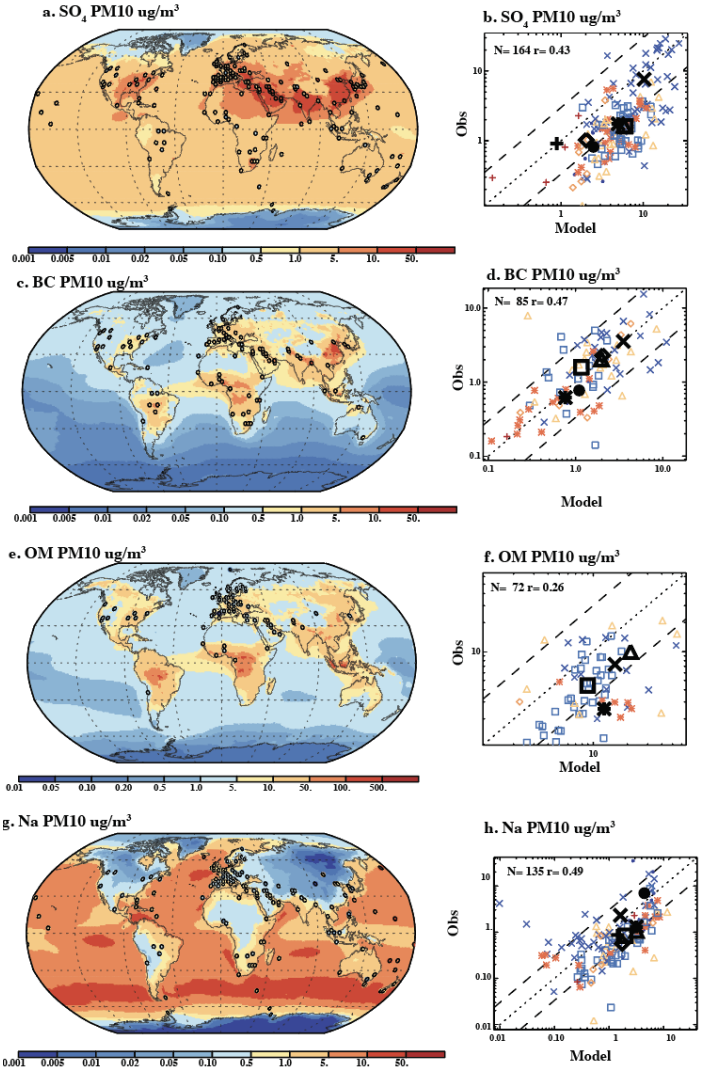
a. SO4 PM10 ug/m3
0.001 0.005 0.01 0.02 0.05 0.10 0.5 1.0 5. 10. 50.
b. SO4 PM10 ug/m3
N= 164 r= 0.43
Obs
Model
c. BC PM10 ug/m3
0.001 0.005 0.01 0.02 0.05 0.10 0.5 1.0 5. 10. 50.
d. BC PM10 ug/m3
N= 85 r= 0.47
Obs
Model
e. OM PM10 ug/m3
0.01 0.05 0.10 0.20 0.5 1.0 5. 10. 50. 100. 500.
f. OM PM10 ug/m3
N= 72 r= 0.26
Obs
Model
g. Na PM10 ug/m3
0.001 0.005 0.01 0.02 0.05 0.10 0.5 1.0 5. 10. 50.
h. Na PM10 ug/m3
N= 135 r= 0.49
Obs
Model

1707

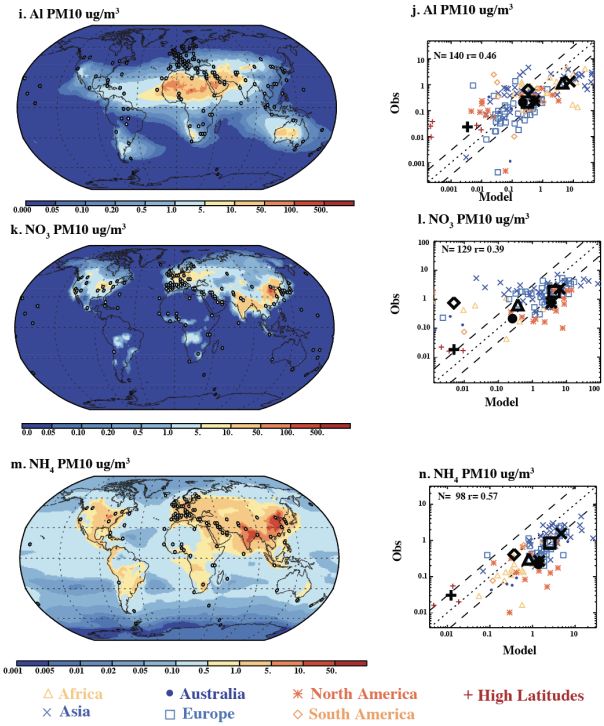

Figure 7: Model results and gridded observations for different types of PM_{10} in $\mu g/m^3$ spatially mapped globally where the model is plotted as the background and the observations are circles with the colors indicating the amount PM_{10} using the same scale for (a) SO_4^{+2}, (c) BC (black carbon), (e) OM (organic material=1.8 times organic carbon (OC)), (g) Na, (i) Al, (k) NO_3^-, (m) NH_4^+. A scatter plot comparison of the model (x-axis) to the observations (y-axis) is shown for the gridded observational data for (b) SO_4^2, (d) BC (f) OM, (h) Na, (j) Al, (l) NO_3^-, (n) NH_4^+. In the scatter plots, the colors and symbols indicate the regions, the bold black symbols are the average across each region (indicated by the symbol), the dotted line is the 1:1 line and the dashed lines are the

1716 factor of 3 uncertainty estimates. More statistics are shown in Table S7, and the maps focused on specific
1717 regions are available in Figure S11-S17 for SO_4^{2-}, BC, OM, Na, Al, NO_3^-, and NH_4^+, respectively.

1718

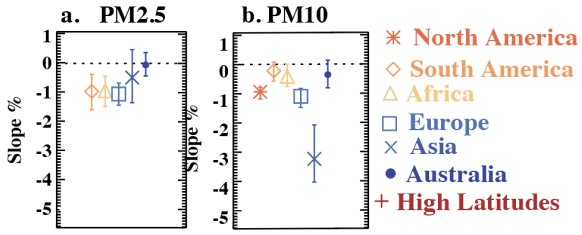

Figure 8: Trends in the observations of aerosols in different regions during the 1980-2000 and 2000-2024 time periods for $PM_{2.5}$ (a) and PM_{10} (b). Error bars indicate the 1-sigma uncertainty using a Thiel regression approach.

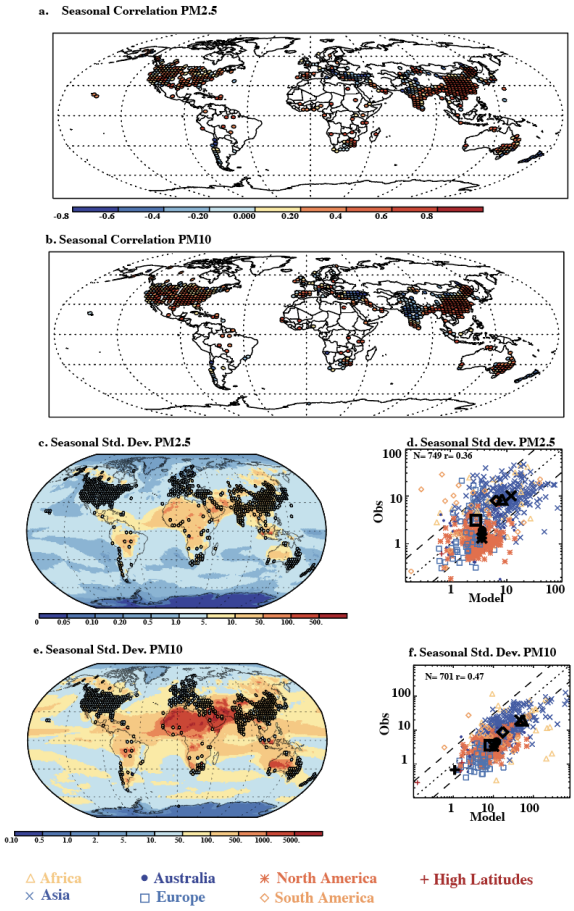

Figure 9: Model data comparison for the seasonal cycle. The correlation coefficient between the 12 climatological monthly means in the observations and the model for those station datasets with a larger seasonal cycle than within monthly variability (see Section 2.5 for more details), averaged to 2°×2° grid for plotting for $PM_{2.5}$ (a) and PM_{10} (b). A comparison of the magnitude seasonal cycle in the observations versus the model (defined as the standard deviation of the 12 climatological monthly means) spatially for (c) $PM_{2.5}$ and (e) PM_{10} and a scatterplot for $PM_{2.5}$

(d) and PM_{10} (f). The correlation coefficient is only calculated in locations where the standard deviation from the seasonal cycle is stronger than the within month variability (see Section 2.5 for details).

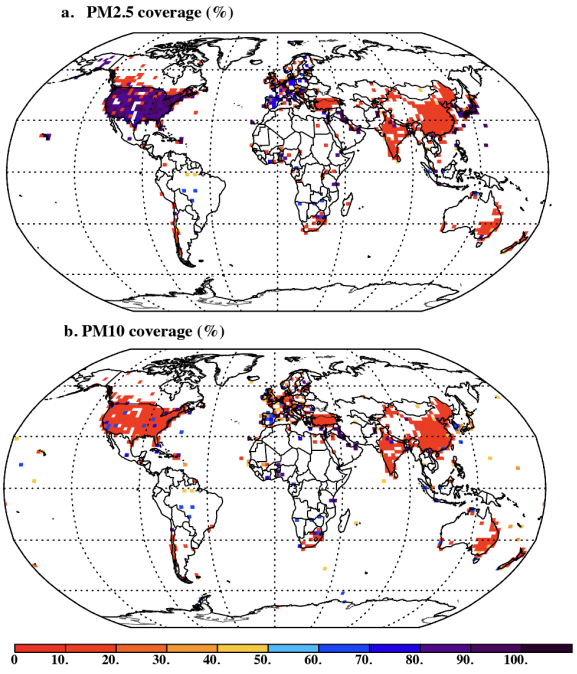

Figure 10: Observational coverage (%) for gridded observations, showing within each grid box (2°x2°) the % of the constituents that are measured assuming that PM, SO_4^{2-}, BC, OM, Na, Al, NO_3^-, and NH_4^+ are required to constrain the PM distribution for (a) $PM_{2.5}$ and (b) PM_{10}.

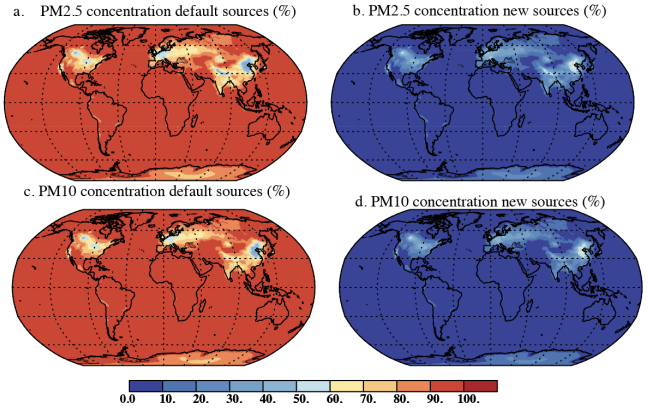

Figure 11: Modelled estimates of what percent of the surface concentration of $PM_{2.5}$ is considered in the default CAM6 climate model (a) or is new in this study (b). Similarly PM_{10} is shown for the default model (c) and new sources in this study (d). The new sources added in this study are the nitrogen oxides as described in Section 2.3.

Table 1: Aerosol measurement types.

Composition	Measurement Method	Variables		Example Networks	Example Citations
Fine and Coarse	Stacked Filter Unit (SFU)	Fine, Coarse		U. Gent	Maenhaut et al., 2002a
PM2.5 and PM10	Reference Method/Federal Equivalent Method (FRM/FEM),	PM2.5, PM10		IMPROVE, CASNET, EMEP	Hand et al, 2019, Putaud et al., 2004
PM2.5 and PM10	Hi Vol Sampler			EMEP, SINCA	Putaud et al., 2004
Elemental	Particle Induced x-ray emission Spectrometry (PIXE), Instrumental nuclear activation analysis (INAA)	Al, S, Na		U. Gent, EMEP	Maenhaut et al., 2002a
Elemental	Inductively Coupled Plasma-Mass Spectrometry (ICP-MS)	Al, S, Na		EMEP, SPARTAN	Putaud et al., 2004; Phillip et al., 2017
Elemental	XRF	Al, S, Na		IMPROVE, CASNET	Hand et al, 2019
Chemistry	Ion Chromatography	SO4--, NO3-, NHr		IMPROVE, CASNET, EMEP	Hand et al, 2019, Putaud et al., 2004
Carbonaceous	Thermal Optical Reflectance	EC, OC		IMPROVE, CASNET	Hand et al, 2019
	Evolved Gas Analysis Non-dispersive Infrared (EGA+NDIR)	OC, EC		EMEP	Putaud et al., 2004

Formatted Table

Table 2: Global Aerosol Modelling Budgets

Global modelled deposition (Tg/year), percentage of aerosol that is $PM_{2.5}$, and globally and annually averaged surface concentration ($\mu g/m^3$) and aerosol optical depth for each of the sources used in the model. An asterisk indicates that there are additions to the model from the default CAM6.

	PM_{10}	$PM_{2.5}$		
	Deposition (Tg/year)	%	Conc ($\mu g/m^3$)	AOD (unitless)

Formatted Table

Sulfate	121	100	2.1	0.018
Black carbon	10	100	0.5	0.009
Primary organic aerosol	34	100	1.6	0.008
Secondary organic aerosol	37	100	1.0	0.007
Sea salts	2520	3	13.0	0.045
Dust	2870	1	19.4	0.030
NH_4NO_3*	20	100	0.4	0.013